Final Report

Improvements and Calibrations of Lower San Joaquin River DO Model

Contract Numbers
CALFED 99-B16
DWR 4600000989

Prepared for

CALFED 2000 Grant
Dr. P. Lehman, Principal Investigator
California Department of Water Resources
3251 S Street
Sacramento, CA 95816

Prepared by

Carl W. Chen and Wanteng Tsai
Systech Engineering, Inc.
3180 Crow Canyon Pl., Suite 260
San Ramon, CA 94583

Tel: 925-355-1780
Fax: 925-355-1778
Email: carl@systechengineering.com

September 2001
Revised March 2002

Executive Summary

The Lower San Joaquin River is on the 301(d) list for low dissolved oxygen. An estuary model was applied to simulate DO, temperature, CBOD, detritus, ammonia, algae, and pheophytin based on real-time tides, river flows, and waste loads. Organic nitrogen is included in the pools of detritus, algae, and pheophytin. The model was calibrated and verified with field data of 1999, 2000, and 2001.

The model shows that low DO are caused by: 1) the dredging of the river from 8-10 ft to 35-40 ft for Stockton Deep Water Ship Channel, which increases hydraulic residence time, 2) the upstream flow diversion through the Old River to the Tracy Export Pumping Facility, which reduces river flow, 3) the point source discharge of Stockton, which contributes BOD and ammonia, and 4) the oxygen consuming materials discharged by wetlands, agricultural drainage, and municipalities in the Upper San Joaquin River.

The ultimate BOD, calculated as a function of flow, CBOD5, ammonia, algae, detritus, and pheophytin, was 3,600 to 3,900 kg/d for Stockton load and 30,000 to 35,000 kg/d for the upstream river load, during the critical periods of July to October in 1999 and 2000. The sinks and sources of DO in the DWSC are +1,500 kg/d for photosynthesis,-3,900 kg/d for algae respiration, -1600 kg/d for nitrification, -1,800 kg/d for sediment oxygen demand, -3,000 kg/d for the decay of CBOD, detritus and pheophytin, and +2,300 kg/d for surface aeration. High temperature lowers DO by: 1) reducing the solubility of dissolved oxygen and 2) increasing the rates that consume DO.

The model sensitivity was evaluated in terms of predicted DO deficit below the target criterion of 5 mg/l for the entire DWSC. A 5% change of decay coefficients for nitrification and BOD decay can only lead 5 to 10% change of predicted DO deficit. A 5% change of temperature correction factors for nitrification and BOD decay can lead to 35 to 70% change of predicted DO deficit. Fortunately, the model predicts the water temperature accurately. The high sensitivity also makes it easier to calibrate the temperature correction factors in order to match the observed DO. A sensitivity analysis was also made to evaluate the effects of boundary conditions on the DO deficit in DWSC. A 5% change of UVM flow leads to a 15% change in DO deficit. A 5% increase of river load can increase the DO deficit by 50%. A 5% decrease of river load can decrease the DO deficit by 34%. A 5% change of Stockton load can only change the DO deficit by 5%. Clearly, the river load has a big impact on the DO deficit in the DWSC. The infrequent (bi-weekly or monthly) river load data was thought to be the reason for model's inability to capture some of the episodic low DO observed in the DWSC. To reduce the model uncertainty, it is necessary to collect more frequent river load data, especially during the period of low UVM flow.

The model predicted the top to bottom DO difference due to algae floating in the stratified Turning Basin to be 8 mg/l. At high UVM flows, this DO difference dropped to less than 1.5 mg/l at Channel Point, where the water from the Turning Basin mixed with San Joaquin river flow from the upstream. At low UVM flow, the DO difference may stay as high as 3.5 mg/l by tidal excursion.

The model was used to evaluate alternative management strategies for low DO in DWSC. If the DWSC is restored to its original depth of 8-10 ft, the DO deficit disappears at the UVM flow of 1000 cfs. However, eliminating the DWSC is not a viable option. Increasing the river flow from 250 to 1000 cfs can decrease the predicted DO deficit from 1400 kg to 32 kg. The benefit of hydraulic flushing appears to have over compensated the higher river loads from upstream. By maintaining a river flow above 1000 cfs, it may be adequate for 10 to 25% reduction of current (1999 and 2000) Stockton and river loads, which is more achievable.

Table of Contents

List of Figures

List of Tables

I. Introduction

Introduction

Dissolved oxygen in the Lower San Joaquin River is controlled by a large number of factors. These factors include tides at the downstream end, the stream flow at the upstream end, channel depth, water temperature, and various dissolved oxygen (DO) sinks, i.e. algae, BOD, ammonia, volatile suspended solids, and sediment oxygen demand. The sediment oxygen demand was derived from organic matter that has been accumulated at the river bottom through years. Other DO sinks are discharged by Stockton, local urban runoff, and the upstream agricultural farms, dairy farms, wetlands, and municipalities.

The controlling factors for the DO can change with time by hour, day, and season. The dynamic nature of the estuary system make it difficult to perform statistical correlations of parameters, measured at discrete places and times. No single factor can be used to explain the observed DO change, because all factors work in concert to affect the DO in the Lower San Joaquin River.

One approach is to develop a mathematical model of the estuary system. Actual tides, river flows, and waste discharges can be inputted to the model. The model can then simulate the physical, chemical, and biological responses. The model output may include the predictions of temperature, BOD, ammonia, DO etc. at various locations and times. Such predictions can be compared to the observed data. If they match well, we can say that the model can explain the observed variations of the estuary system.

Systech Engineering, Inc. has developed such a model for the Lower San Joaquin River (Schanz and Chen 1993, Chen and Tsai 1997). The model was adapted and modified from the link-node model of Chen and Orlob (1975). The model formulations and coefficients must be calibrated so that the model predictions match the observed data. For the multiple parameter model like this, the more calibrations can be made the more reliable it becomes.

During the model calibration, the observed data is compared to the model prediction. The model can make predictions for times and locations not covered by the monitoring program. The model can be used to explain why the water quality behaved as observed. Such explanation (or understanding) is crucial to the formulation of adaptive water quality management plans. After the calibration, the model can be used to calculate the maximum daily loads of oxygen consuming materials to meet the DO standard.

During the CALFED 2000 grant, field data was collected in the summer and fall of 1999 and 2000. This report documents the model improvements and calibrations using the new data sets.

Hypothesis

The working hypothesis of this project is as follow: The Lower San Joaquin River DO model, which already accounts for tide, channel depth, river flow, headwater quality, sediment oxygen demand, point source and nonpoint source loads, can be improved to track the new field data collected in the CALFED 2000 grant. The model can also calculate various mass fluxes to support integrated data analysis and hypothesis testing. The calibrated model can be used to predict the response of dissolved oxygen in the river under various management scenarios of waste load reductions and river flow manipulations.

Scope of Work

Specific tasks to be performed in the project are as follow:

1. *Peer review of the model*: The model was subjected to two peer reviews. The USEPA has conducted a peer review of the model and has found no problem with its formulations. They suggested an adjustment of some coefficients (theda values) and the outputs of hourly results and frequency distribution plots. The second review was made as a part of the CALFED 2000 grant, which required an external science review of the entire project. We responded to both reviews.

2. *Compilation of data:* We compiled all relevant data to support modeling activities, including the preparation of input data and the comparison of model results to the observed data. Relevant data included tide, meteorology, San Joaquin River flow at Vernalis, UVM flow, delta export, head of the Old River barrier operation, and continuous water quality monitoring at Vernalis, Mossdale, and Rough and Ready Island, the sediment flux data collected by Dr. Gary Litton of the University of Pacific, the receiving water monitoring data collected by the City of Stockton and by Dr. Peggy Lehman of the Department of Water Resources. We also compiled the daily discharge data for Stockton Regional Wastewater Control Facility.

3. *Model enhancements:* In addition to algae, we added detritus (VSS), its sedimentation, resuspension, and sediment oxygen demand (SOD) to the model. We added algorithm to simulate phytoplankton growth in Turning Basin under a specified mixing depth. The algae grown under such condition would be transported to exert oxygen demand in the Deep Water Ship Channel. We made changes to output the hourly results instead of the daily values.

4. *Model calibration:* The decay coefficient, SOD rate, and particle settling velocity, measured by Dr. Gary Litton, were used to the extent possible by the model. The model predictions were compared to flows measured by ADCP and water quality concentrations measured by the collaborators of the CALFED grant. Slight adjustments of model coefficients were made to improve the match

between model result and observed data. Some sensitivity analyses were also performed.

5. *Hypothesis testing:* We used the model to calculate various fluxes to help test various hypotheses about how water quality changed with time and space as observed.

6. *Management scenarios:* We used the model to predict the DO concentrations in the Stockton Deep Water Ship Channel under various scenarios of river flow, river loads, and Stockton load. The results were given to Dr. Chris Foe of the Central Valley Regional Water Quality Control Board to prepare the Strawman TMDL allocation report. The analyses were repeated for the 1999 and 2000 conditions.

Acknowledgement

The financial support for this study was provided by CALFED. The work was carried out under the leadership of Dr. Peggy Lehman of DWR, who served as the principal investigator of the overall project. Technical Advisory Committee of the project has reviewed the progress and provided internal critiques. The Steering Committee of the San Joaquin River Dissolved Oxygen TMDL provided an oversight of the project.

The model project requires a large amount of data collected by other investigators. Dr. Peggy Lehman of DWR and Dr. Steve Hayes of DWR have furnished us their data set for algae, nutrients, DO, current velocity, and others. Dr. Gary Litton of the University of Pacific has furnished his sediment flux, BOD incubation, and light attenuation data. The City of Stockton has furnished their effluent data as well as the monitoring data collected in the San Joaquin River.

Dr. G. Fred Lee of G. Fred Lee & Associates provided a detail review of this report. His comments have been incorporated into this final report.

II. Model Description

Model History

The root of the model can be traced back to the link-node model of Chen and Orlob (1975). The basic hydrodynamic formulations can be found in Feigner and Harris (1970). The analogy of model node to a chemical reactor and the formulations to track the mass and concentration of multiple constituents interacting within the reactor can be found in Chen (1970). The model has been adapted into EPA WASP5, under the code name DYNHYD5.

In 1993, we adapted the model to the Lower San Joaquin River for the City of Stockton (Schanz and Chen 1993). For this application, the model was modified to accept real tides (spring and neap tides) throughout the year instead of a single repeating tide (i.e. dynamic steady state tide). The tidal boundary conditions were calculated as a function of tidal exchange coefficient instead of a specified constant. Anti-numerical dispersion term was introduced to hold back the numerical dispersion that was known to exist in link-node model. The model was calibrated with 1991 data, including a special tracer study of 1992. The model was used to predict the water quality impact of waste discharge from Stockton Regional Wastewater Control Facility (RWCF) and was used in the NPDES negotiation between the City and the Central Valley Regional Water Quality Control Board.

In 1993, we applied the model to evaluate the impact of the Interim South Delta Program on the dissolved oxygen resources of the Lower San Joaquin River (Chen and Tsai 1997). In this study, the model calibration was confirmed with 1993 and 1996 data. The work was performed at the request of State Water Resources Control Board. The results were presented at the 1998 Water Right Hearing of the State Water Resources Control Board.

Model Domain

Figure II-1 presents the domain of the Lower San Joaquin DO model. The model started at the head of the Old River in the south, extended northward to Stockton, and then westward to Light 18 in the Deep Water Ship Channel, near McDonald Tract.

The stations numbered R1to R8 are the water quality stations, monitored by the City of Stockton as a part of its NPDES requirements. The Stockton Regional Wastewater Control Facility discharges its treated effluent at the location marked “outfall”, between station R2 and R3.

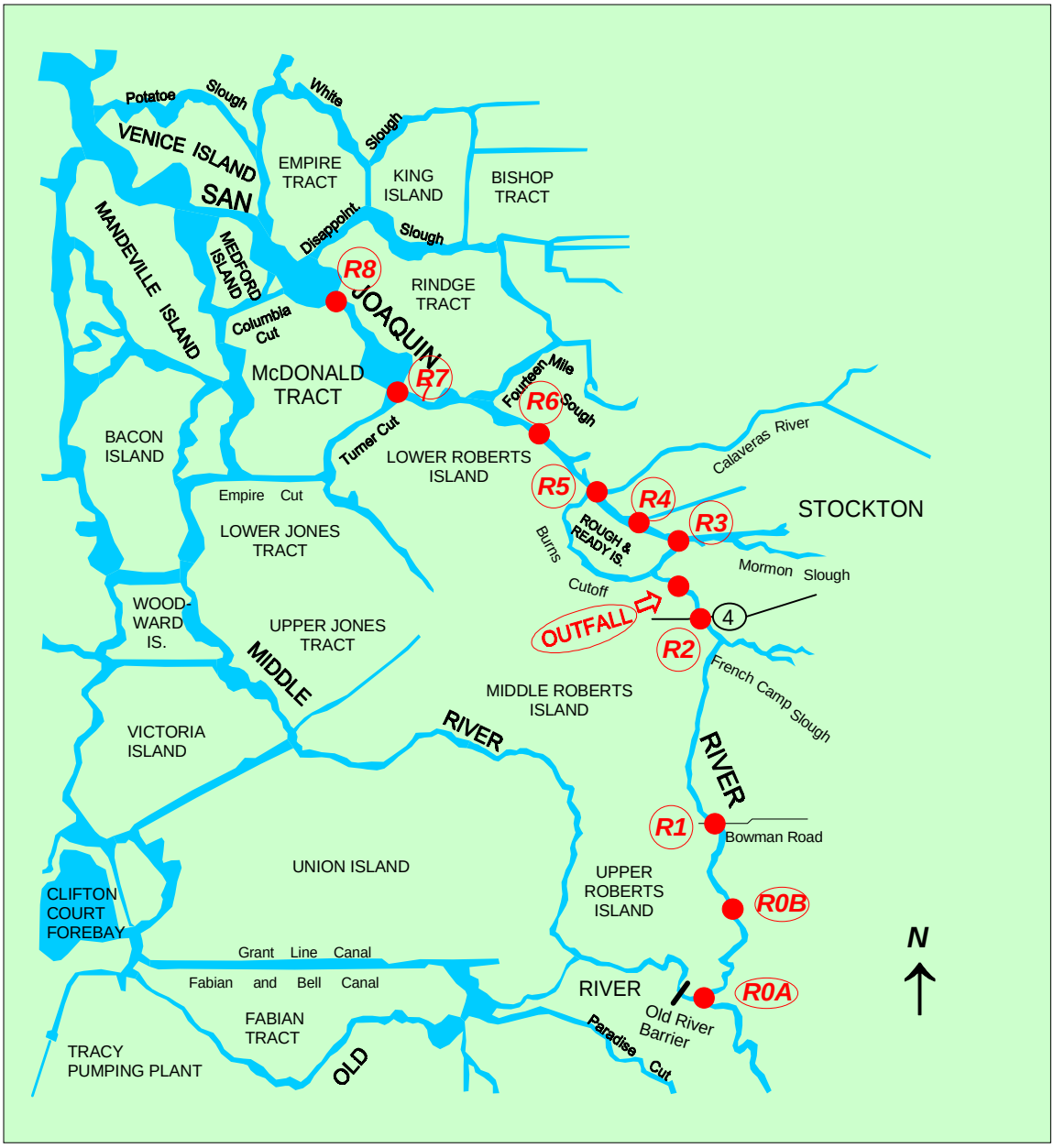

Figure II-1

Domain of the Lower San Joaquin River DO Model

The model domain also includes the slough around the Rough and Ready Island, Smith Canal, Turning Basin, and French Camp Slough. These sloughs are included so that correct volumes are used to adsorb tidal flows. In principal, they can accept storm water inflows and nonpoint source loads, which are assumed to be zero for lack of data at this time.

Link-Node Concept

For modeling purpose, the Lower San Joaquin is divided into river segments (nodes). Between nodes, there are channels that allow the water to move back and forth by tides. The channels are referred to as links. Figure II-2 depicts the concept of link-node model.

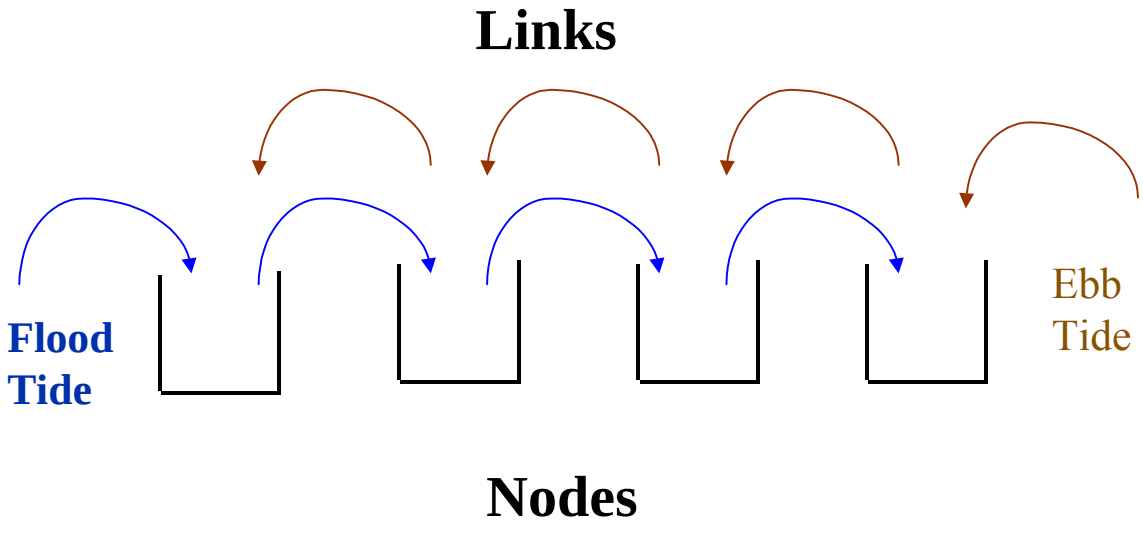

Figure II-2
Link-Node Concept.

Hydrodynamics

The first step of the model is to calculate how the water will move from one node to the next. The flow velocity is controlled by the equation of motion:

$$\frac{dU}{dt} = -U\frac{dU}{dX} - g\frac{dH}{dX} - nUU \qquad \text{(II-1)}$$

where U is flow velocity, t is time, X is horizontal distance, g is gravity acceleration, H is head or water surface elevation, and n is Manning's friction factor. This equation says that the changing rate of flow velocity is a function of momentum (first term), head differential (second term), and friction loss at the bottom (third term).

Equation II-1 is in differential form. For numerical solution by computer, it was transformed into Equation II-2:

$$U(t) = U(t-1) - [U\frac{dU}{dX} + g\frac{dH}{dX} + nU(t-1)U(t-1)] \quad \text{(II-2)}$$

where (t) is used to denote the parameter value at the current time step and (t-1) is used to denote the parameter value at the previous time step.

The calculated flow velocity (U) is multiplied by cross sectional area (Xa) of the channel (link) to obtain the flow (Q) in Equation II-3.

$$Q = UXa \quad \text{(II-3)}$$

The flows for various channels connected to a node can be summed and divided by the surface area (Sa) of the node to calculate the new water surface elevation H(t) as shown in Equation II-4. Equation II-4 is the continuity equation for water.

$$H(t) = H(t-1) - \frac{\sum Q}{Sa}\Delta t \quad \text{(II-4)}$$

The computer program of the Lower San Joaquin DO model solves Equations II-2, II-3, and II- 4 in an iterative manner from (t-1) to (t). The time step is in the order of seconds. The outputs are time series of flow velocity and volumetric flow for links and water surface elevation and water volume for nodes.

Water Quality

With the flow information known, the next step is to calculate the concentrations of water quality parameters. The calculation is based on the principle of mass balance. The general mass balance equation is as follow.

$$\frac{dVC}{dt} = \sum QC + \alpha\frac{dC}{dX} - AND - Sinks + Sources \quad \text{(II-5)}$$

where V = volume of water in the node, C = concentration of a water quality constituent, Q = flow in link. C = upstream concentration, α = diffusion coefficient, dC/dX = horizontal concentration gradient, AND = anti numerical dispersion term, Sinks = loss to decay, uptake, or diversion, Sources = gain from waste discharge, chemical transformation, or biological growth.

Equation II-5 was written to account for the fact that both volume and concentration can change with time in the dynamic estuary. The equation can be decomposed to.

$$V\frac{dC}{dt} = -C\frac{dV}{dt} + \sum QC + \alpha\frac{dC}{dX} - AND - Sinks + Sources \quad \text{(II-6)}$$

with the values of V and Q obtained from hydrodynamic solution, Equation II-6 can be solved numerically for the changing rate of concentration (dC/dt), which can be used to calculate C(t), based on the value of C(t-1) of the previous time step.

$$C(t) = C(t-1) + \frac{dC}{dt}\Delta t \qquad \text{(II-7)}$$

In Equation II-6, we use the upstream concentration to calculate the mass flow occurring in links. This procedure introduces a numerical dispersion, which causes the mass of pollutant to advance too fast from one node to the other.

In the computational fluid dynamics by Roache (1972), a theoretical derivation was made for the magnitude of numerical dispersion using the UPWIND scheme. For our link-node model, we adopted the equation to calculate the magnitude of numerical dispersion and subtracted it from the transport term. We named the term "anti numerical dispersion" (AND).

$$AND = \frac{1}{2}u\Delta x(1-c) \qquad \text{(II-8)}$$

$$c = \frac{u\Delta t}{\Delta x} \qquad \text{(II-9)}$$

DO Sinks and Sources

Equation II-5 is written for any water quality constituent. Different constituents will have difference sinks and source terms. For the conservative substance, the sink term will be limited to water diversion and the source term will be limited to waste discharge. For non-conservative substance, there is additional sink for decay.

For dissolved oxygen, sinks and sources become more complicated. Figure II-3 shows various sinks and sources of DO. The sinks include BOD decay, ammonia nitrification, sediment oxygen demand, algal respiration, and decay of volatile suspended solid. The model does not simulate organic nitrogen as a separate water quality parameter. Organic nitrogen is included in three pools (algae, pheophytin, and volatile suspended solid). When the parent pools decay, they release ammonia, which is a sink of dissolved oxygen. While Algal respiration is a DO sink, algal photosynthesis is DO source that contributes DO to the water.

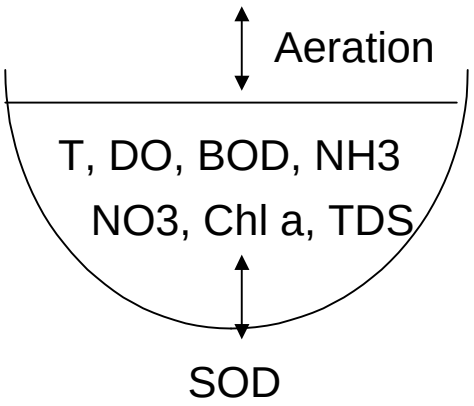

O2(s)=f(T)
Aeration=a(O2(s)-O2)
BOD+O2=CO2
NH3+O2=NO3
SOD+O2=CO2
Chla+N+P+CO2=Chla+O2
Chla+O2=Chla+CO2
VSS+O2=CO2+NH4

Figure II-3
Sinks and Sources of Dissolved Oxygen.

As shown in Figure II-3, the water in the node has a temperature and concentrations of DO, BOD, NH3, NO3, Chl a, TDS, etc. Based on water temperature, we can calculate the solubility of dissolved oxygen. If the DO solubility is higher than the DO concentration, the surface aeration will add DO to the node. If the DO solubility is lower than the DO concentration (in the case of super saturation due to algal bloom), the aeration will vent DO from water to the air.

The aeration rate was based on O'Connor and Dobbins equation with an added term for the wind:

$$K_a = \frac{12.9U^{1/2}}{D^{3/2}}\theta^{(T-20)} + \frac{0.15W^2}{D} \qquad \text{(II-10)}$$

Where K_a = composite aeration coefficient; U = current velocity in ft/sec; W = wind speed in m/s; and D = water depth in ft. The flux of oxygen mass transfer across the water surface is:

$$F = K_a A[DO_s(T) - DO] \qquad \text{(II-11)}$$

where F = surface aeration, A = surface area of the node; DO_s = dissolved oxygen solubility at the temperature T, and DO = dissolved oxygen concentration in the water.

Other sinks include the decay of BOD, NH3 and SOD, all of which consume DO. For algae (Chl a), it can be a source in the photic zone and a sink in the non-photic zone at the bottom.

Photosynthesis Oxygenation

The model calculates the light extinction coefficient as a function of total suspended sediment and algae concentration (Chl a and pheophytin), all of which can vary with time. Figure II-4 shows the simulated light attenuation with depth at station R3.

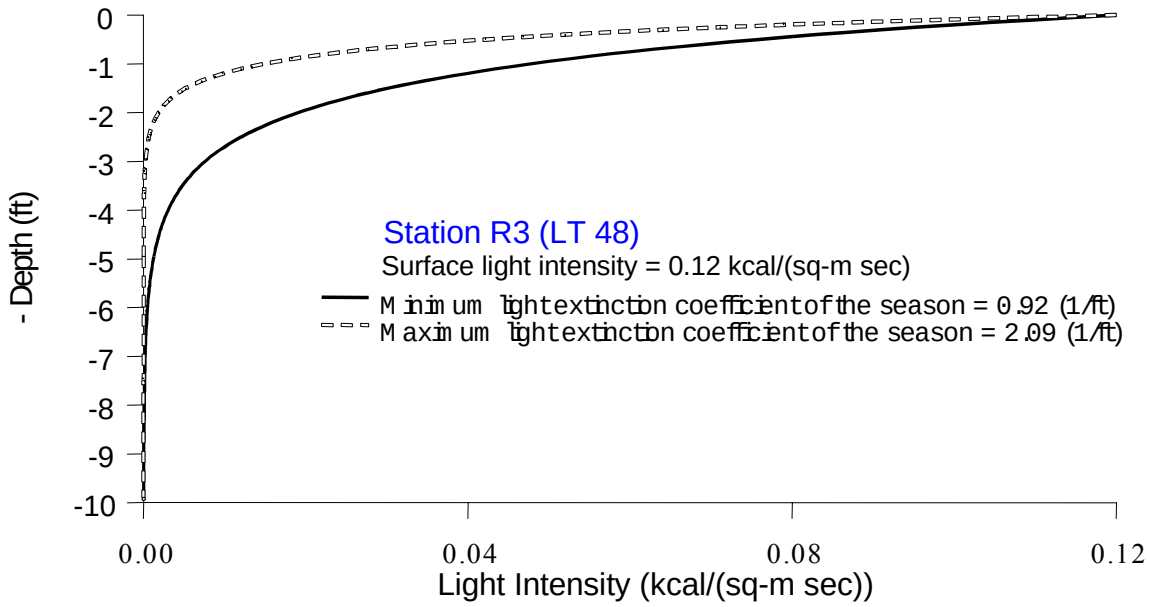

Figure II-4
Simulated Light Attenuation With Depth at Station R3.

The algal growth can be limited by light or concentrations of P (phosphate) and N (ammonia and nitrate). In a vertically mixed system, P and N concentrations are uniform throughout the depth, but light is not. One can assume that algae spend equal time at each depth in the course of vertical mixing. The light intensity can be calculated at foot intervals and then used to calculate the growth rate at each depth. The growth rates at each depth can be averaged for the growth rate of algae in the water column.

Alternatively, one can use an integrated equation for the same result. As it was documented in QUAL2E (Brown and Barnwell 1985), light intensity varies with depth according to the Beer's law:

$$Iz = I \exp(-\lambda Z) \qquad \text{(II-12)}$$

where Iz = light intensity at depth Z, I = surface light intensity, λ = light extinction coefficient, Z = water depth from surface. This equation was used to predict the light attenuation curves shown in Figure II-4.

QUAL2E has described three formulations for the light limitation on algae growth. They are Monod expression, Smith function, and Steel's equation. The Monod expression is as follow:

$$Gz = \frac{Iz}{K + Iz} \qquad \text{(II-13)}$$

where Gz = growth rate at depth Z; Iz = light intensity at depth Z, and K = half saturation constant of light.

If Equation II-10 is substituted into Equation II-11 and integrated over depth, it results in the following equation:

$$Gd = (1/\lambda d)\ln\frac{K + I}{K + Ie^{(-\lambda d)}} \qquad \text{(II-14)}$$

where Gd = depth averaged algae growth if light is limiting, d = total water depth, and I = light intensity at the surface.

When algae grow, it removes an equivalent amount of nitrogen and phosphorus to make biomass. When algae respire, it looses biomass and releases ammonia and phosphorus to the water column.

The model was expended to track the mass of pheophytin, which was measured in the recent field program. It was assumed that algae die at a mortality rate to become pheophytin. In addition, algae also settled at a specified velocity. Once settled, the mass is converted to volatile solid in the sediment. The model does not include the grazing of algae by zooplankton or benthic animals at the present time.

Sediment Transport

In the earlier version of San Joaquin River DO model, SOD was treated as a lump parameter that included the error term for unaccounted for local nonpoint source loads. In the CALFED 2000 grant, Dr. Gary Litton would measure the flux of sedimentation and BOD of the sediment samples and re-suspended particles. The program was modified to track the sediment fluxes for a better match of model prediction and field data. By separating the SOD to their components, the original value of SOD was reduced to a smaller number.

The equations for scouring, deposition, and transport of sediment have previously been incorporated into the model version, used to evaluate the transport and fate of copper discharged to San Francisco Bay (Chen, Leva, and Oliveri 1996). These equations are derived after a careful reviews of literature contained in ANSWERS (Beasely and Higgins 1991) and Graf (1971).

The model tracks five settleable groups of particles: chlorophyll-a, pheophytin, detritus, inorganic solids, and sand. Chlorophyll-a is live algae; pheophytin is dead algae; detritus is land derived organic matter; and inorganic solid is fine silt or clay. Each group will settle to the bottom according to their settling velocities. The model assumes that settled algae become pheophytin. For that reason, the model accumulates only four groups of sediment: pheophytin, detritus, inorganic solid, and sand.

The settled materials may be scoured from the bottom to become suspended particles again. Scouring is assumed to occur when the flow velocity exceeds a critical value:

$$V_{CR} = \sqrt{25 * 0.65 g d^{0.8} D^{0.2}} \qquad \text{(II-15)}$$

where V_{CR} = critical velocity (Graf 1971); g = acceleration due to gravity (9.81 m/s^2); d = particle diameter; and D = water depth. The rate of scouring is:

$$S = KA_W (V_{AVE} - V_{CR})^b \qquad \text{(II-16)}$$

where S = scouring rate in kg/s; K = a calibration parameter; A_W = area of the wetted channel bed; V_{AVE} = average flow velocity in m/s; V_{CR} = critical velocity; b = a calibration parameter.

The re-suspended are added to their respective pools in the water column and are subjected to transport, dispersion and settling again.

The heavier sand is subjected to the bed load transport, which is different from other suspended particles. The bed load transport capacity is a function of the shear velocity, shear stress, Reynolds Number, and critical shear stress:

$$V^* = \sqrt{gDS} \qquad \text{(II-17)}$$

$$Y = \frac{V^{*2}}{(\gamma - 1) g d} \qquad \text{(II-18)}$$

$$NR = \frac{V^* d}{\nu} \qquad \text{(II-19)}$$

$$Y_{CR} = f(N_R) \qquad \text{(II-20)}$$

where V* = shear velocity in m/s; g = acceleration due to gravity; D = hydraulic radius (water depth) in m; Y = shear stress; γ = specific gravity of the soil particles; d = diameter of soil particles in m, N_R = Reynolds Number; ν = kinematic viscosity of water in m^2/s; and Y_{CR} = critical shear stress, taken from Shield Diagram (Graf 1971).

The Yalin equation is used to calculate bed load transport capacity of sand:

$$T_f = P_S \gamma \rho_w dV * W \quad \text{(II-21)}$$

$$P_S = 0.635\Delta[1 - \frac{\ln(1+\Sigma)}{\Sigma}] \quad \text{(II-22)}$$

$$\Delta = \frac{Y}{Y_{CR}} - 1 \quad \text{(II-23)}$$

$$\Sigma = 2.45\rho^{-0.4}\Delta\sqrt{Y_{CR}} \quad \text{(II-24)}$$

where ρ_w = density of water in kg/m3 and W = wetted perimeter of channel in m. The value of $\Delta = 0$ when Y is less than Y_{CR}.

The eroded sand in excess of T_f is immediately re-deposited to the riverbed. Only the excess remains in suspension, which occurs only at high Reynolds number.

Tidal Boundary

In earlier link-node model, tides at the boundary node were typically specified as a stationary wave that repeats its tidal stages every 24.5 hours. The concentration at the tidal boundary was specified as a constant.

For the Lower San Joaquin River DO model, the algorithm was changed to use real tides for continuous simulation throughout the year. The input data for the tidal boundary was also changed to a background concentration (Co) and an exchange coefficient, which can be measured by a tracer study. The model was modified to track the parcels of water that exit during the ebb and re-enter during the flood. The concept is depicted in Figure II-5.

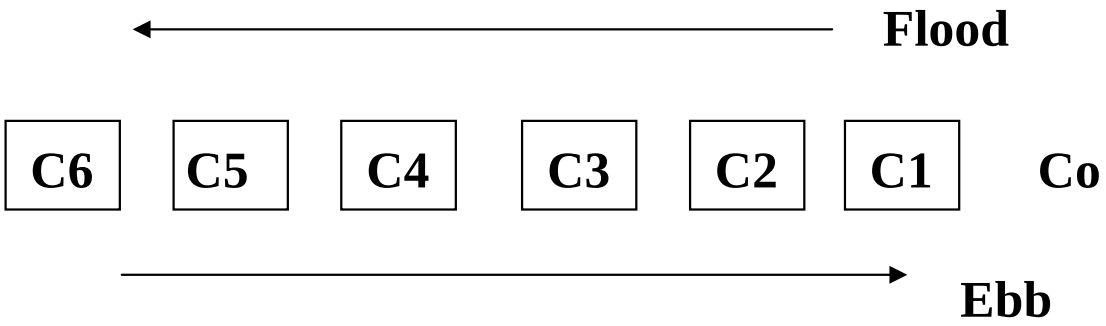

Figure II-5
Definition Sketch of Tidal Exchange Algorithm

The model tracks the parcels of water exiting the tidal boundary during the ebb tide. The first parcel (C1) exits in the first hour of ebb. The second parcel (C2) exits in the second hour. The last parcel of water is C6. During the flood tide, C6 re-enters first, then C5, C4 and so on. C1 will spend 6 hours outside of the model domain.

Each hour the parcel of water stays outside of the tidal boundary, the water in the parcel is assumed to exchange with the background water by the following equation:

$$C_i = C_{i+1}E + (1-E)C_o \qquad \text{(II-25)}$$

Computer Model

Flow Chart Diagram

The computer model was developed to simulate the hydrodynamics and water quality of Lower San Joaquin River according to the formulations outlined above. The model has two modules, hydrodynamics (H.D.) and water quality (W.Q), as shown in Figure II-6.

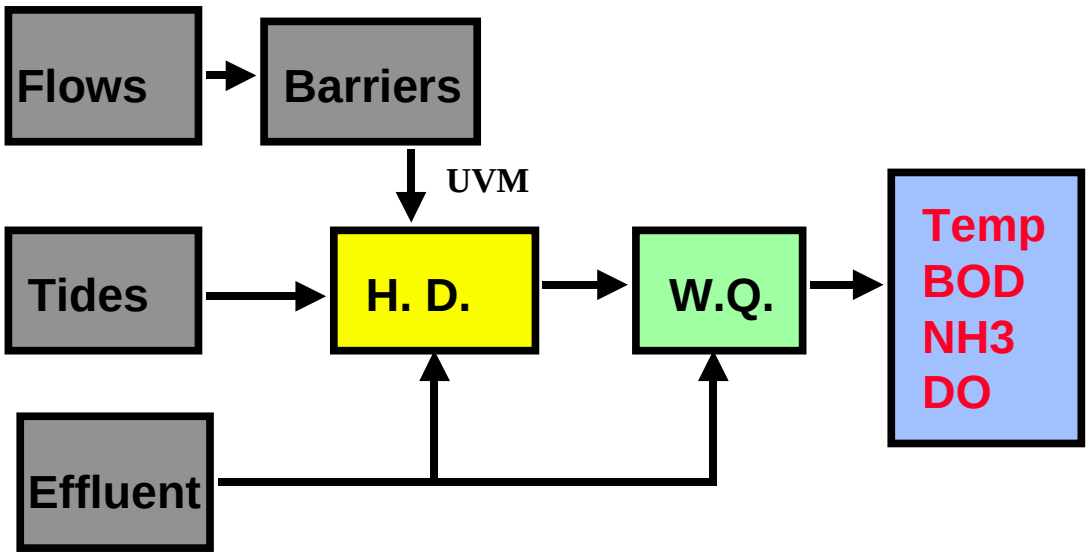

Figure II-6
Flow Chart of The Lower San Joaquin River DO Model

As shown in Figure II-6, the hydrodynamic module accepts its upstream flow at the head of Old River and real times for the downstream boundary. The daily effluent form Stockton Regional Wastewater Control Facility is discharged into appropriate node. The hydrodynamic module simulates flow and volume for the link-node system every 10 seconds Results are integrated to hourly values, which are then fed to the water quality

module. The water quality module simulates the temperature and concentrations of various constituents for all nodes and every hour throughout the simulation.

Input Data

The model requires the following input data:

Real tides at the downstream boundary
Tidal exchange and background concentration
River flow
Channel geometry
Meteorological data
Point source data
River load data
Model coefficients

The real tides were obtained from the tide tables published by the National Oceanic and Atmospheric Administration. We started with the Golden Gate tides and adjusted to Light 18 according to the adjustment factors provided in the tide tables.

The tidal exchange was assumed to be 3% for every hour outside of the tidal boundary. This amounts to a net exchange of approximately 10% over a tidal cycle. The background concentrations were estimated in part from the water quality data measured at station R8.

For the river flow, we previously used DWR empirical equations to calculate it as a function of Vernalis flow and Delta pumping. One equation is used when the temporary barrier at the head of Old River is up. Another equation is used when the barrier is removed. The method was found not accurate. In cooperation with USGS, an UVM gauging station was installed to measure the actual flow past Stockton. The model is now driven by the UVM flow.

The channel geometry was derived from a limited number of cross sections, provided by the Corps of Engineers. During the tracer study of 1992, we have measured some cross sections up and down the river near the Stockton outfall area. Some interpolations and extrapolations were made to obtain the channel geometry for the entire river domain.

The meteorological data was obtained for Lodi station, which is a cooperative station of agricultural communities. The data was downloaded from their web site CIMIS.

For the point source loads, the model used the daily flows and their pollutant concentrations discharged by Stockton Regional Wastewater Control Facility s. For the river loads, the flow was based on UVM and pollutant concentrations were estimated from the monitoring data of Mossdale station. The Mossdale data, however, is not as frequent, as the Stockton data. This may contribute errors to the model.

Model coefficients includes decay rate of BOD, ammonia, growth rate of algae etc. Table II-1 presents the model coefficients for parameters affecting dissolved oxygen. These rate coefficients must be adjusted to the prevailing temperature. The EPA recommended temperature coefficients are shown in Table II-2.

Table II-1
Model Coefficients for Parameters Affecting Dissolved Oxygen

Parameter	Unit	Value
BOD5 Decay Coefficient	per day	0.10
Ultimate BOD/BOD5	mg/mg	2.54
Ammonia decay coefficient	per day	0.05
DO/ammonia ratio	mg/mg	4.57
Detritus decay	per day	0.01
DO/Detritus ratio	mg/mg	1.6
N/Detritus	mg/mg	0.08
P/Detritus	mg/mg	0.012
Algae		
maximum growth rate	per day	1.80
half saturation constant of light	cal/m2/sec	4.3
half saturation constant of P	mg/l	0.003
half saturation constant of N	mg/l	0.1
Algae respiration rate	per day	0.25
Algae settling rate	m/day	0.15
DO/algae ratio	mg/mg	1.6
Chl a to pheophytin	per day	0.13
Pheophytin decay	per day	0.1

Table II-2
Theta Values for Temperature Correction

Process	EPA Recommended Theta Values
Nitrification	1.08
Aeration	1.024 (use 1.02)
BOD decay	1.04
SOD decay	1.04

Output Comparison

A deterministic model will accept the input data and perform simulations to make predictions. The basic predictions of the San Joaquin River DO model include the time series of tidal stage and volume for each node, flow for each link, and concentrations of various water quality constituents for each node. The model predictions can be compared to their corresponding measurements performed at comparable locations and times.

The basic model predictions can be used to plot time series of parameter values with time at a given location. They can also be plotted as concentration profiles with distance at a given time. They can also be transformed into the frequency distribution of predictions made for a given location.

In addition, the model was made to output various fluxes that caused the dynamic changes of variables. Some of these fluxes can be compared to the fluxes that have been measured in the field by Dr. Peggy Lehman of DWR and Dr. Gary Litton of UOP.

Peer Review

The San Joaquin River DO model has been subjected to two peer reviews: one by the EPA and the other by CALFED. Written responses to each review have been submitted.

The EPA reviewers found no major problem with the model formulation. However, they suggested that the model output be changed to hourly and the frequency distribution be used to compare model results to observed data. They also found that the theta (θ) values for temperature correction should be higher. Those suggestions were incorporated into the San Joaquin River DO model.

The CALFED reviewers raised concerned about whether a vertically stratified (2D vertical) model is needed and whether the data is available to support such model development. The reviewers urged us to consider non-vertically mixed factors such as light, surface aeration, sediment oxygen demand, and others that might affect dissolved oxygen balances. One of the reviewers worried about the use of anti-numerical dispersion term and suggested us to switch to DWR DSM2 model, which is a Lagrangian model without numerical dispersion problem.

To the extent possible, we have considered the suggestion made by CALFED reviewers. We placed a large emphasis on the effect of light, surface aeration, sediment oxygen demand on the surface and bottom DO. The change of model to 3D, 2D vertical or DSM2 is beyond the scope of work. The 3D and 2D models will require detailed data (wind, channel morphology, boundary condition, vertical water quality profiles), which is not available to our knowledge. Whether the new models can provide better predictions remains to be proven by more research. We believe that the link-node model with proper calibration can provide adequate information for TMDL decisions now. After the TMDL implementation, new data can be collected to verify and further improve the model.

III. Model Calibration

Introduction

As discussed earlier in this report, the Lower San Joaquin River DO model has been calibrated with 1991, 1993, and 1996 data. With the CALFED 2000 grant, the model parameters were expanded to include VSS, TSS, and pheophytin. Algorithms were added to simulate the settling of suspended particles, the scouring of sediment from bottom, and their effects on SOD. The model was also enhanced to simulate the growth of flagellate algae that stays in the upper layer of Turning Basin.

For the calibration of the enhanced model, the CALFED 2000 grant also collected a dataset from July to October 2000. The DO Steering Committee also sponsored the collection of a dataset from July to September 1999.

It is important to clarify what we mean by model calibration. The model is driven by the boundary conditions and a set of model coefficients. For each year of simulation, we prepare the year specific data of river flow, meteorology, tide, Stockton discharge and upstream water quality concentrations. With the year specific data and model coefficients, the model simulates the dynamic variations of flow and water quality (parameters) at various nodes of the San Joaquin River. The model predictions are compared to the observed values in time series and concentration profiles. If the match for a specific parameter (e.g. flow) is not close, we identify the model coefficient (e.g. friction coefficient) that has an influence on the predicted values. The said coefficient is adjusted to improve the match. By this procedure, we developed a set of calibrated coefficients for all parameters, which will be used for all years of simulation.

After the completion of modeling project, additional water quality data was collected in 2001 with CALFED 2001 grant. There was a desire to run the model for the 2001 condition. CALFED approved a redirection of some 2001 funding to modeling. Under a subcontract from Jones and Stokes, we ran the model for the 2001 condition. The results were presented at the end of this chapter.

1999 Simulation

Solar Radiation

The meteorological data of Lodi station was used to drive the model. The model used the daily meteorology data to calculate short wave radiation for heat budget and algal growth simulation. Short wave radiation has also been measured directly at the Lodi station.

Figure III-1 compares the measured solar radiation against the theoretical values calculated by the model. They match very well. The noon radiation decreased from 0.24 kcal/m^2/sec in July 1, 1999 to 0.15 kcal/m^2/sec in October 31, 1999.

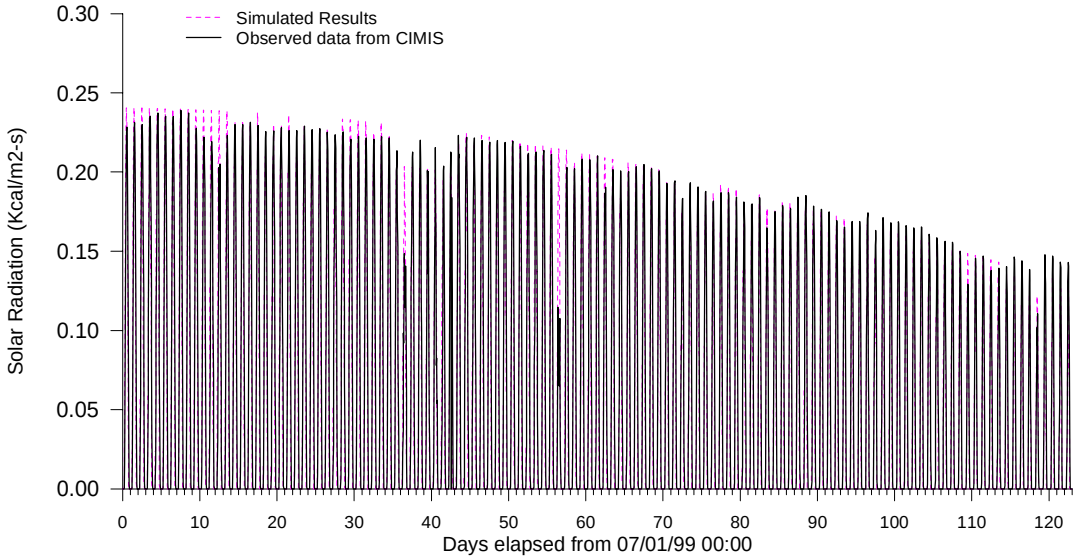

Figure III-1
Measured vs. Simulated Short Wave Radiations

River Flow

Figure III-2 presents the UVM flow for the sampling period of 1999. The river flow fluctuated between 750 to 1250 cfs in most of the summer. In approximately 10 days of late September, the flow dropped below 250 cfs. The flow went back to 500-600 cfs range in October.

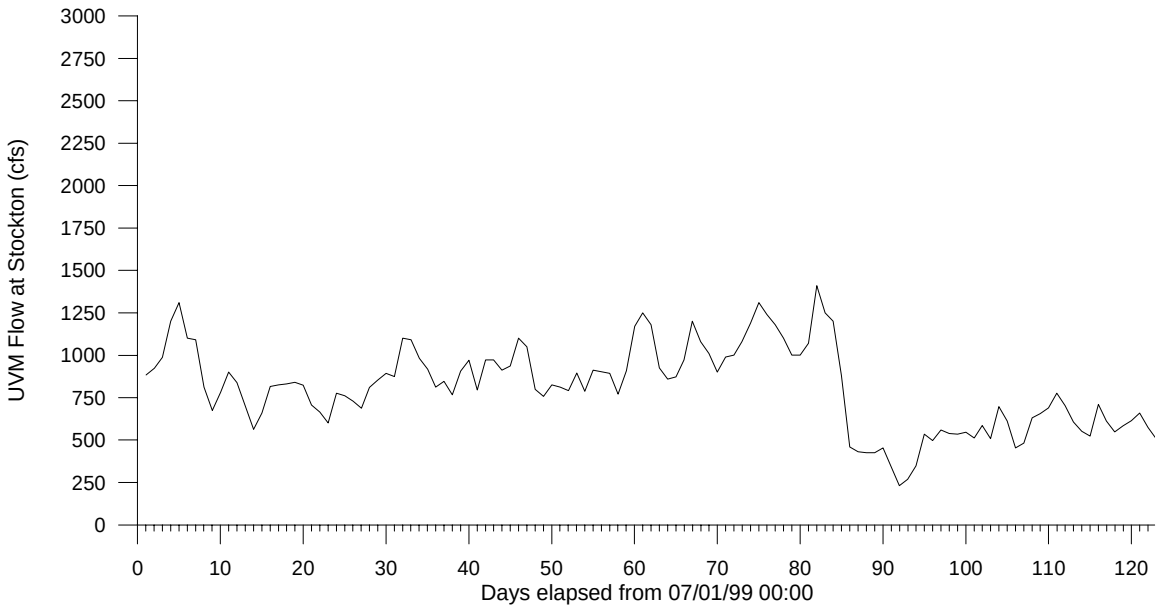

Figure III-2
UVM Flow, July to October 1999

The drop of flow near the end of September could be caused by a combination of factors. The Sacramento River flow, delta export pumping, the removal of Grant Line barrier and the operation of the Delta Cross Channel could be such that the water level in the Delta was lowered and more San Joaquin River flow was diverted to the Old River. Regardless of reasons, the UVM data was used to drive the model.

Stockton Discharge

Figure III-3 presents the daily discharge of treated effluent from Stockton Regional Wastewater Control Facility (RWCF). The maximum discharge was 70 cfs (45 MGD). The discharge was zero on some weekends.

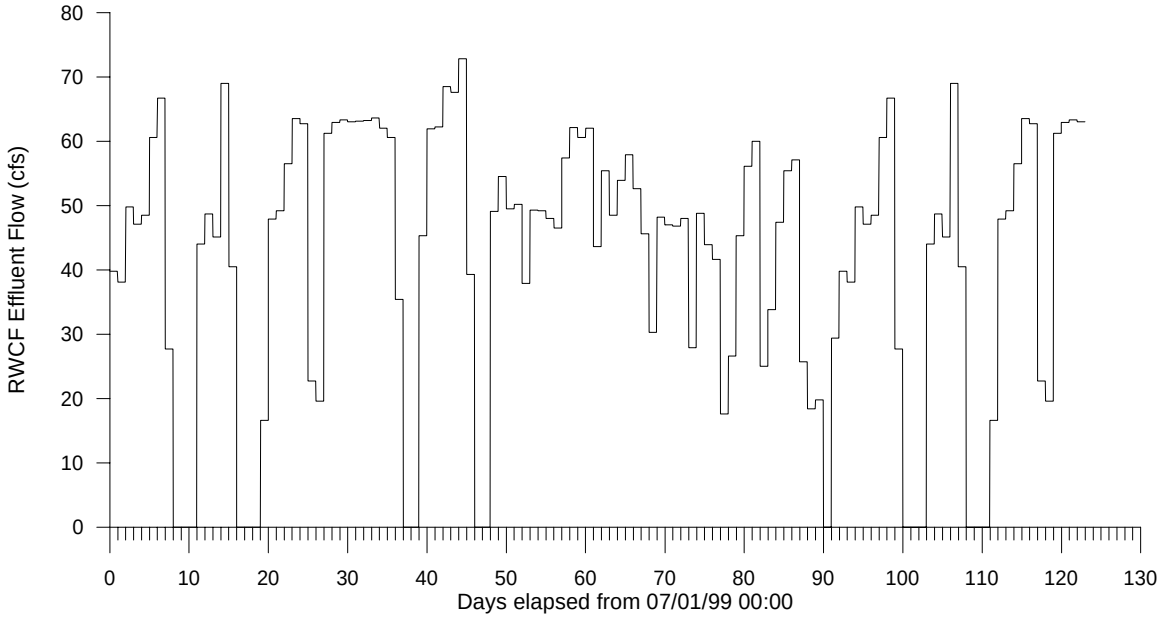

Figure III-3
Daily discharge from Stockton Regional Wastewater Control Facility

Pollution Loads

There are two major sources of pollution loads: the river load from the upstream and the point source load from Stockton RWCF. The pollution loads are specified by discharge flows and pollutant concentrations.

The Stockton RWCF provided the daily concentrations of pollutants contained in the treated effluent. For some parameters like VSS, no daily values were available. Interpolation was made to derive the daily values. The daily flows and their pollutant concentrations are inputted to the model.

For the river load, the flow was continuous measurement, but water quality data was collected infrequently. Interpolation was made to derive the daily values for input to the model

Average loadings were calculated for comparative analyses. Table III-1 shows the river load and Stockton load for the 1999 sampling period. On the average, the river received 6 times more CBOD5, 14 times more VSS, and 16 times more chlorophyll a (algae) from river load than from Stockton discharge. For ammonia, however, Stockton discharged 3 times more than the river load during the year 1999 sampling period.

Table III-1
Pollution Loads for the 1999 Sampling Period

Items	CBOD5	NH3-N	VSS	Chl-a
River load at Mossdale, kg/d	2,929	315	16,439	52
Stockton load average, kg/d	470	929	1,144	3.2
River load at Mossdale, lb/d	6,444	693	36,166	114
Stockton load average, lb/d	1,034	2,044	2,517	7.0

Figure III-4 presents the ammonia concentration in the effluent of RWCF. The Stockton RWCF has algae ponds in its treatment system. From July 1 to early August, the algae ponds reduced ammonia concentration to below 1 mg/l. From mid August to end of October, the algae stopped photosynthesis to remove ammonia. The ammonia-nitrogen concentration rose steadily to 25 mg/l.

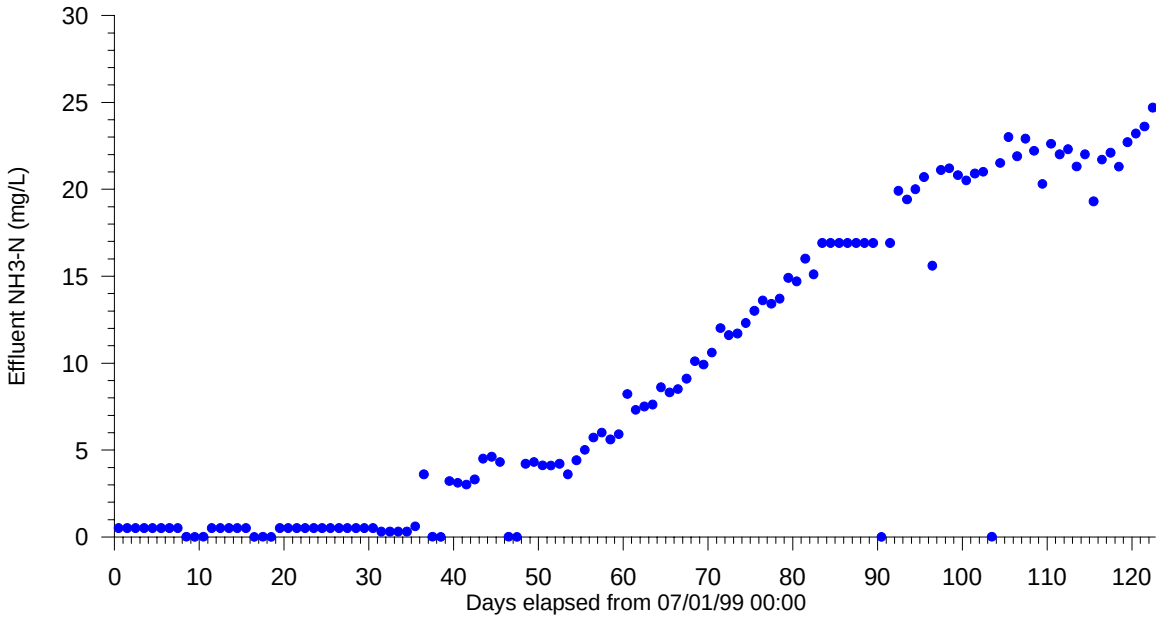

Figure III-4
Ammonia Concentration in the Effluent of Stockton RWCF.

Flow Simulation

The model predicted tidal stage and flow for various points of the river. Observed data was typically available only for tidal stage. So, previous model calibration could only compare the simulated and observed tidal stages.

From July to September 1999, Dr. Peggy Lehman of DWR measured flows at 3 sites 2 times with portable ADCP current meter. This afforded an opportunity to compare simulated flow to observed flow.

Site 1 is located near Light 45 or the mouth of Smith Canal. Site 2 is near Light 48, upstream of Channel Point. Site 3 is in the main channel upstream of the Turning Basin. The comparisons of simulated and observed velocity are shown in the following 6 figures. The model predictions matched the observed very reasonably.

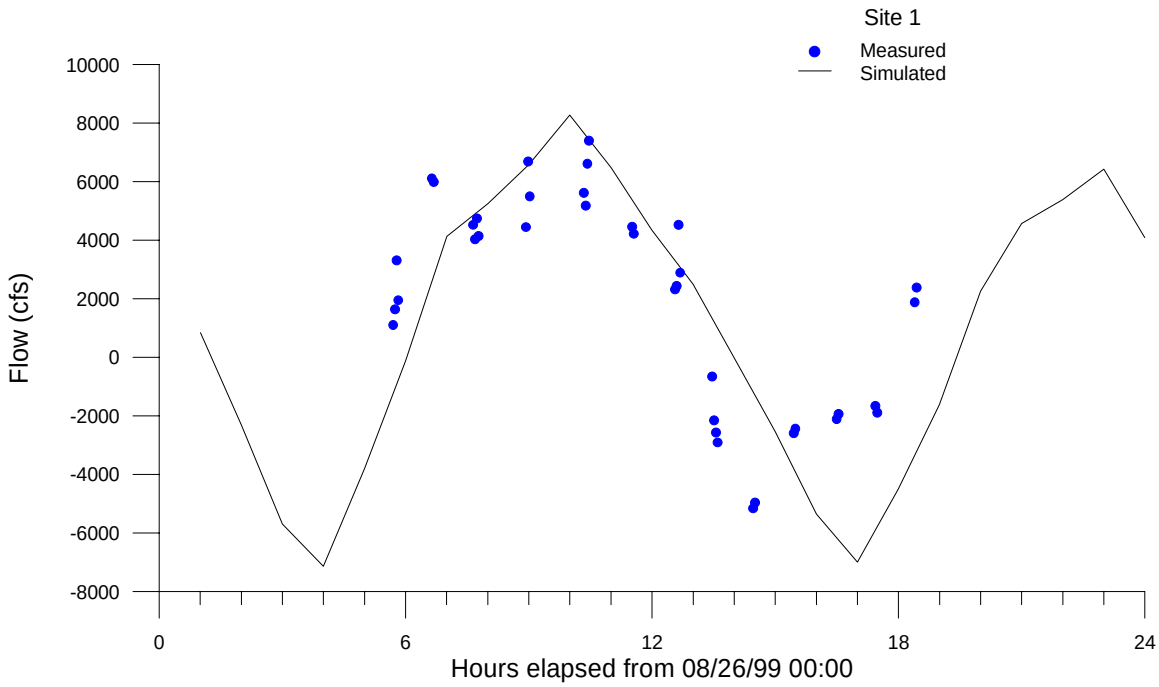

Figure III-5
Simulated vs. Observed Flow at Site 1, on 8/26/99.

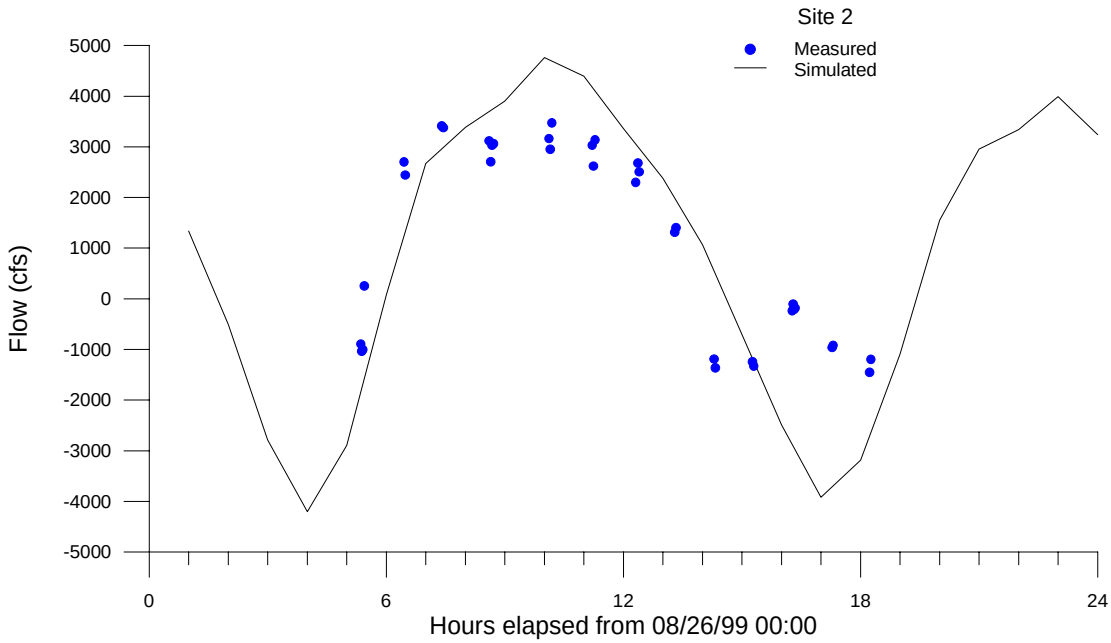

Figure III-6
Simulated Vs. Observed Flow at Site 2, on 08/26/99.

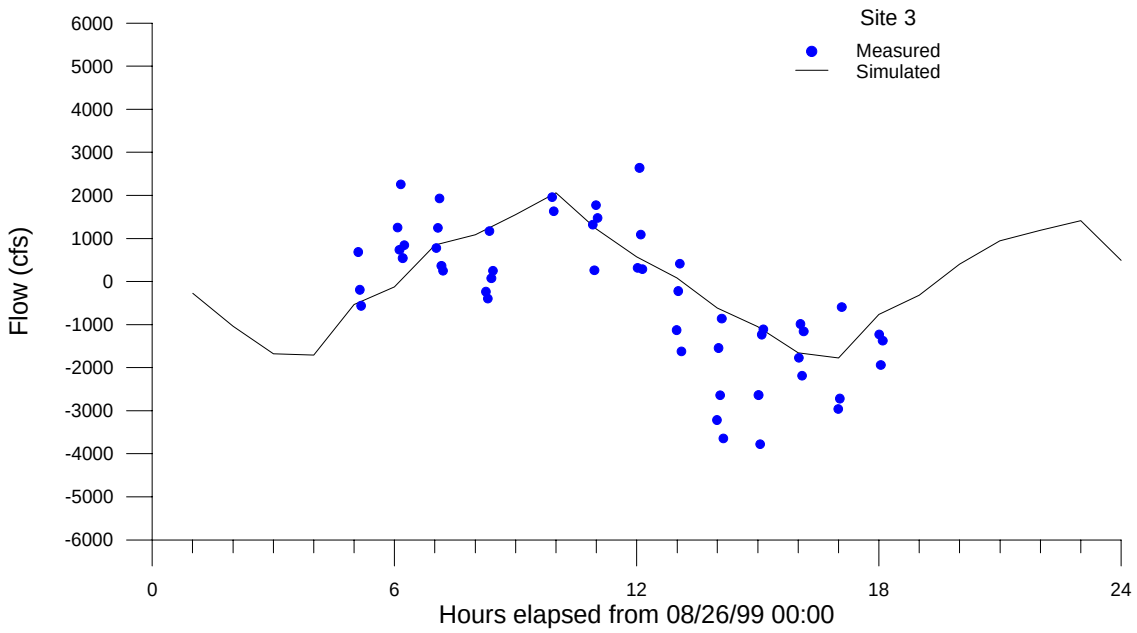

Figure III-7
Simulated Vs. Observed Flow at Site 3, on 08/26/99.

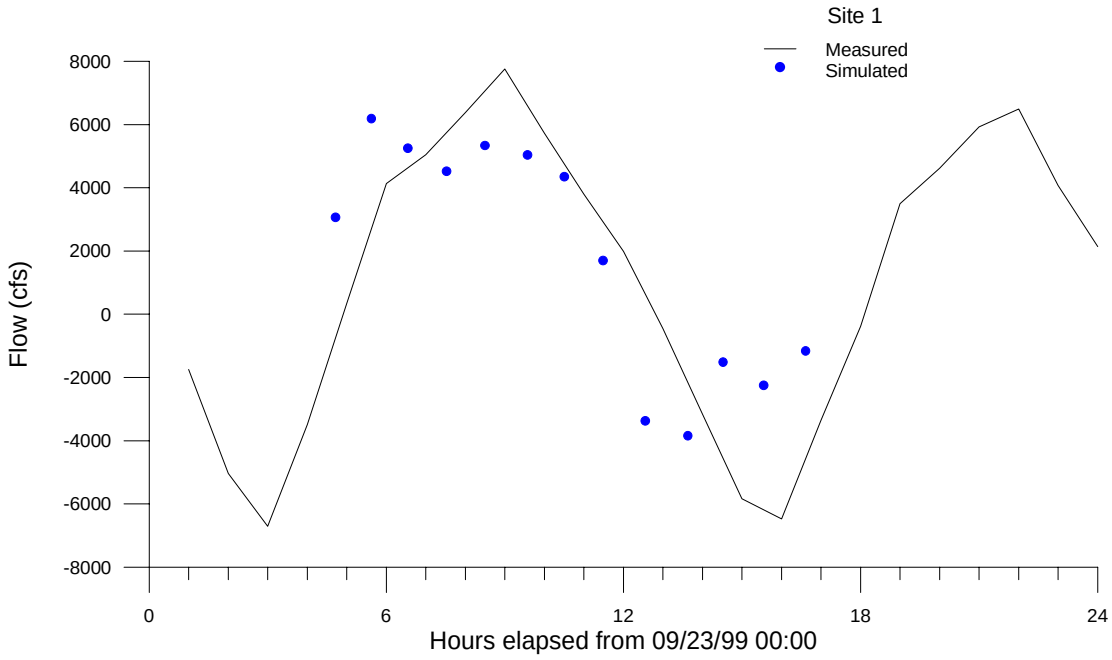

Figure III-8
Simulated Vs. Observed Flow at Site 1, on 09/23/99.

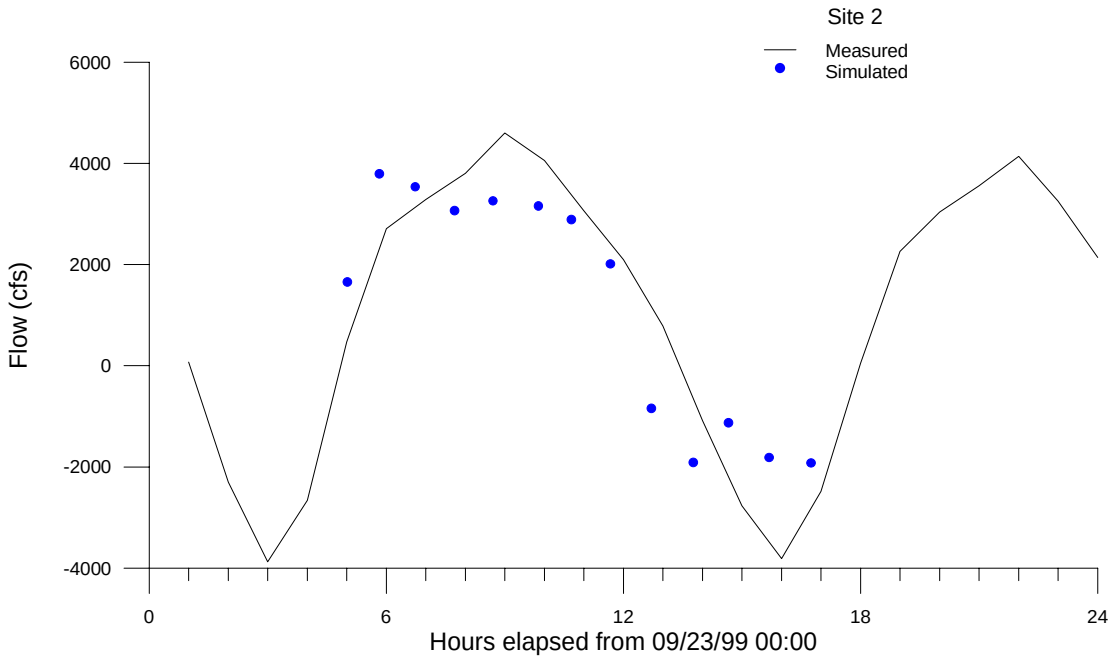

Figure III-9
Simulated Vs. Observed Flow at Site 2, on 09/23/99.

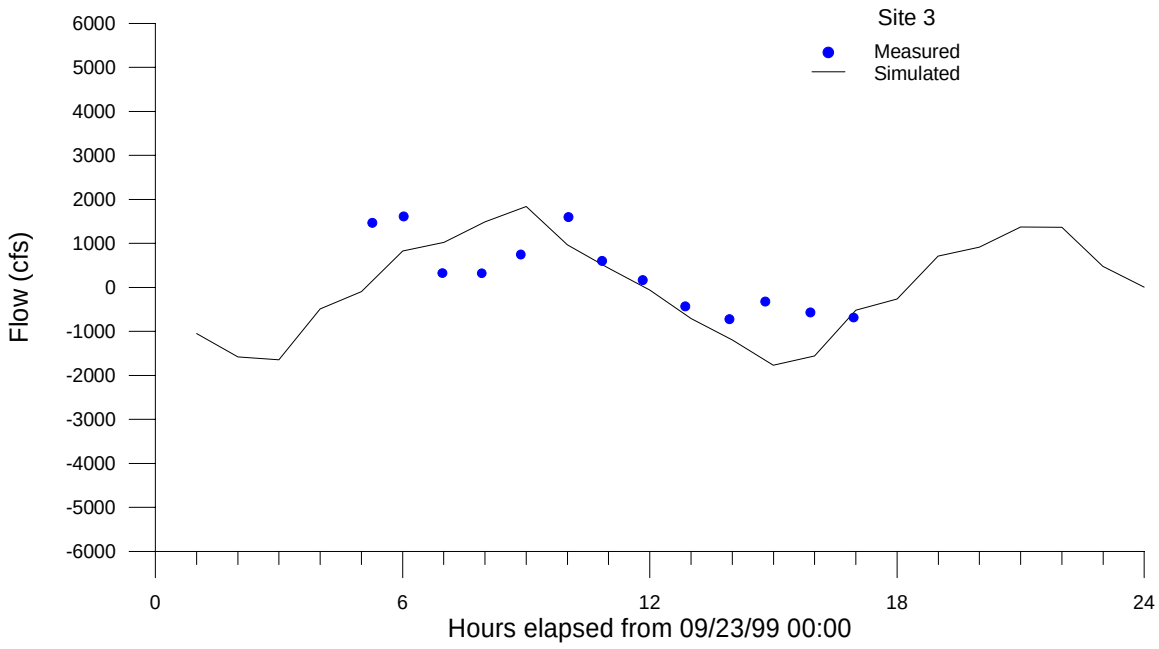

Figure III-10
Simulated Vs. Observed Flow at Site 3, on 09/23/99.

Temperature Simulation

Time series plots were made to compare simulated and observed temperatures for various monitoring stations. Figures III-11 and 12 are representative plots for station R3 and R4, both in the Stockton Deep Water Ship Channel. The model simulated the decreasing trend of temperature from August to October as the weather changed from summer to fall.

Figure III-13 compares the simulated and observed temperature profile for August 31, 1999. The model has followed the spatial variation of temperature from the head of Old River (ROA) to Deep Water Ship Channel (R8).

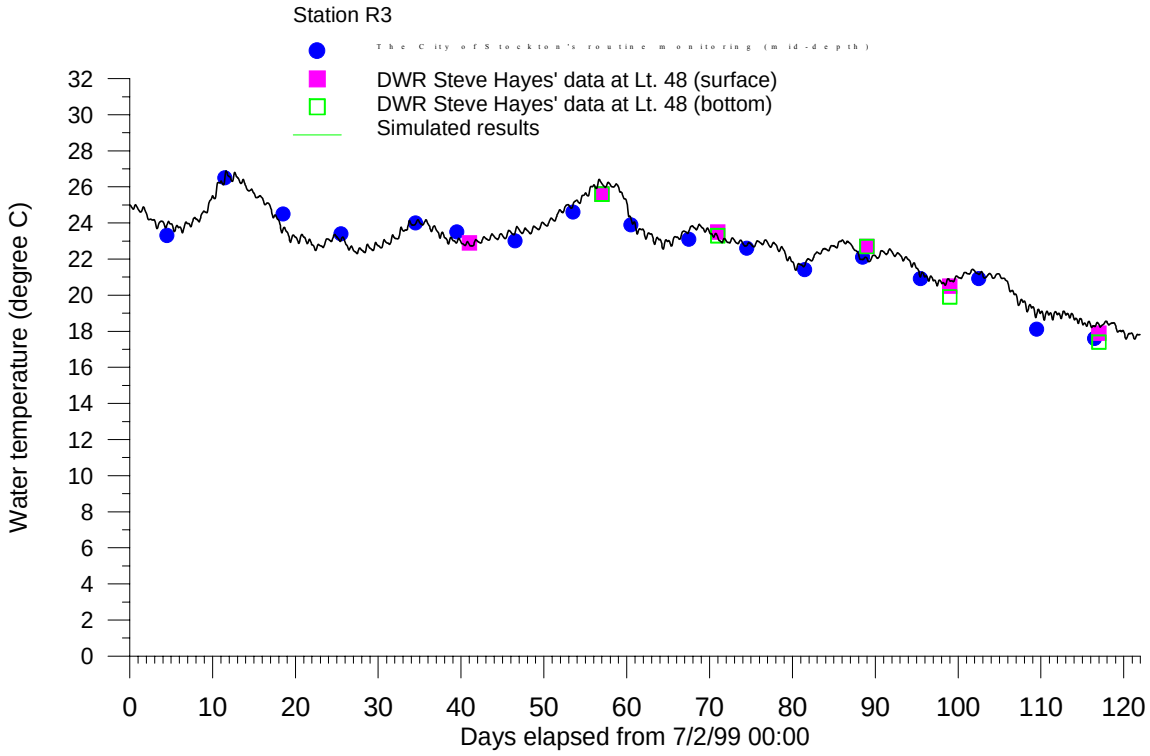

Figure III-11
Simulated and Observed Temperatures at Station R3, 1999.

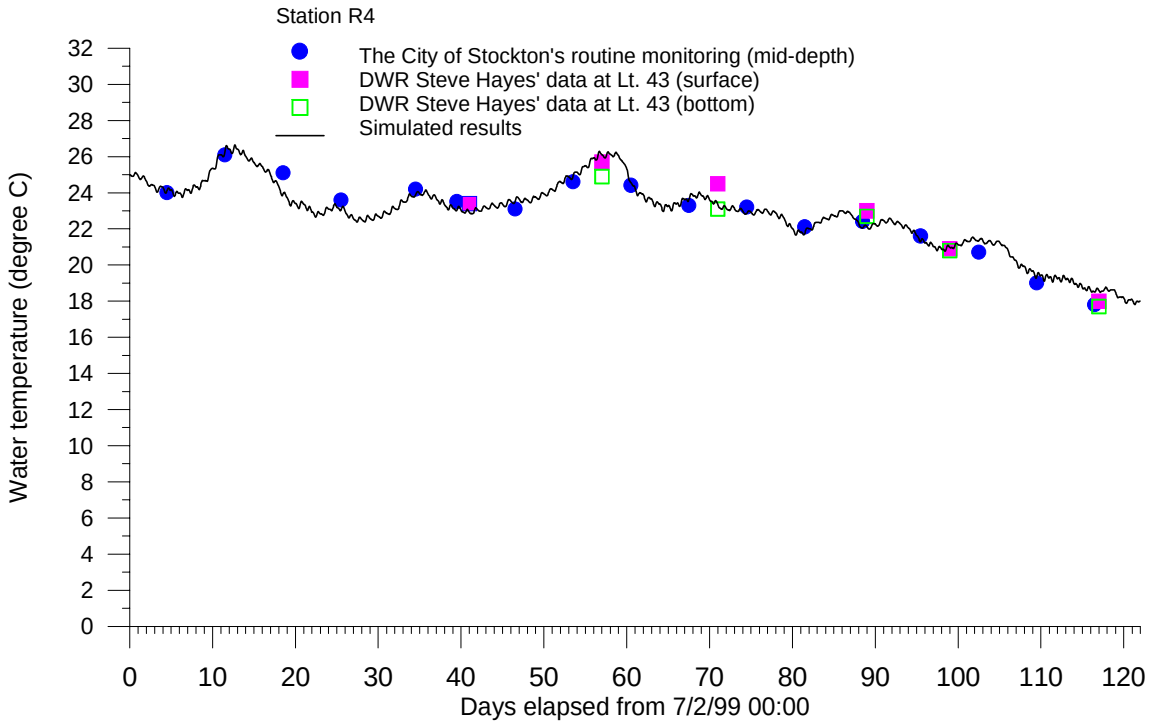

Figure III-12
Simulated and Observed Temperatures at Station R4, 1999.

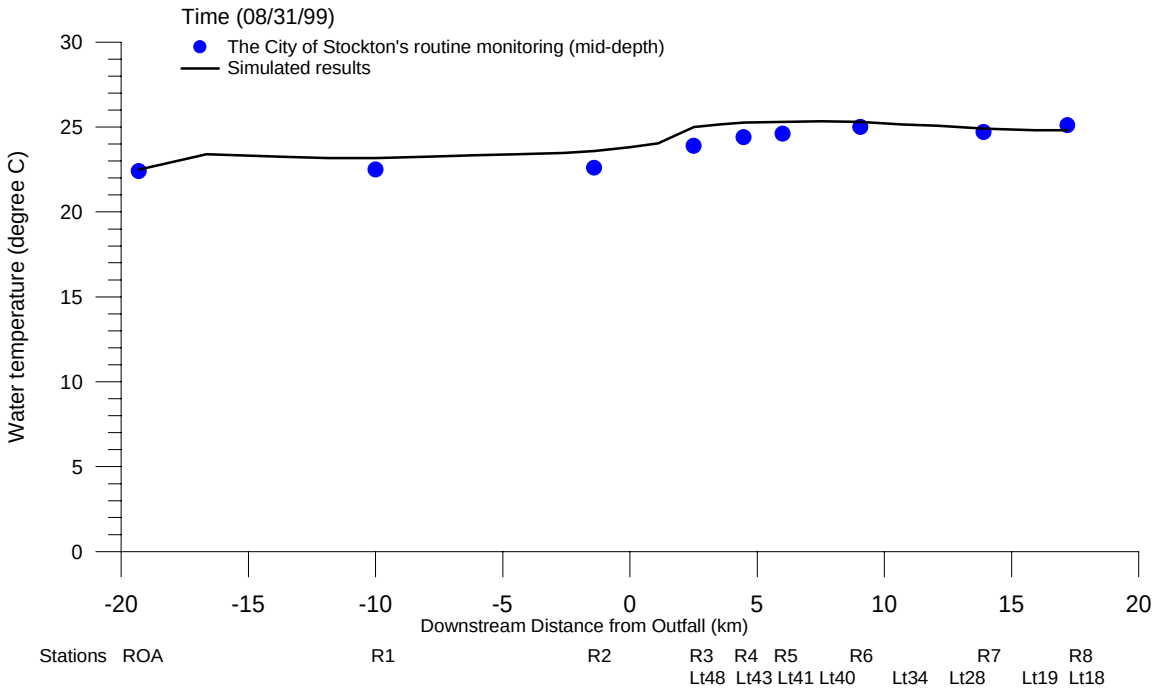

Figure III-13
Simulated and Observed Temperature Profile for August 31, 1999.

Dissolved Oxygen Simulation

Figures III-14, III-15 and III-16 compare the simulated and observed dissolved oxygen for station R3, R4 and R5, respectively. The plots indicate that the model follows the general time trend of DO variations. However, the model did not track the episodic DO drops, which occurred once in mid July and once in late August of 1999. Those events were triggered by boundary conditions that were not reflected in the model input.

Figure III-17 compares the simulated and observed concentration profile of DO for August 31, 1999. The model appears to have simulated correctly that the DO depression occurred mostly in the Deep Water Ship Channel (stations R3 to R6). The DO dropped below 5 mg/l in many stations within the Deep Water Ship Channel in the 1999 sampling period.

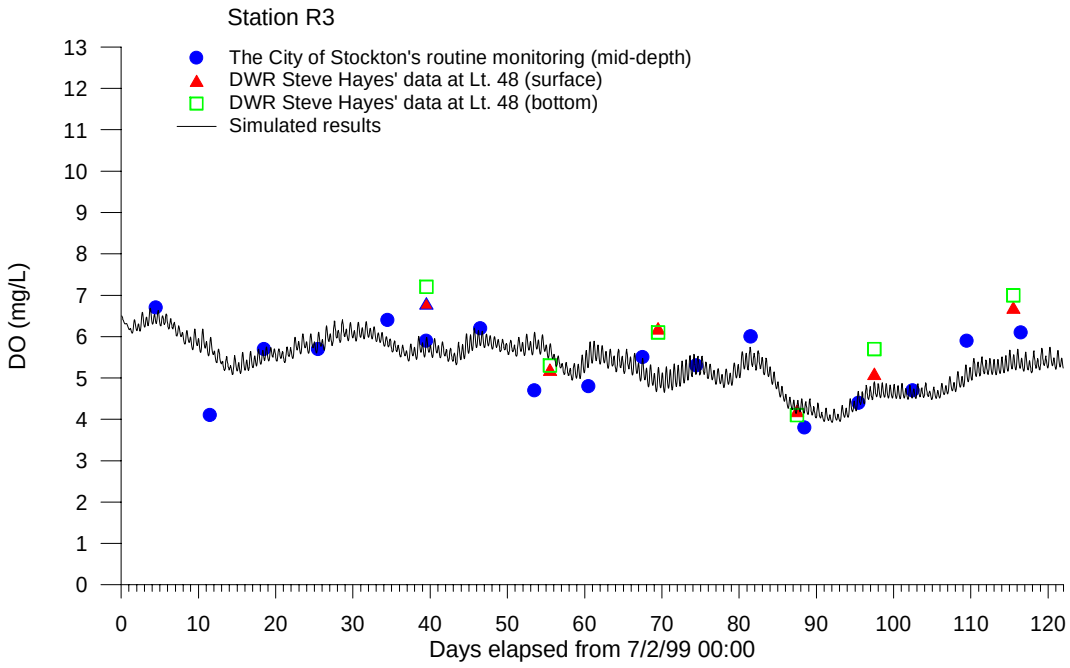

Figure III-14
Simulated and Observed DO at Station R3, 1999.

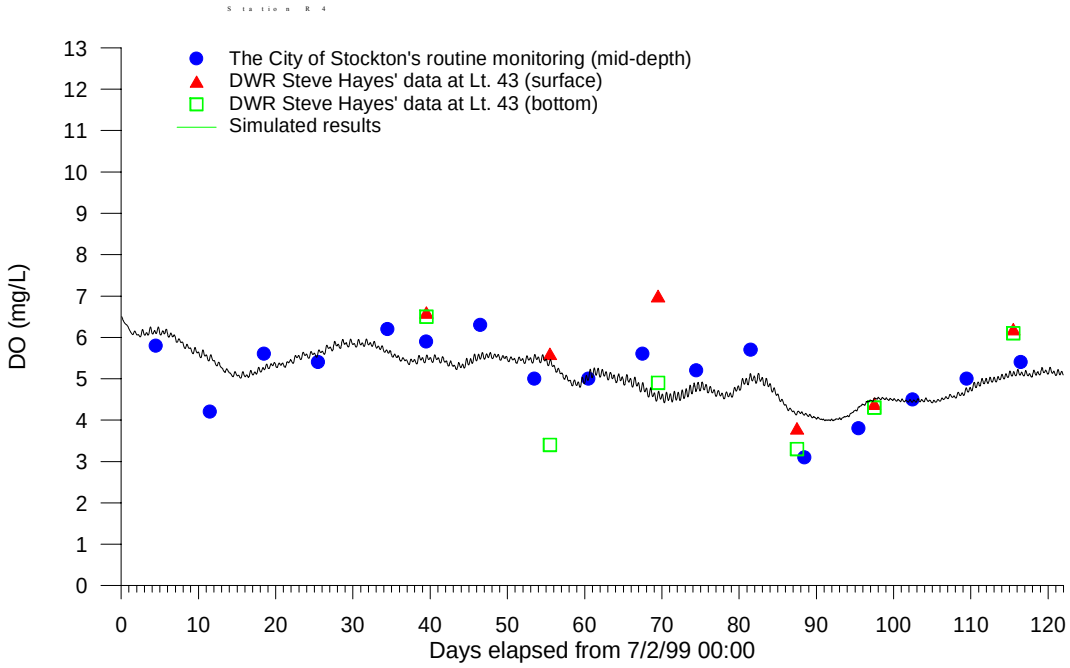

Figure III-15
Simulated and Observed DO at Station R4, 1999.

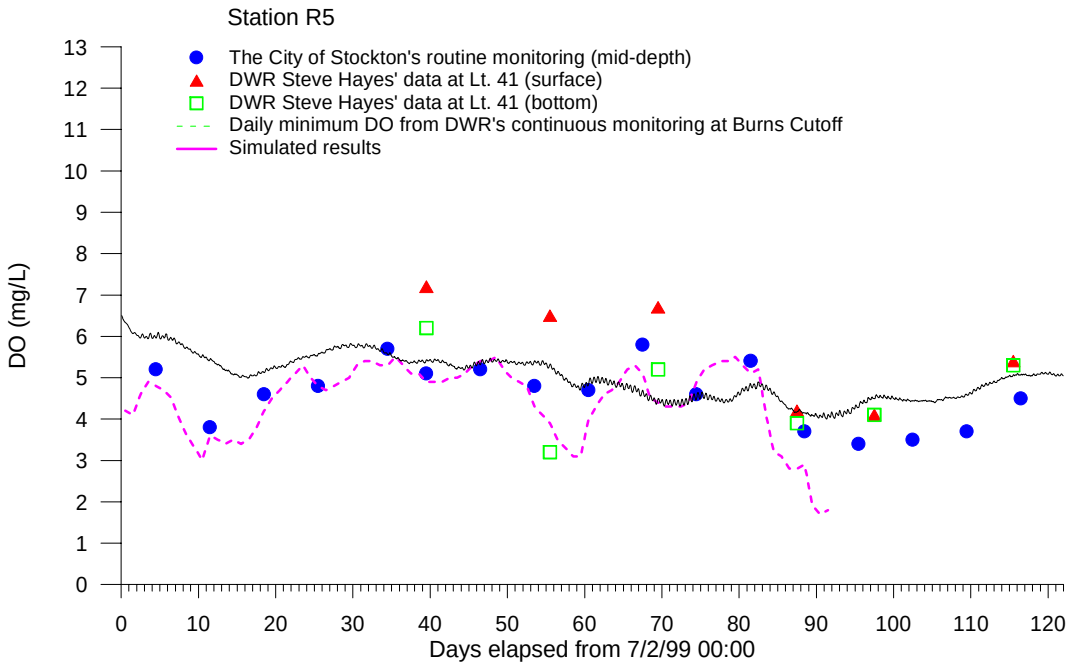

Figure III-16
Simulated and Observed DO at Station R5, 1999.

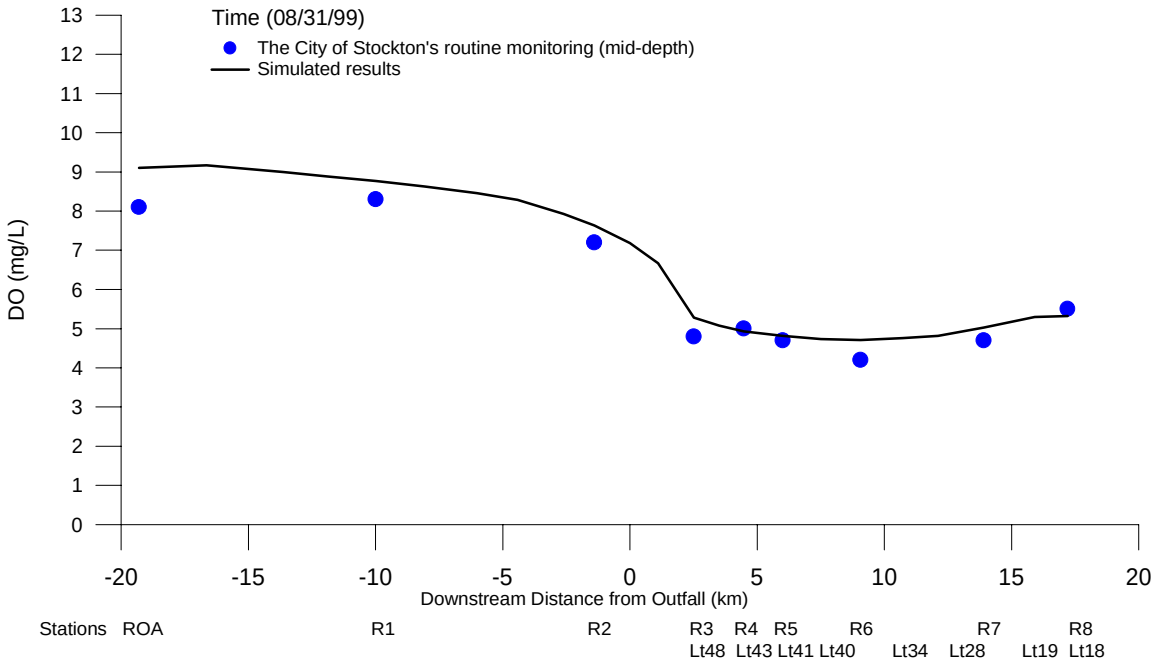

Figure III-17
Simulated and Observed DO Profile for August 31, 1999

Algae Simulation

Figures III-18 and III-19 compare the simulated and observed chlorophyll-a concentrations for stations R3 and R4. The model simulates a decreasing time trend of chlorophyll-a concentrations from August (20 µg/l) to October (5 µg/l) for station R3. This is probably caused by the seasonal decrease of solar radiation from summer to fall (Figure III-1).

DWR Peggy Lehman's data consistently shows that the surface chlorophyll was higher than the bottom chlorophyll. The City of Stockton data, on the other hand, consistently showed higher chlorophyll for the bottom samples in the Deep Water Ship Channel. The chlorophyll data from different sources have wide variations. The model predictions appear to go through the middle of the variations.

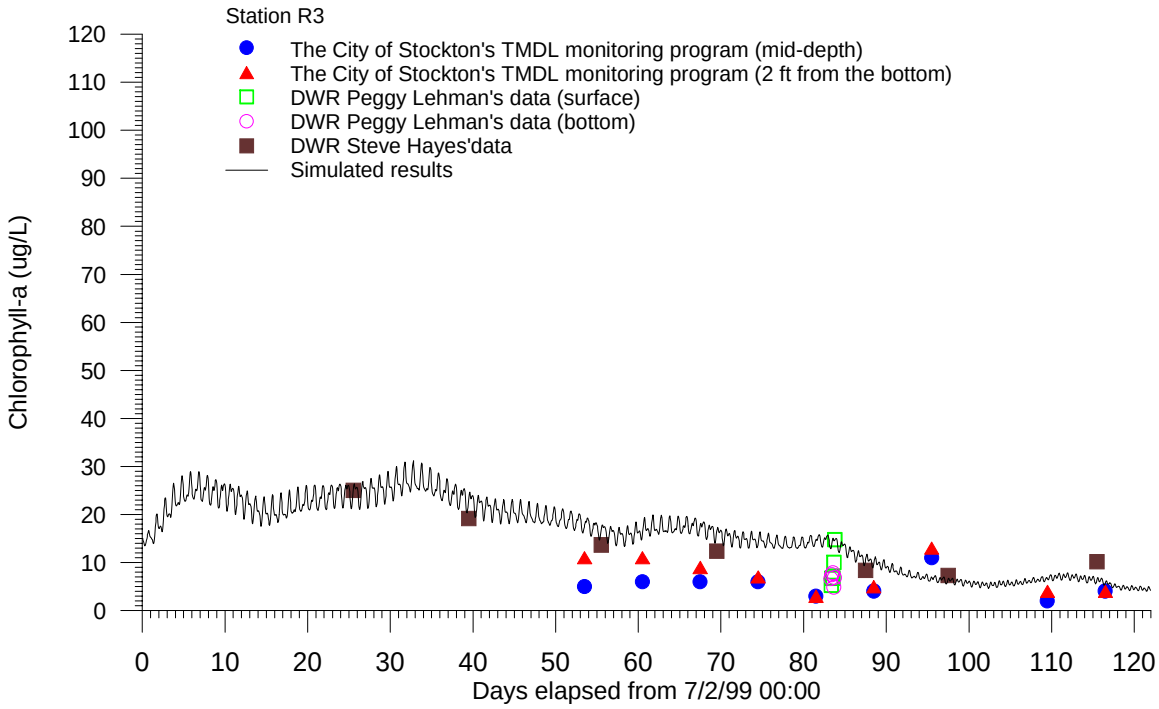

Figure III-18
Simulated and Observed Chlorophyll-a for Station R3, 1999

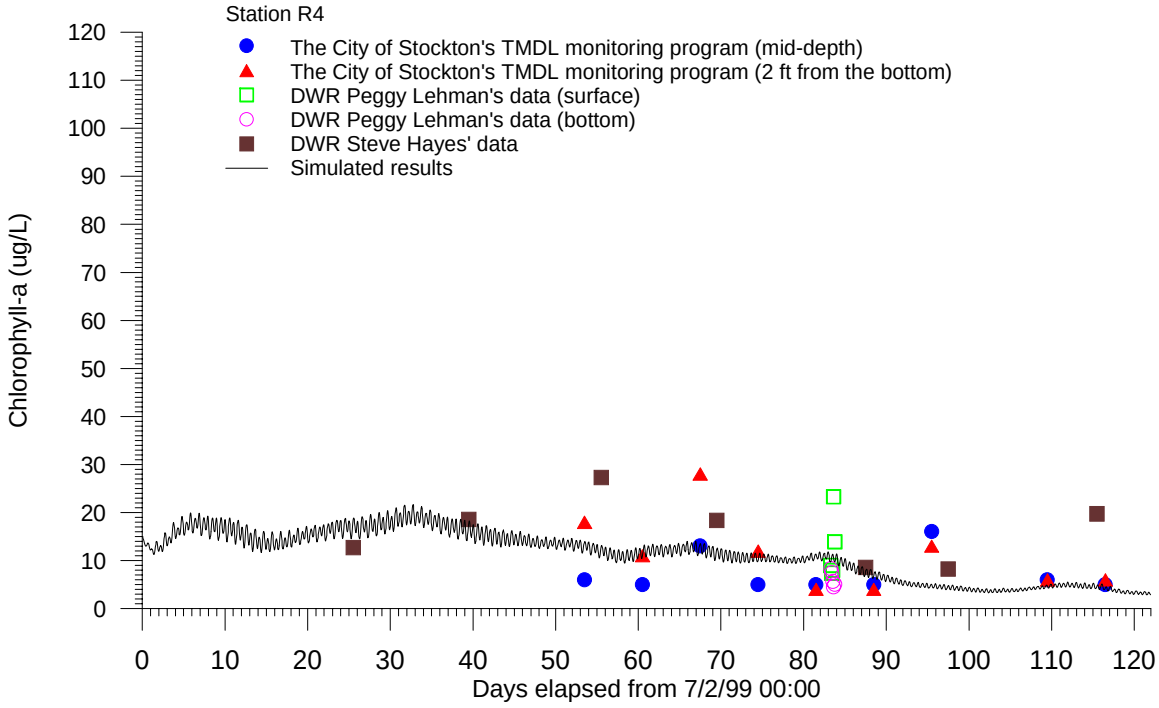

Figure III-19
Simulated and Observed Chlorophyll-a for Station R4, 1999.

Figure III-20 presents the concentration profiles of algae along the San Joaquin River for August 31, 1999. The model simulates a decreasing trend of chlorophyll from ROA (20 µg/l) to R5 (<5µg/l). This is because the water depth at ROA is relatively shallow. In shallow water, the light was not as limiting and photosynthesis was able to sustain a higher algal biomass. At the Deep Water Ship Channel, algae only grows on the top but is mixed to the entire depth, which results in a lower concentration.

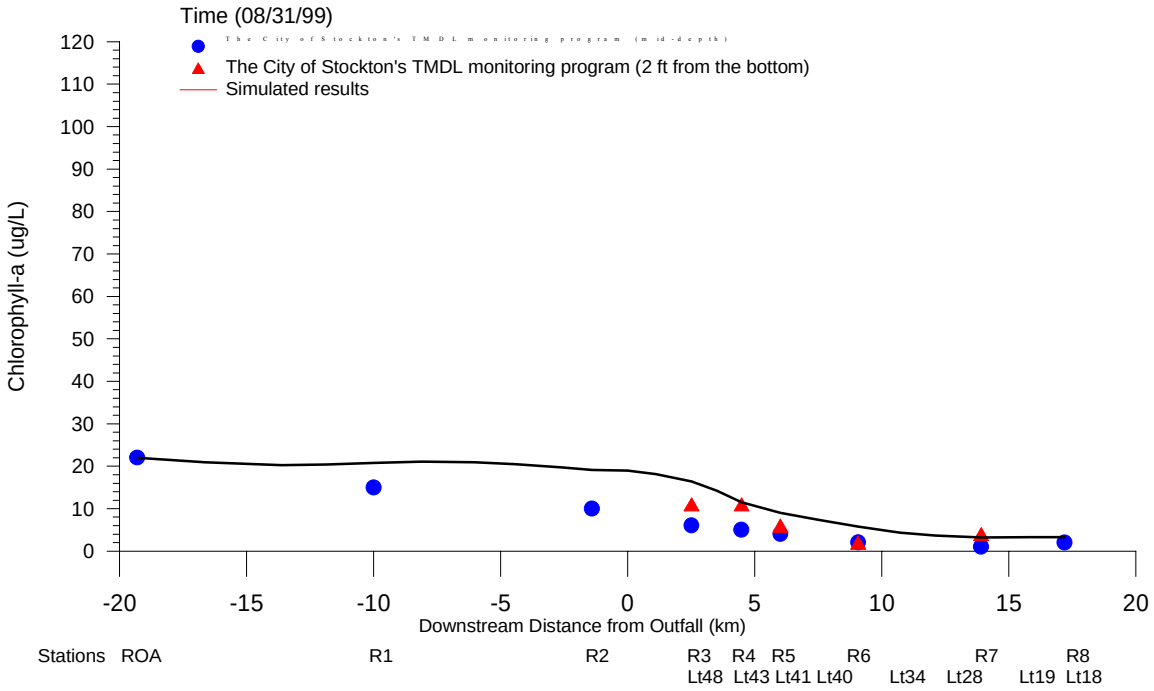

Figure III-20
Simulated and Observed Chlorophyll-a Profile for August 31, 1999

Pheophytin Simulation

Figure III-21 and III-22 compare the simulated and observed pheophytin for stations R3 and R4, respectively. The match is comparable to the result of chlorophyll simulation.

Based on model simulation and observed data, the pheophytin concentration was approximately the same as chlorophyll-a concentration at stations R3 and R4. Light limitation at the Deep Water Ship Channel not only caused algae to respire more than photosynthesis but also caused algae to die.

Figure III-23 compares the simulated and observed concentration profile of pheophytin from head of the Old River (ROA) to Deep Water Ship Channel for August 31, 1999. The match is reasonably good. The concentration profile is similar to that of chlorophyll-a.

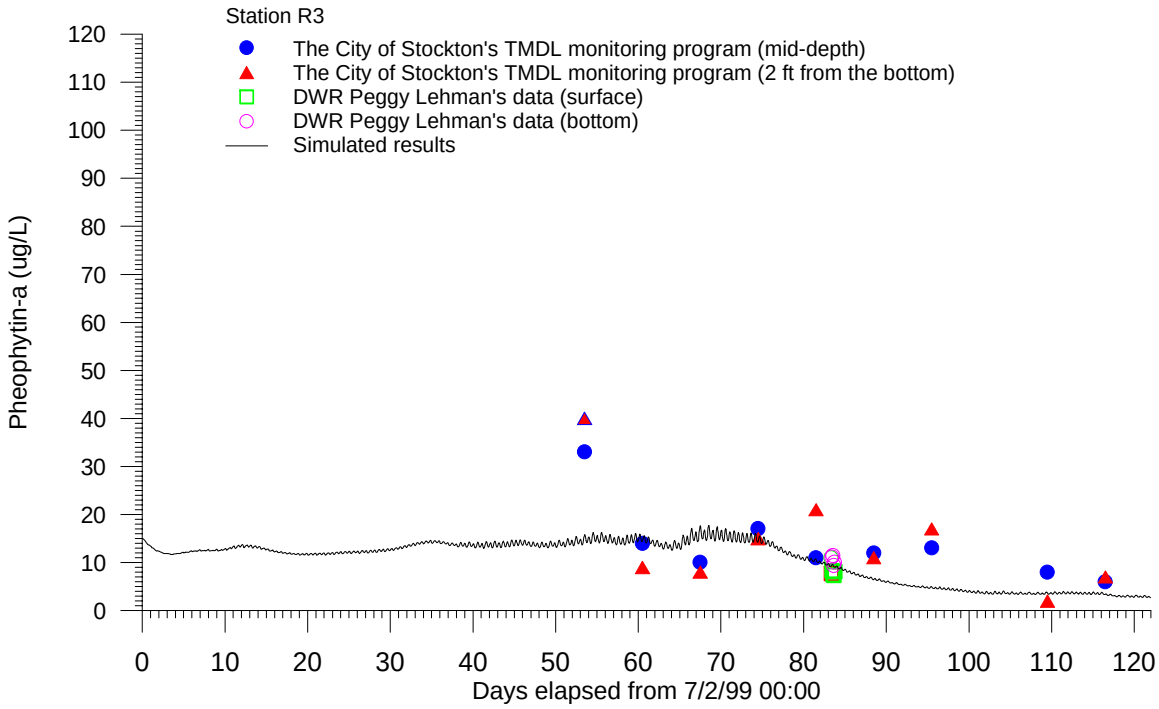

Figure III-21
Simulated and Observed Pheophytin for Station R3, 1999.

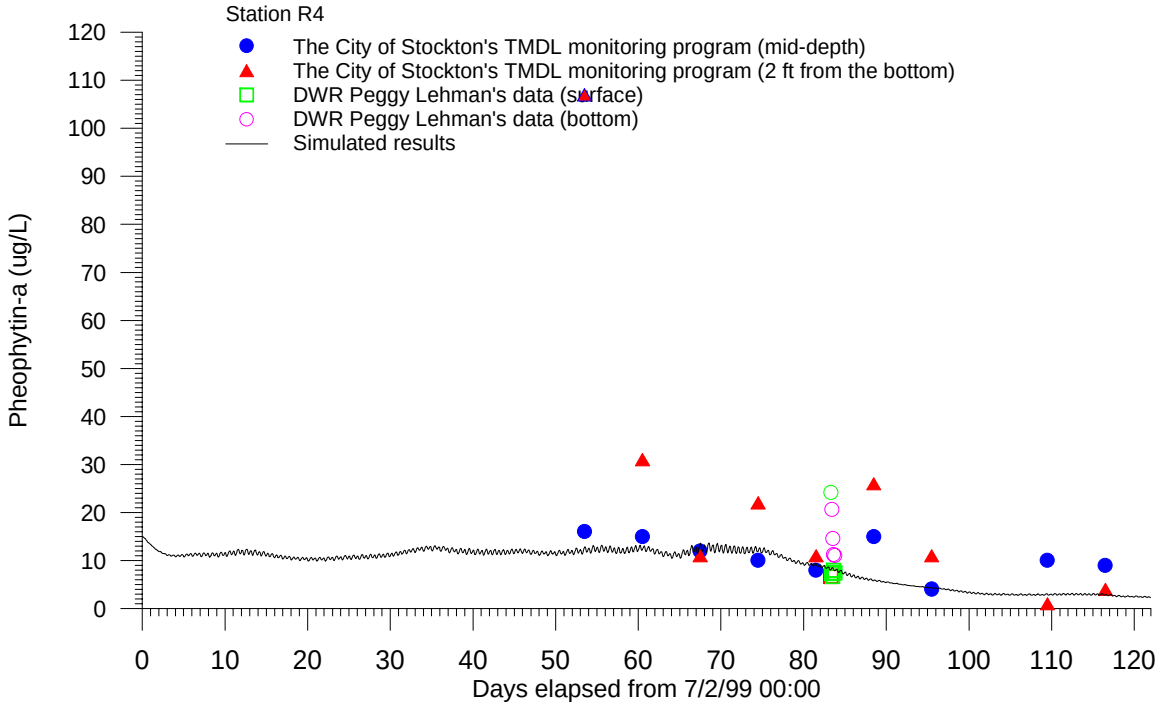

Figure III-22
Simulated and Observed Pheophytin for Station R4, 1999.

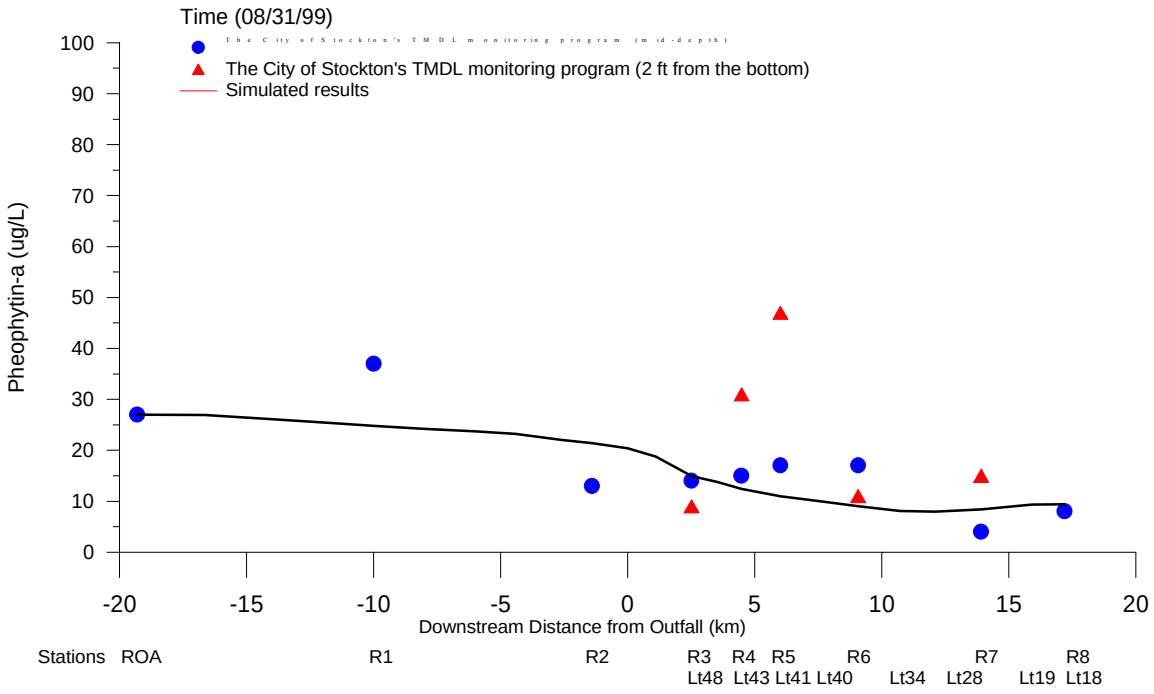

Figure III-23
Simulated and Observed Pheophytin Profile for August 31, 1999.

Ammonia Simulation

Figure III-24 and III-25 compare the simulated and observed ammonia concentrations for station R3 and R4, respectively. The model tracked the rise of ammonia concentration from August to September of 1999, in response to higher ammonia discharge from Stockton RWCF.

Figure III-26 compare the simulated and observed concentration profile of ammonia in the San Joaquin River for August 31, 1999. The general shape of simulated concentration profile matches that of the observed. Both the data and the model showed a decreasing trend of ammonia concentration from R3 to R8.

The spatial trend was caused by the tidal mixing of high ammonia water from the Stockton discharge with the low ammonia water from the downstream boundary. Using ammonia as a tracer, the model predicted a correct pattern of tidal dispersion. The model did not appear to have excessive numerical dispersion, which would have flattened the bell shape curve of ammonia distribution. However, there was a longitudinal shift of position. This could be caused by the tidal phase shift of time or the error in river flow input. The model could be predicting the distribution when the tide pushed the water

upstream, while the sampling could be for the condition when the tide receded downstream.

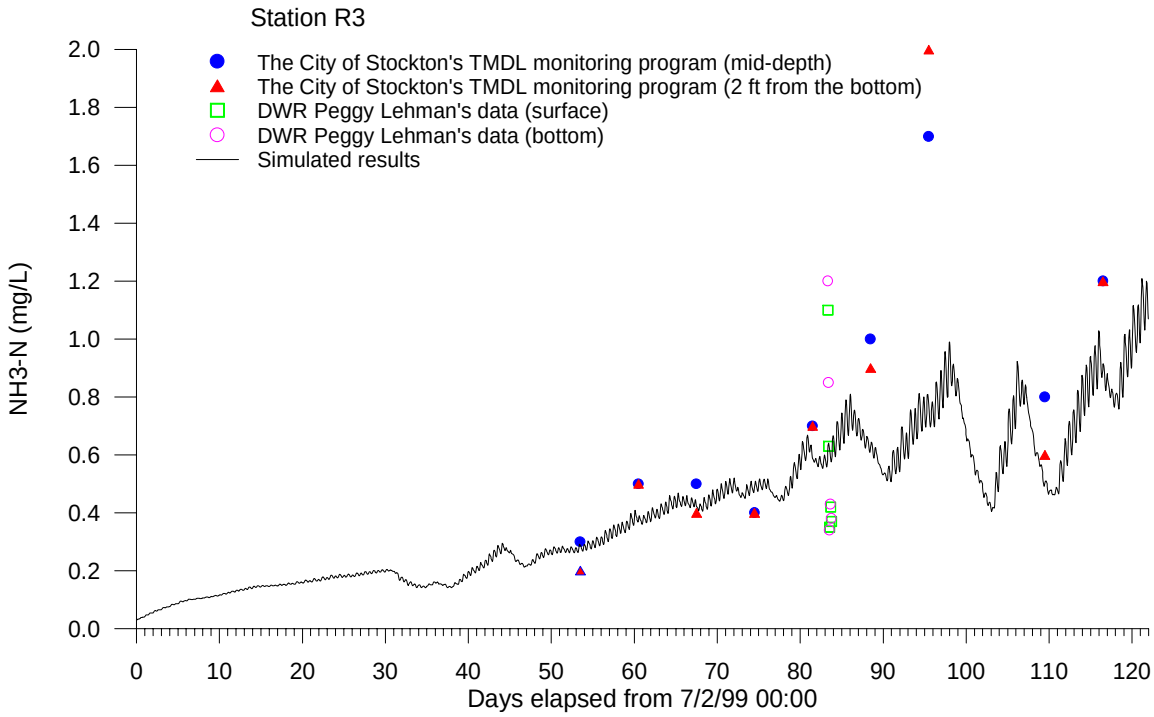

Figure III-24
Simulated and Observed Ammonia Nitrogen for Station R3, 1999.

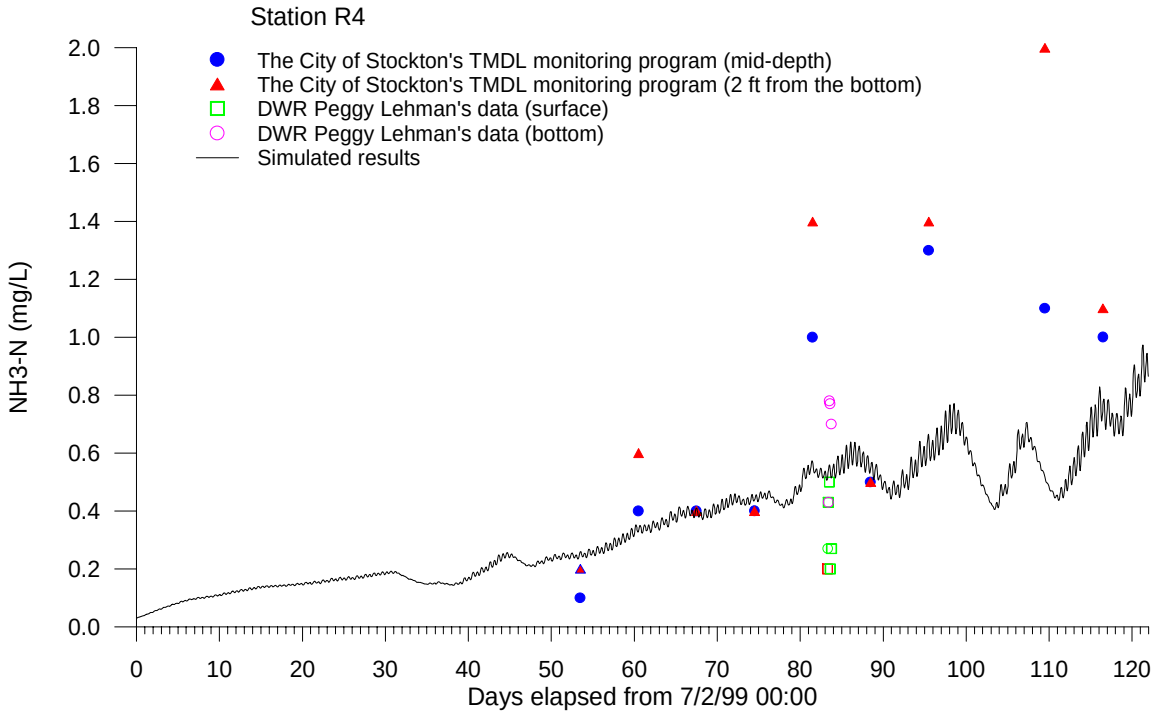

Figure III-25
Simulated and Observed Ammonia Nitrogen for Station R4, 1999.

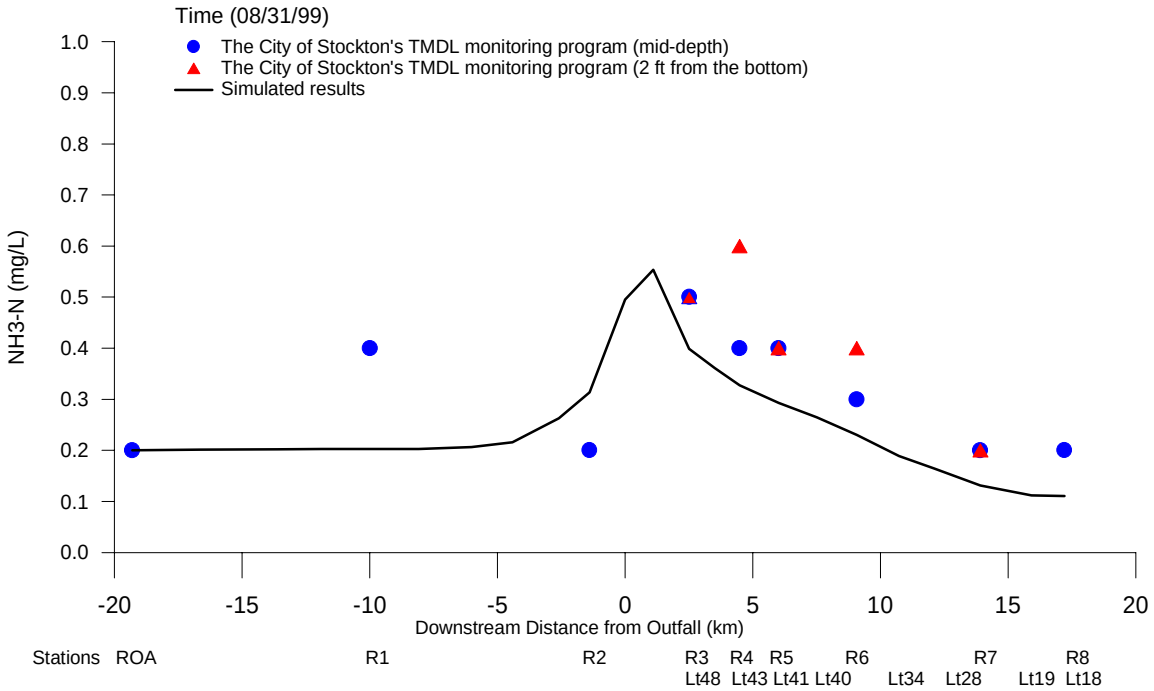

Figure III-26
Simulated and Observed Ammonia Profile for August 31, 1999

Nitrate Simulation

Figures III-27 and III-28 compare the simulated and observed nitrate nitrogen for the 1999 sampling season. The match between model prediction and observed concentration is reasonable.

Figure III-29 compares the simulated and observed concentration profile of nitrate nitrogen in the San Joaquin River for August 31 1999. The model results matched the observed data reasonably well. Since nitrate is derived from ammonia, the nitrate concentrations mimicked the decreasing trend of ammonia concentrations from R3 to R8.

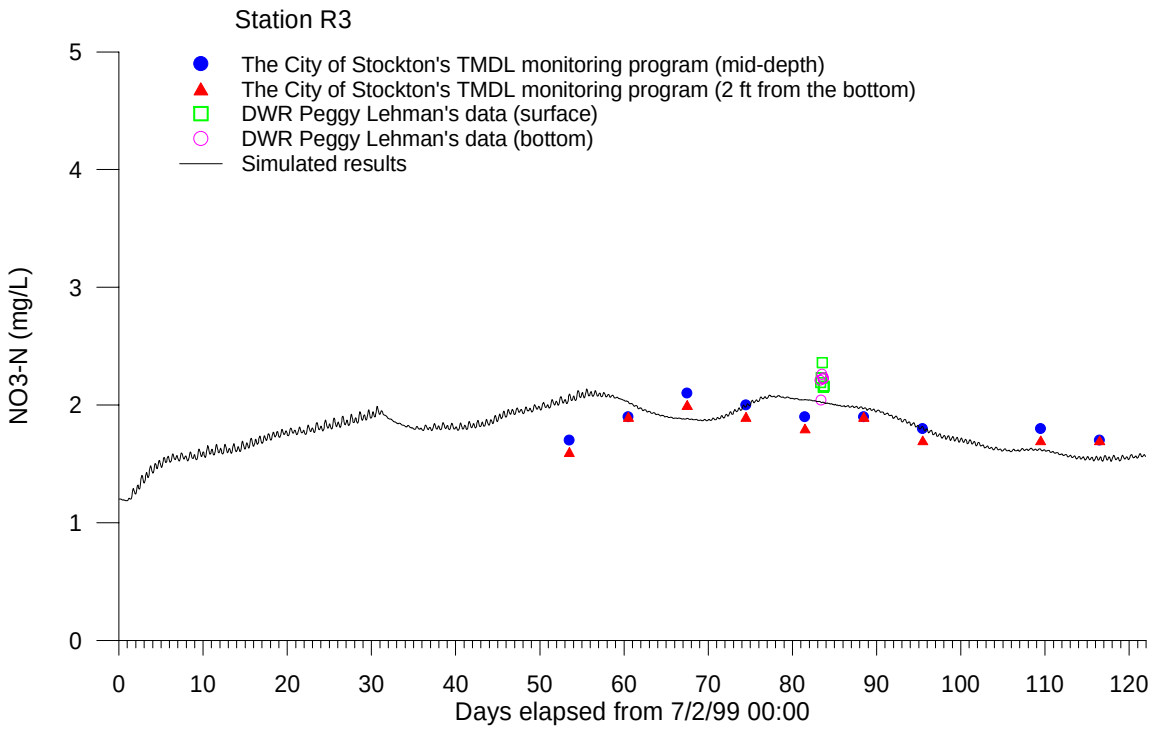

Figure III-27
Simulated and Observed Nitrate Nitrogen for Station R3, 1999.

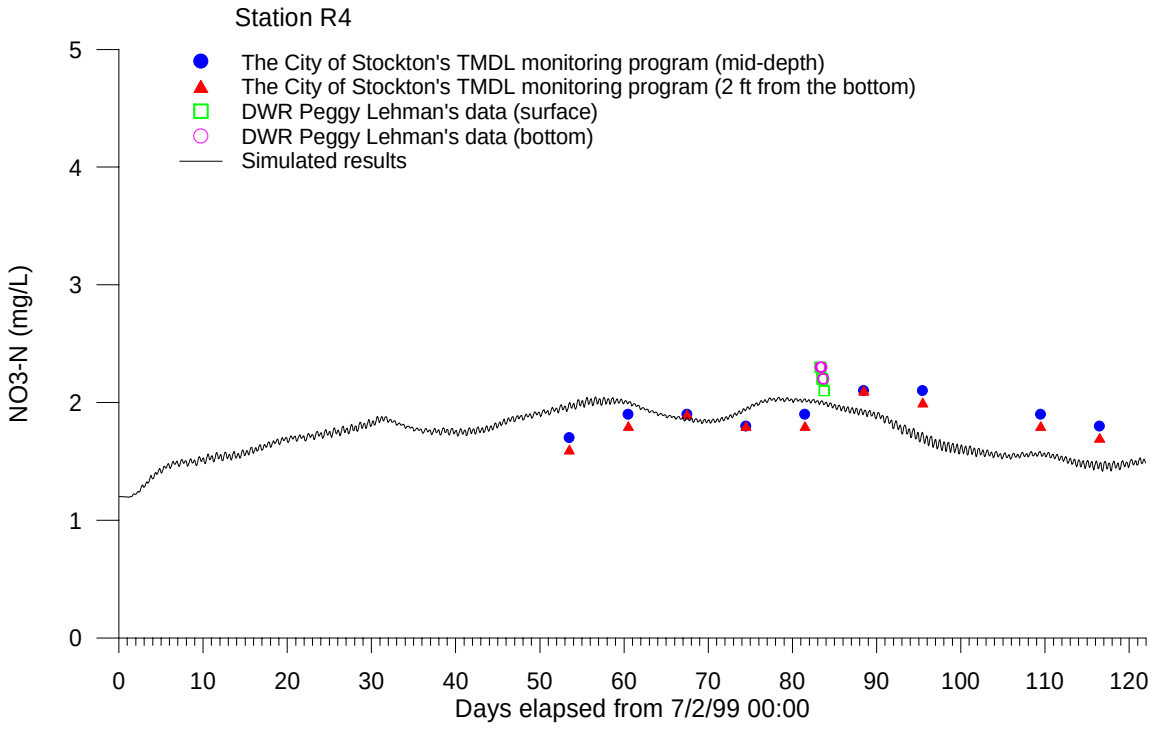

Figure III-28
Simulated and Observed Nitrate Nitrogen for Station R4, 1999.

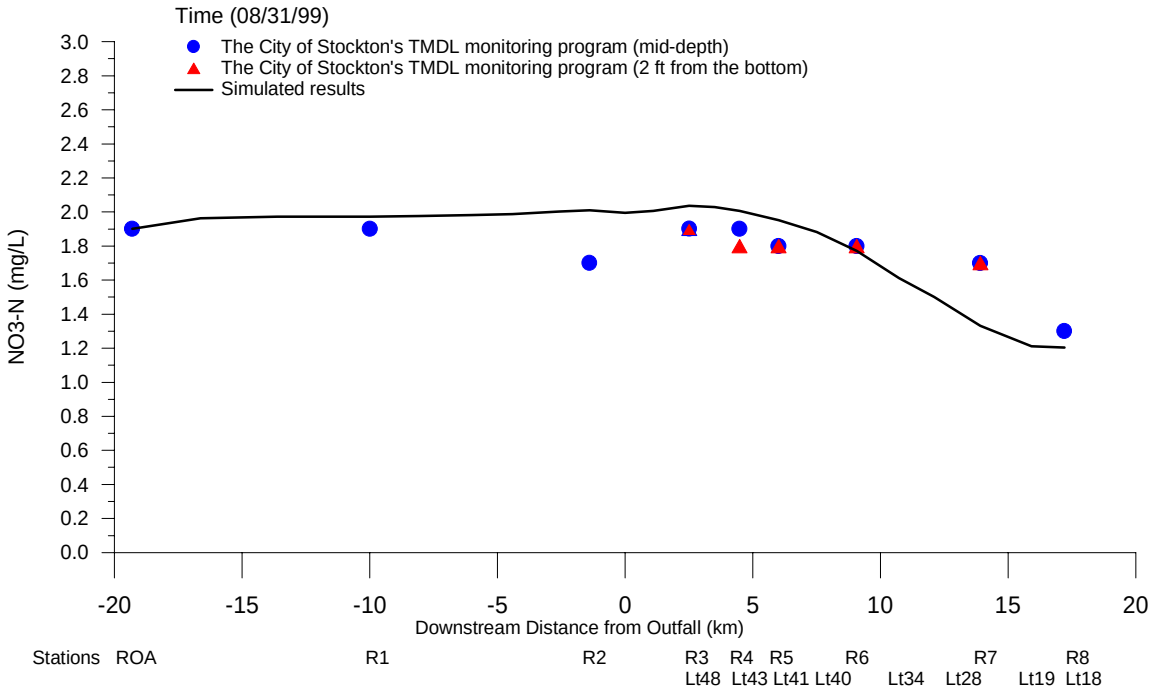

Figure III-29
Simulated and Observed Concentration Profile of NO3-N, 08/31/99.

Phosphorus Simulation

Figures III-30 and III-31 compare the simulated and observed total phosphorus for stations R3 and R4, respectively. The match was reasonably good.

Figure III-32 compares the simulated and observed concentration profile of total phosphorus for August 31 1999. The match was also good.

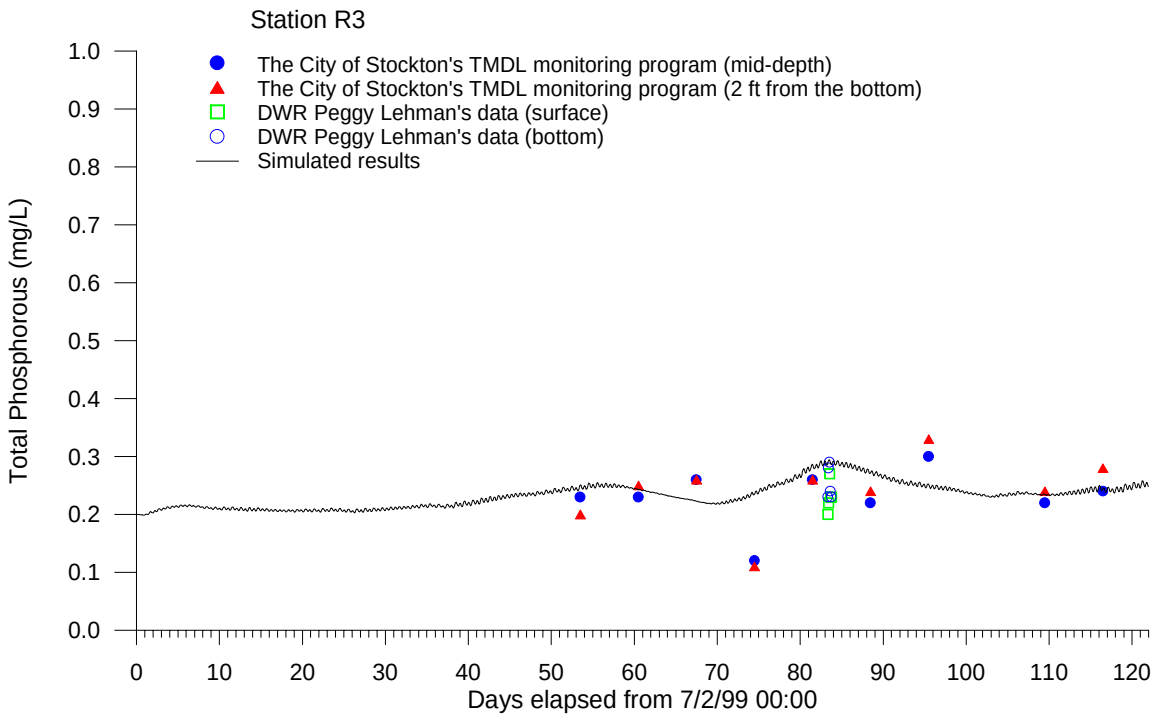

Figure III-30
Simulated and Observed Phosphorus for Station R3, 1999.

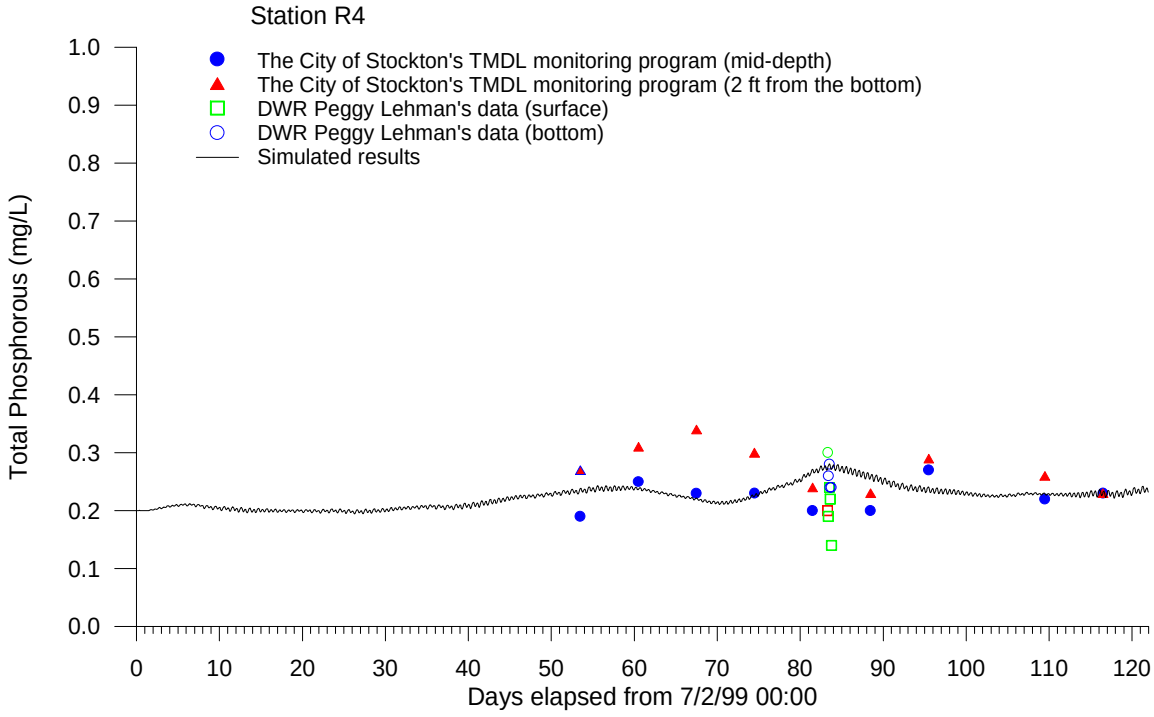

Figure III-31
Simulated and Observed Phosphorus for Station R4, 1999.

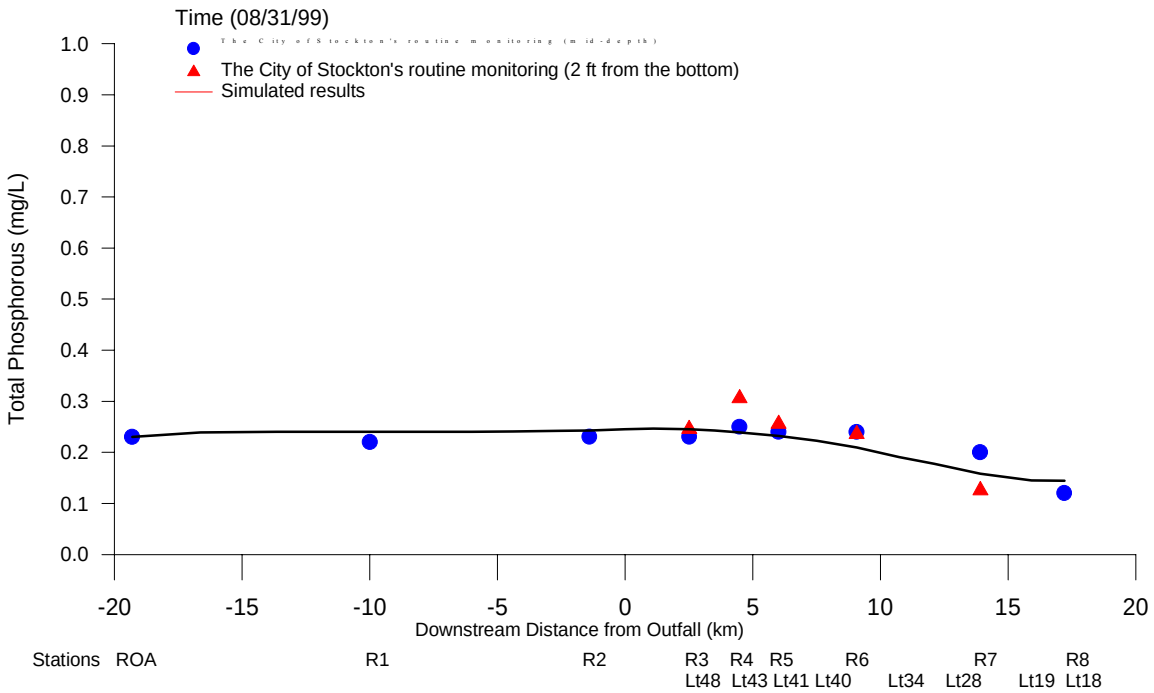

Figure III-32
Simulated and Observed Concentration Profile of PO4-P for 08/31/99.

TSS Simulation

Figures III-33 and III-34 compare the simulated and observed total suspended solid for stations R3 and R4. The observed values of TSS scattered widely. The model predictions were within the observed ranges.

Dr. Peggy Lehman' data showed higher TSS concentrations in the bottom samples than in surface samples. The City of Stockton data also showed higher TSS concentrations in their bottom samples than in their mid-depth samples. These were caused by active settling of suspended particles, re-suspension of sediment from the bottom, and/or both at stations R3 and R4 in the Deep Water Ship Channel.

Figure III-35 compares the simulated and observed concentration profile of TSS for August 31, 1999. The model tracked the observed trend of decreasing TSS from R3 to R8 in the Deep Water Ship Channel. The concentration differences between mid-depth and bottom samples also decreased from R3 to R8, as the river load of TSS settled out in the upstream section of the Deep Water Ship Channel. By the time, it reached station R6, most of the materials were settled and the concentration difference between the surface and bottom samples diminished.

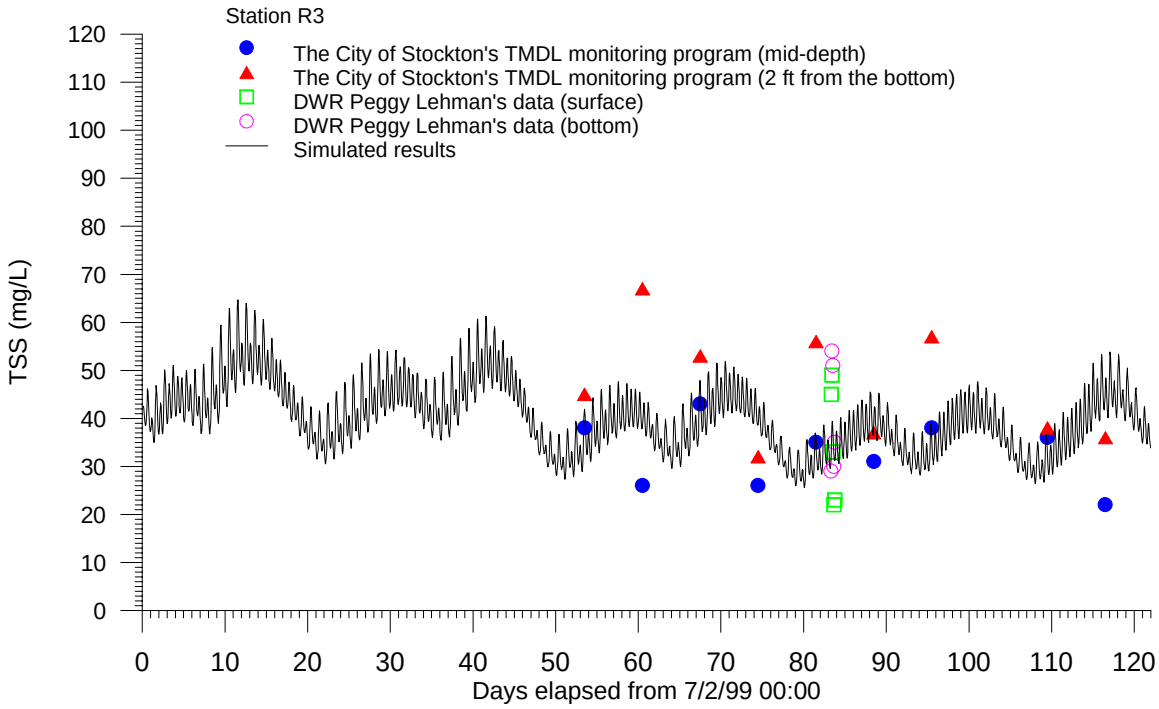

Figure III-33
Simulated and Observed Total Suspended Solid for Station R3, 1999.

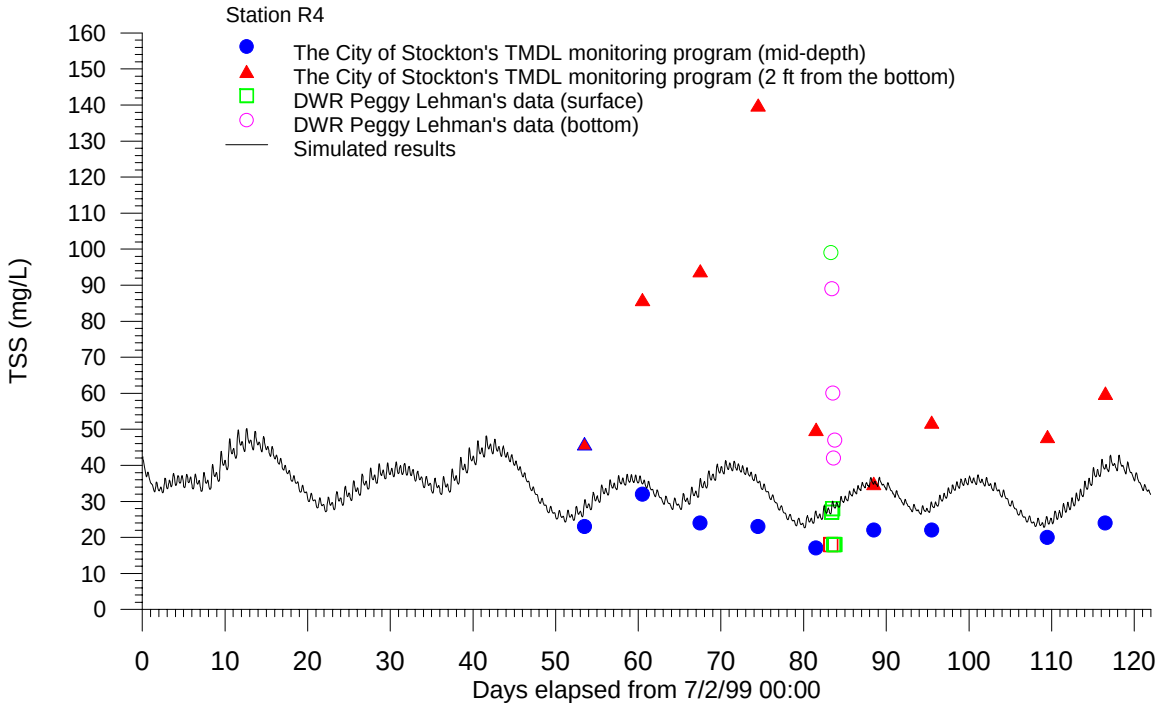

Figure III-34
Simulated and Observed Total Suspended Solid for Station R4, 1999.

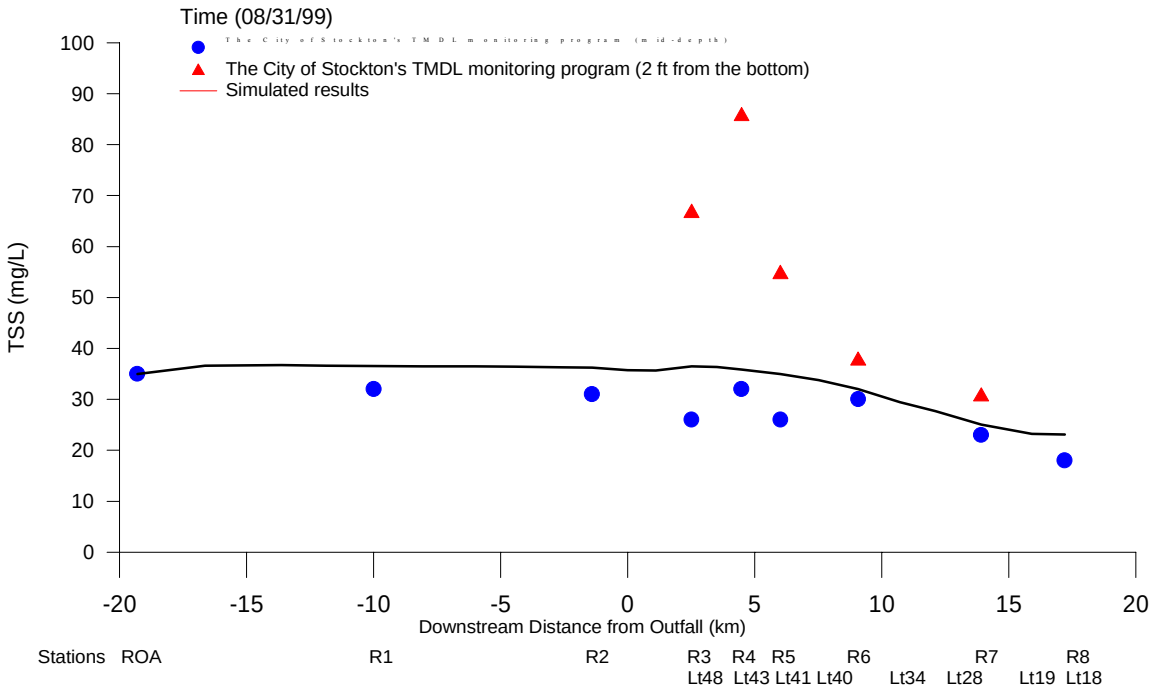

Figure III-35
Simulated and Observed Concentration Profile of TSS for 08/31/99.

VSS Simulation

Figures III-36 and III-37 compare the simulated and observed volatile suspended solid (VSS) for stations R3 and R4, respectively. The model tracked the observed VSS reasonably well.

Both Dr. Peggy Lehman's data and the City of Stockton data showed higher VSS for the bottom samples than for the surface or mid-depth samples. Apparently, VSS was settling out like TSS.

Figure III-38 compares the simulated and observed concentration profiles of VSS in the San Joaquin River for August 31, 1999. The model tracked the decreasing trend of VSS from R3 to R8, similar to the situation for TSS.

By comparing the plots for TSS and VSS, there are some noticeable differences. In both TSS and VSS, the concentration differences were highest for station R4. For TSS, the concentration differences decreased gradually from R4 to R7, with a residual difference due to the re-suspension of sediment from the bottom. For VSS, the concentration differences also decreased gradually from R4 to R7, but the residual difference

diminished to near zero. This suggested that the river load of VSS was completely trapped in the Deep Water Ship Channel.

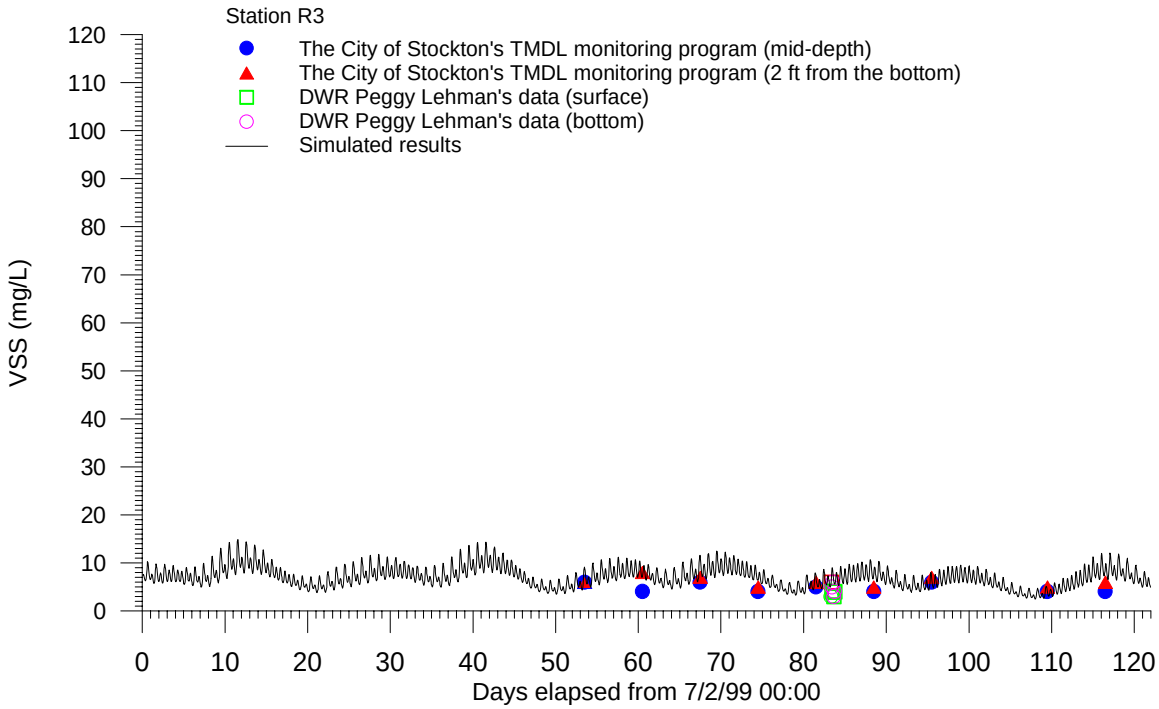

Figure III-36
Simulated and Observed VSS for Station R3, 1999.

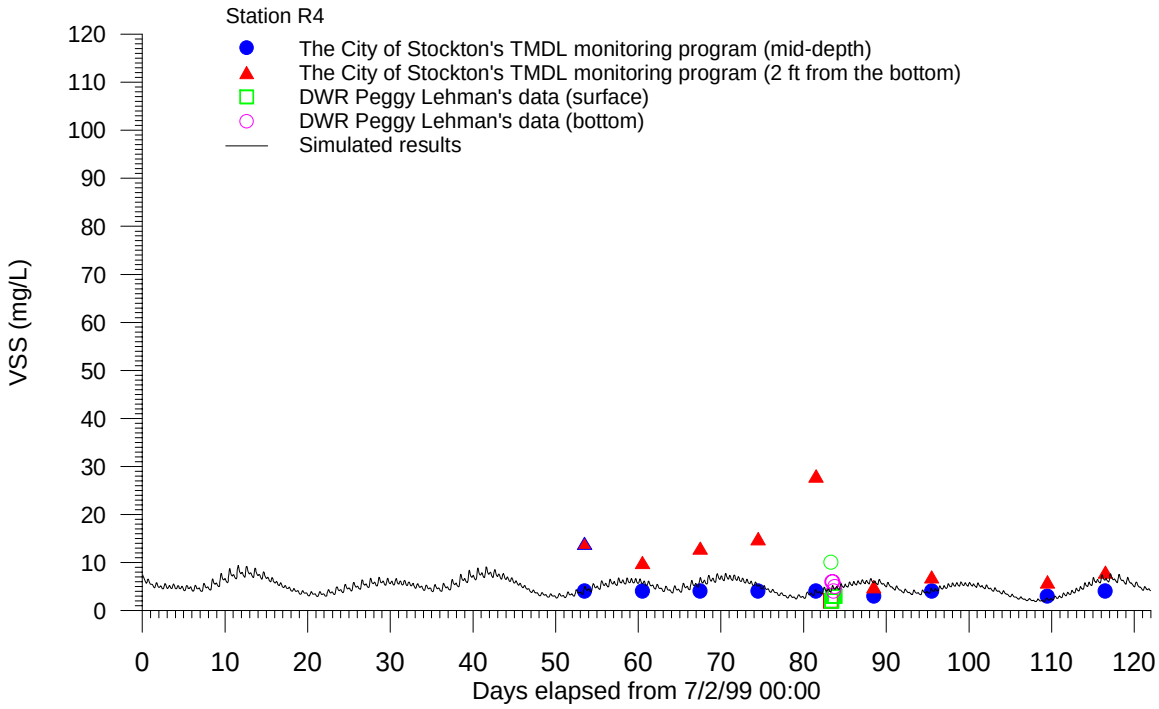

Figure III-37
Simulated and Observed VSS for Station R4, 1999.

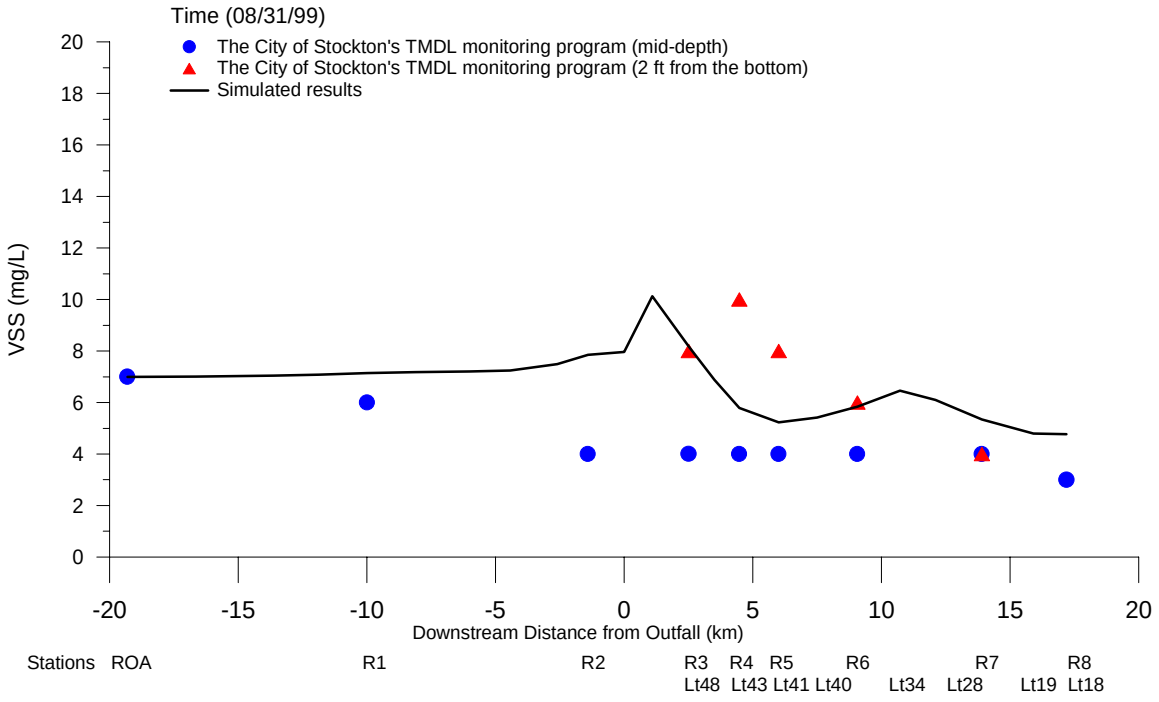

Figure III-38
Simulated and Observed Concentration Profile of VSS for 08/31/99.

2000 Simulation

Solar Radiation

The model calculated the hourly short wave radiations for the year 2000 sampling period. The DWR measured the short wave radiations at Rough and Ready Island. The theoretical and measured values are compared in Figure III-39. The match is as good as for the year 1999. The model has used correct solar radiation in heat budget and algal growth calculations.

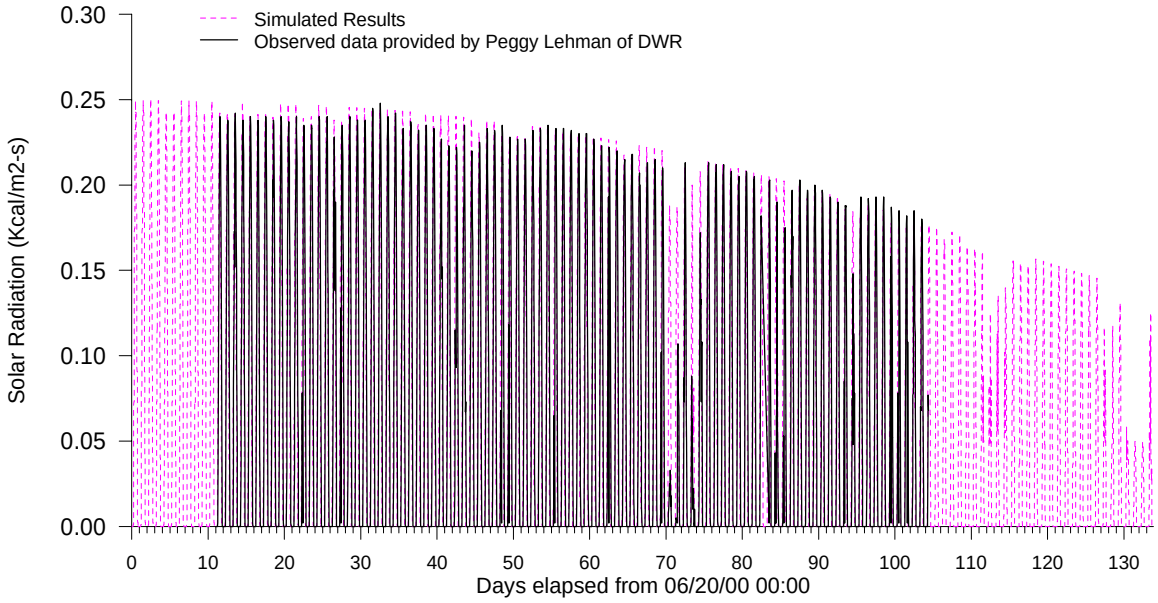

Figure III-39
Theoretical and Measured Solar Radiations, 2000.

River Flow

Figure III-40 presents the UVM flow for the year 2000 sampling period. The pattern of river flow for year 2000 was very different from that for year 1999. In year 1999, the river flow was maintained fairly steady at 1000 cfs until late September, when the river flow dropped precipitously to near zero. In year 2000, the river flow fluctuated between 500 cfs and 1000 cfs from June to mid-August. The river flow was raised to between 1250 and1750 cfs in September. In late September and early October, there were two periods, when the river flow also dropped precipitately as in 1999. However, the lowest flow did not drop below 500 cfs during the year 2000 sampling period.

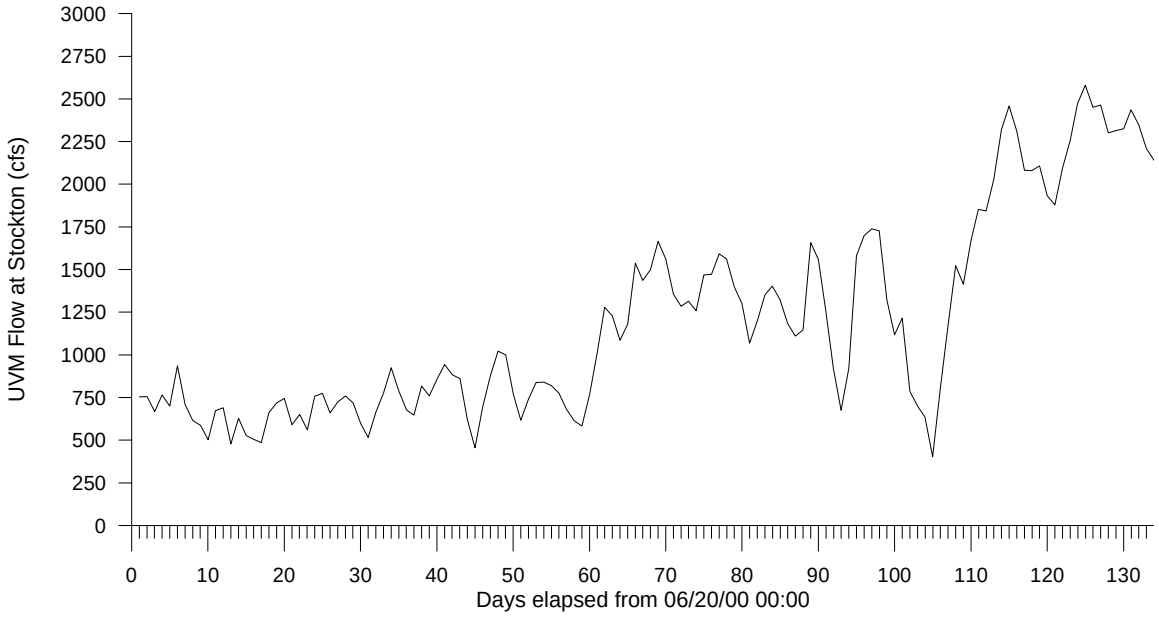

Figure III-40
UVM Flow at Stockton, 2000.

Stockton Discharge

Figure III-41 presents the daily discharge of treated effluent from Stockton RWCF for the year 2000 sampling period. The Stockton discharge did not change too much between 1999 and 2000. The highest value was still about 70 cfs (45 MGD). There was no discharge for one week in mid-July of 2000.

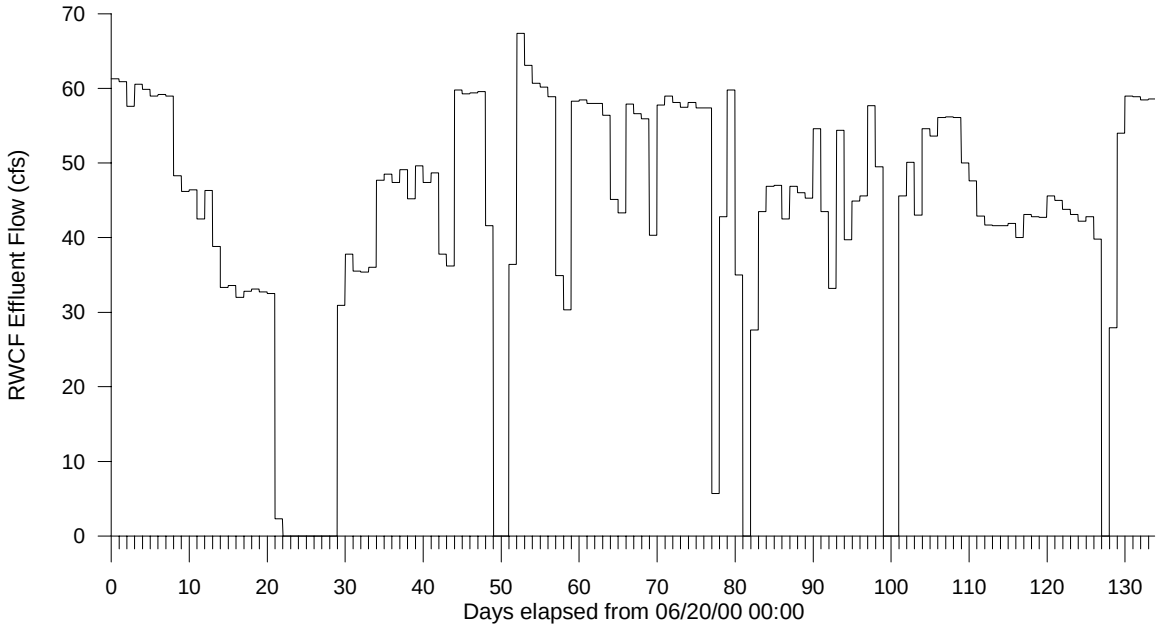

Figure III-41
Daily discharge from Stockton RWCF, 2000.

Pollution Loads

Table III-2 shows the river load and Stockton load for the sampling period, July to October 2000. The river loads of CBOD, VSS, and chlorophyll continued to be substantially higher than the Stockton loads, as they were in 1999. The ammonia river load was still lower than the Stockton load, whose effluent continued to have high ammonia concentration in year 2000 (Figure III-41). The magnitudes of differences were altered slightly.

An analysis of data indicates that the Stockton loads were similar for 1999 and 2000. The river loads were different due to the changes in flow and pollutant concentrations. The river load of ammonia was 589 kg/d, which was nearly the same as the Stockton load (966 kg/d). Clearly, the river load can contribute as much ammonia nitrogen as the Stockton load. Some of the ammonia river load might have come from the wetlands releases in the Mud and Salt Sloughs in the upstream of San Joaquin River.

Table III-2
Pollution Loads for the 2000 Sampling Period

Items	CBOD5	NH3-N	VSS	Chl-a
River load at Mossdale, kg/d	1,459	589	18,133	114
Stockton load average, kg/d	411	966	985	3.1
River load at Mossdale, lb/d	3,210	1,296	39,893	251
Stockton load average, lb/d	904	2,125	2,167	6.9

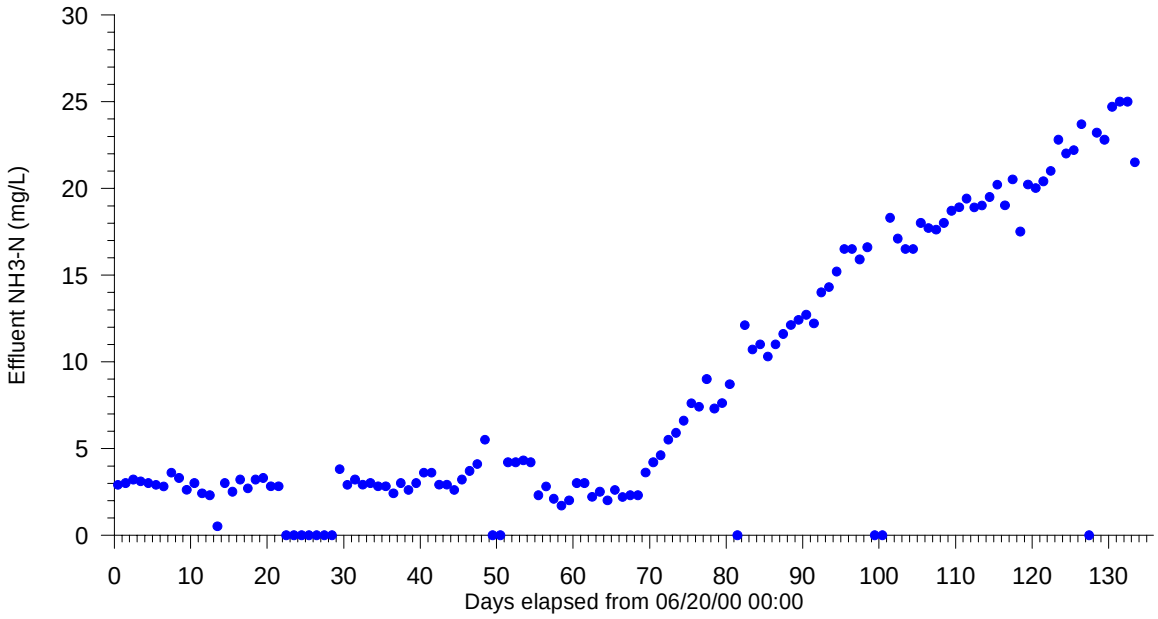

Figure III-42
Ammonia Concentration in Stockton RWCF Effluent, 2000.

Flow Simulation

In year 1999, the ADCP was mounted on a boat and the currents were measured for a few days at three sites. In year 2000, DWR installed a permanent ADCP at Rough and Ready Islands. The ADCP measured the current and flows at 15 minutes intervals, similar to the UVM measurements at Stockton.

DWR provided the flow data at 15 minutes intervals for each month, from July to November, 2000. There are too much data to show the comparison between observed and simulated flow for the entire sampling period. It was decided to select one date each month for the comparison. Figures III-43 to III-46 are the comparisons for July, August, September, and October, respectively.

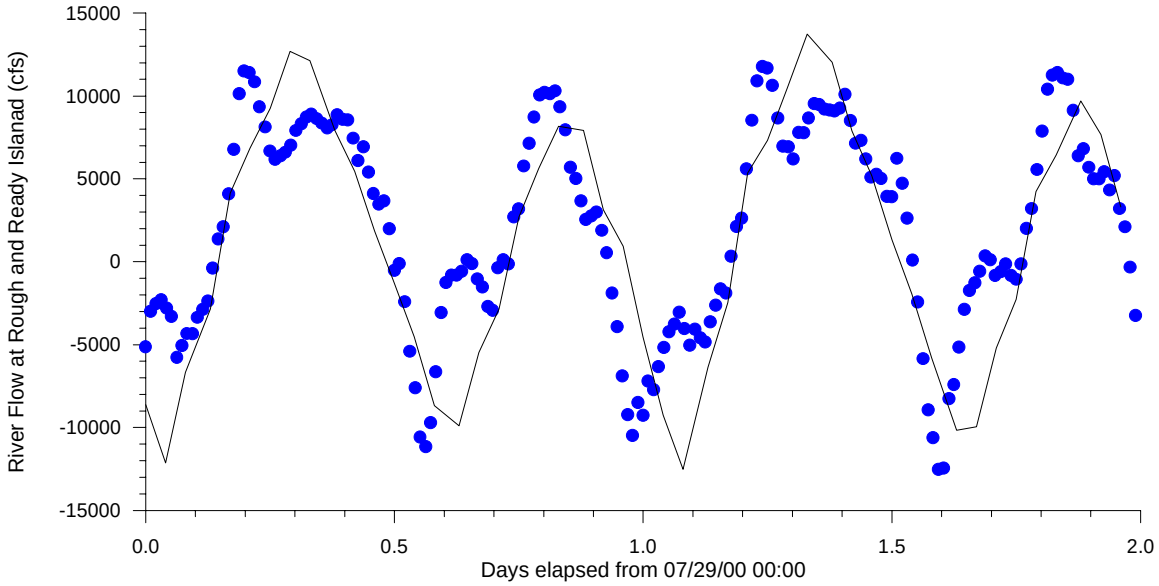

Figure III-43 Simulated and Observed Flow at Rough and Ready for 7/29/00

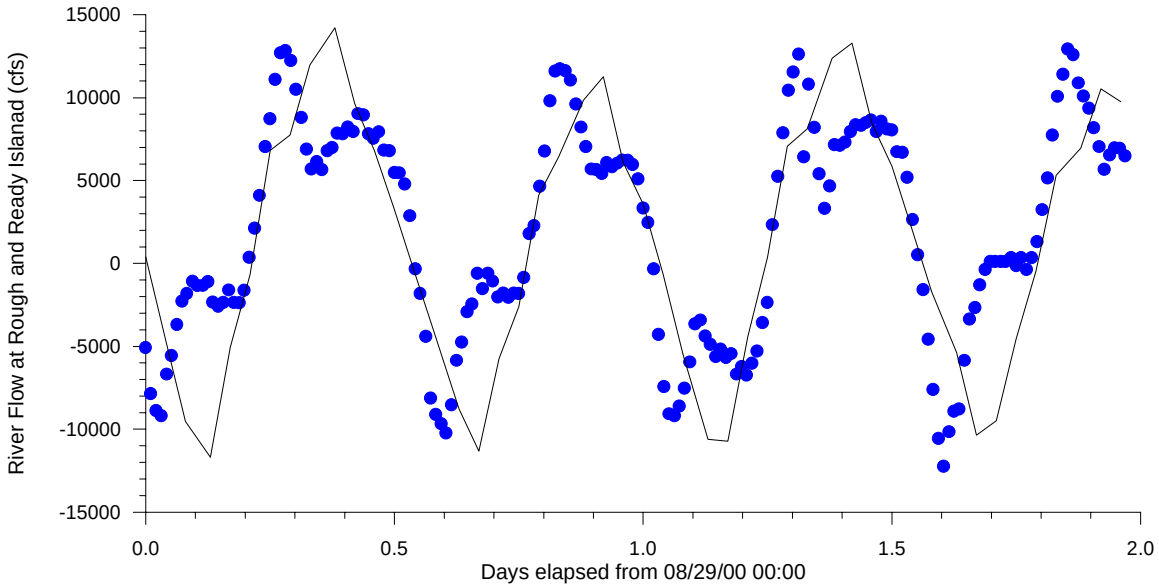

Figure III-44 Simulated and Observed Flow at Rough and Ready for 8/29/00

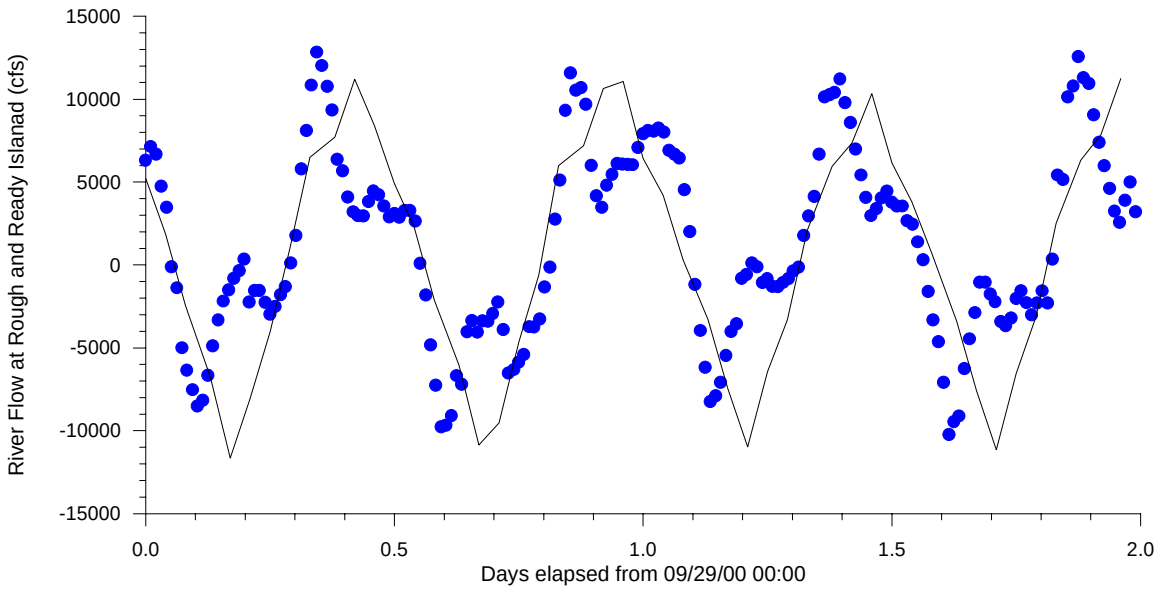

Figure III-45 Simulated and Observed Flow at Rough and Ready for 9/29/00

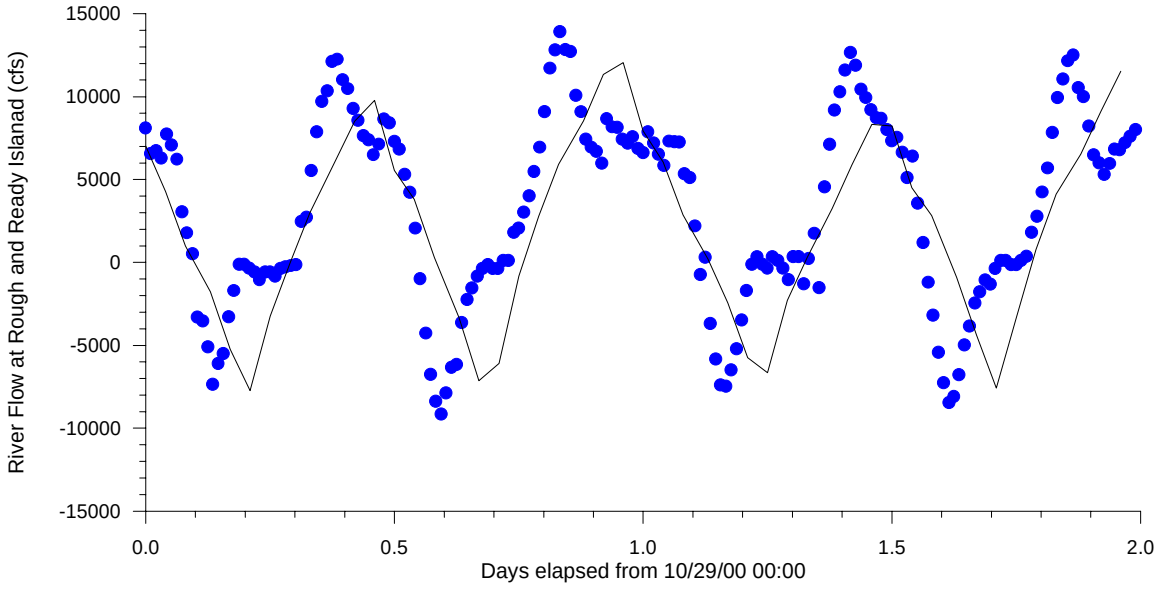

Figure III-46 Simulated and Observed Flow at Rough and Ready for 10/29/00

The results show that the model has simulate the tidal flow at the Rough and Ready accurately. While the net river flow varied from 500 cfs in early July to 2,600 cfs in October, the tidal flow varied between +14,000 cfs to –10,000 cfs. Clearly, the water movement in the Deep Water Ship Channel is dominated by tides.

Temperature Simulation

Figure III-47 compares the simulated and observed temperature for station R3. Figures III-48 and III-49 show the comparison for stations R4 and R5, respectively. Figure III-50 compares the simulated and observed temperature profile for September 12, 2000.

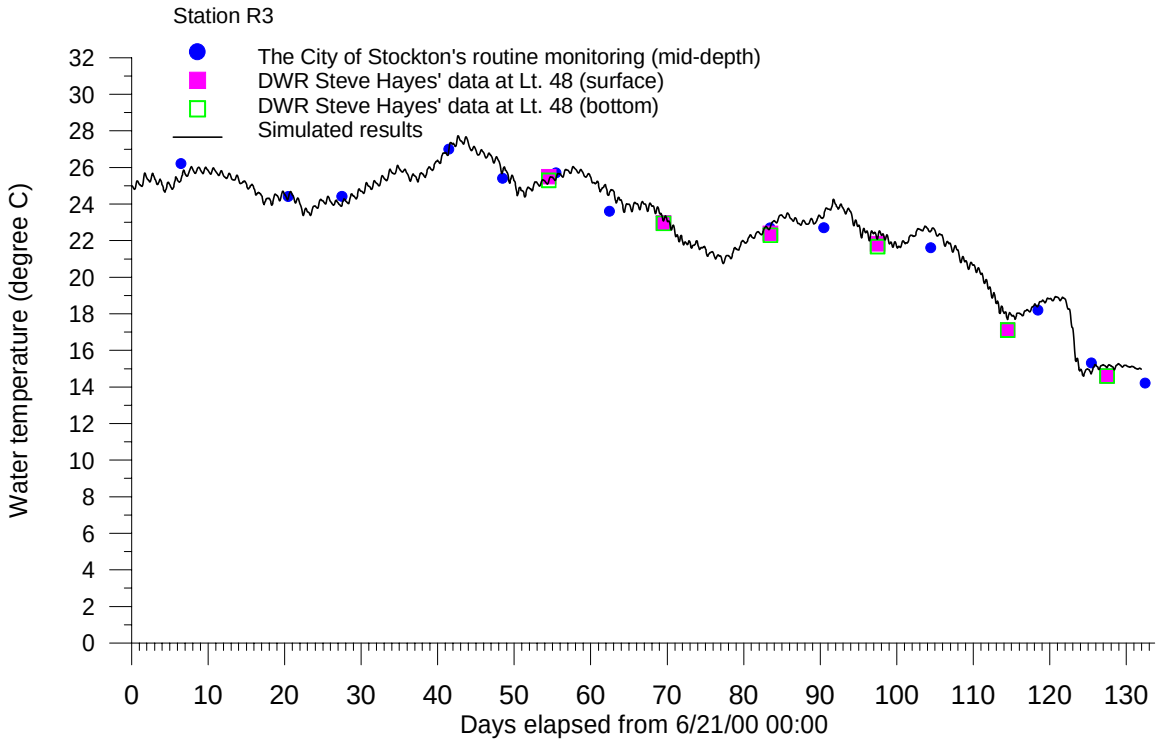

Figure III-47
Simulated vs. Observed Temperature at Stations R3, 2000.

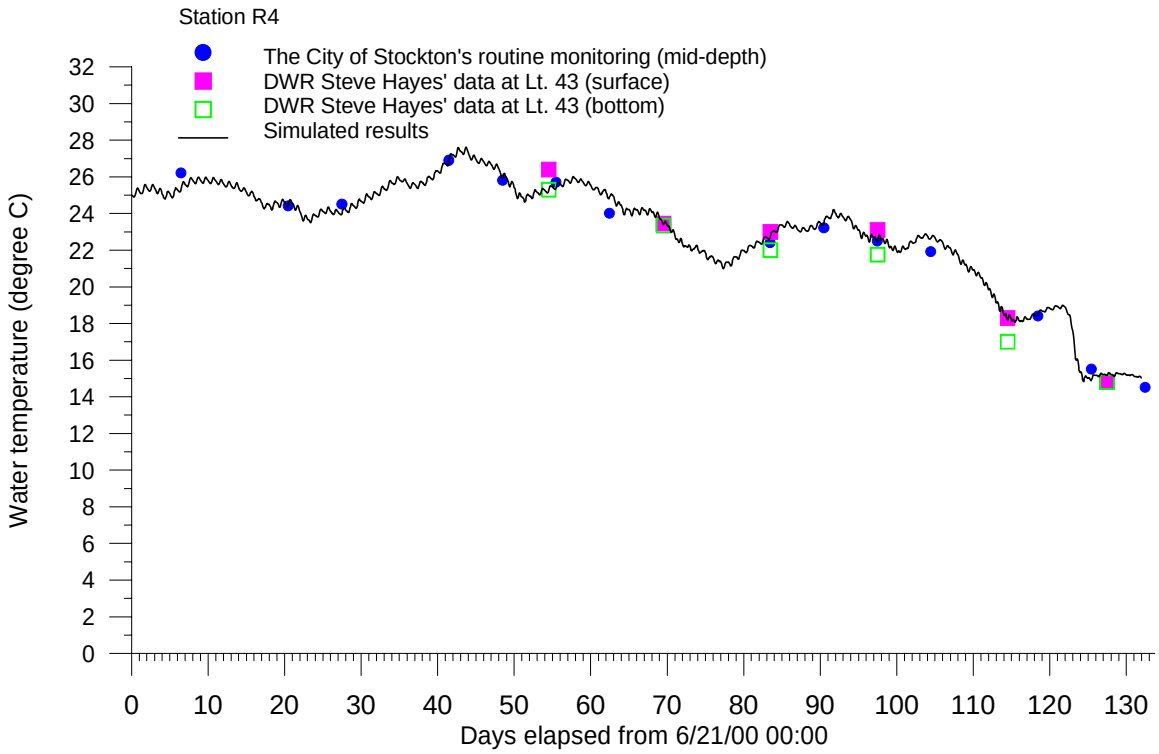

Figure III-48
Simulated vs. Observed Temperature at Stations R4, 2000.

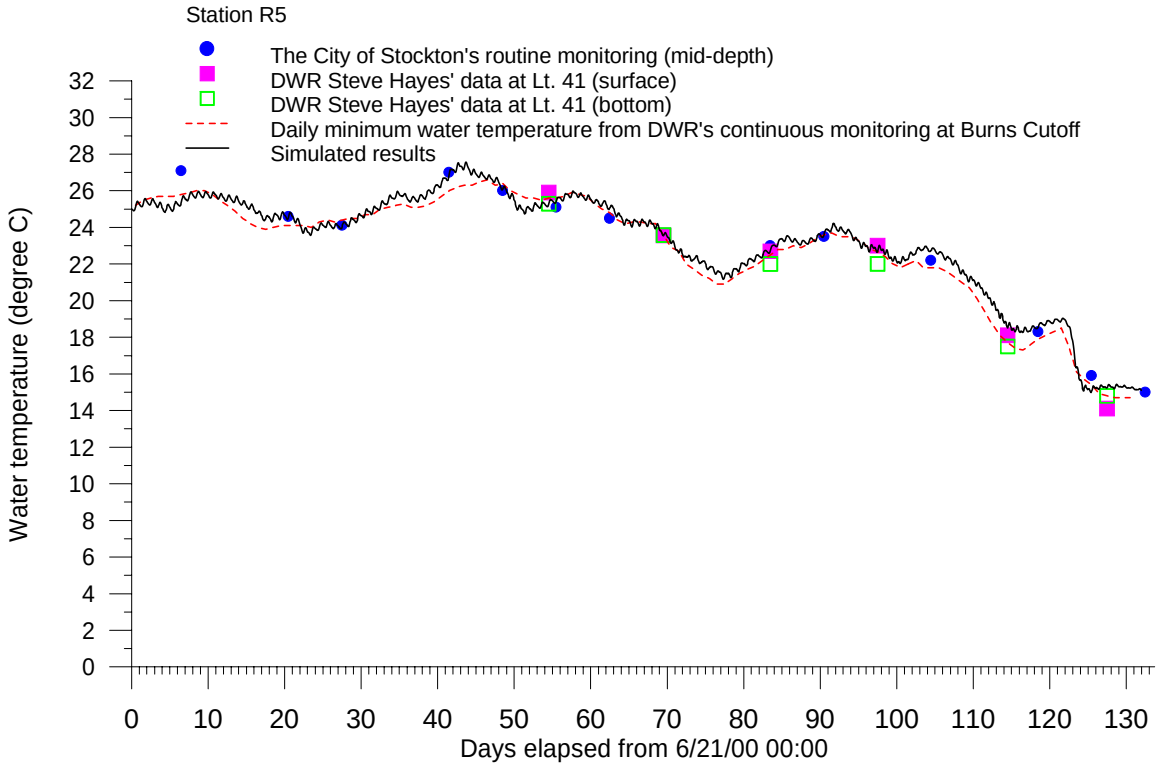

Figure III-49
Simulated vs. Observed Temperature at Stations R5, 2000.

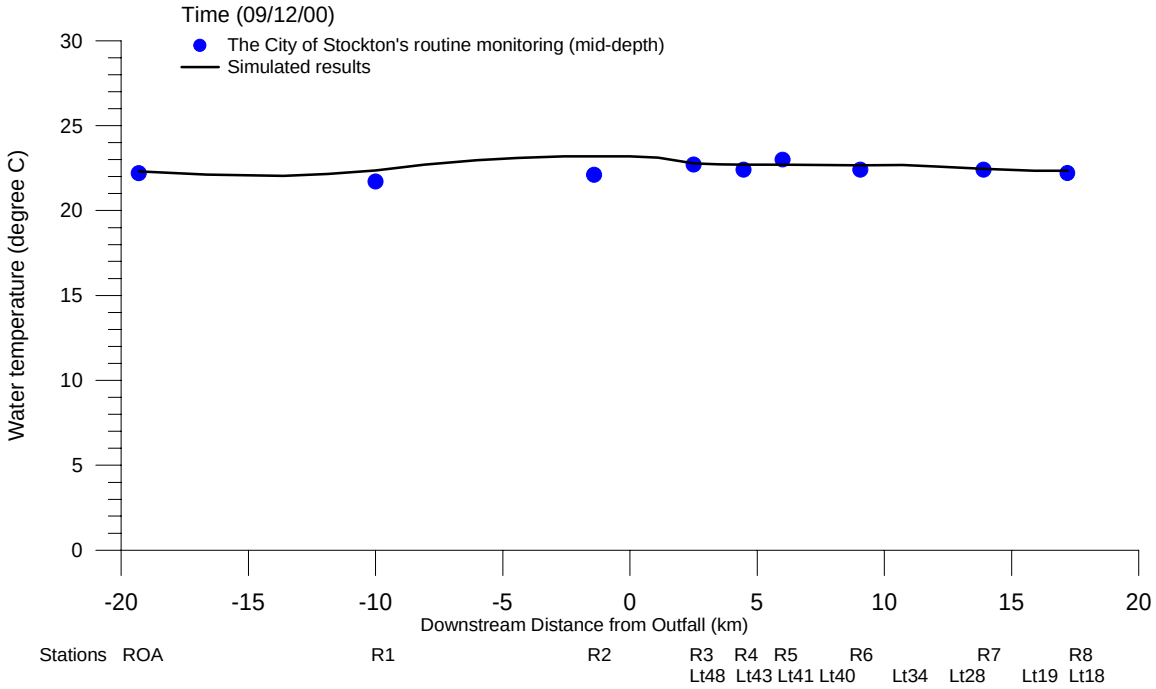

Figure III-50
Simulated vs. Observed Temperature Profile for 09/12/00.

The observed data was derived from the mid depth temperature measured by Stockton; the surface temperature measured by Dr. Hayes of the Department of Water Resources (DWR); and the bottom temperature measured by Dr. Hayes of DWR. The DWR also maintained a continuous water quality monitoring station at Burns Cutoff near Rough and Ready Island. The continuous temperature at Burns Cutoff was used to compare against the continuous model simulation (Figure III-49). The model has predicted the water temperature accurately for the year 2000 sampling period.

Dissolved Oxygen Simulation

Figures III-51, III-52 and III-53 show the comparisons of simulated and observed dissolved oxygen for stations R3, R4 and R5, respectively. The observed DO was derived from City of Stockton (mid-depth measurements) and Dr. Hayes of DWR (surface and bottom DO). The continuous daily minimum DO monitored at Burns Cutoff was also plotted to compare against the continuous model simulation.

The model appears to match the mid-depth values well. The DWR data showed substantially higher DO for surface and bottom measurements. A concentration as high as 10 mg/l was reported for stations R3 and R4 in mid September. The water samples might have been collected at pockets of algal bloom.

The minimum daily DO of DWR's continuous data was lower than the mid-depth DO, which was matched by the model simulation. The continuous monitoring data had a DO as high as 9 mg/l in mid September. The model could not provide an explanation for the anomaly.

Figure III-54 compares the simulated and observed concentration profile of DO for September 12 2000. The match was reasonable. The DO depression occurred mostly in the Deep Water Ship Channel similar to what happened in 1999. But, the DO did not drop below 5 mg/l during the year 2000 sampling period.

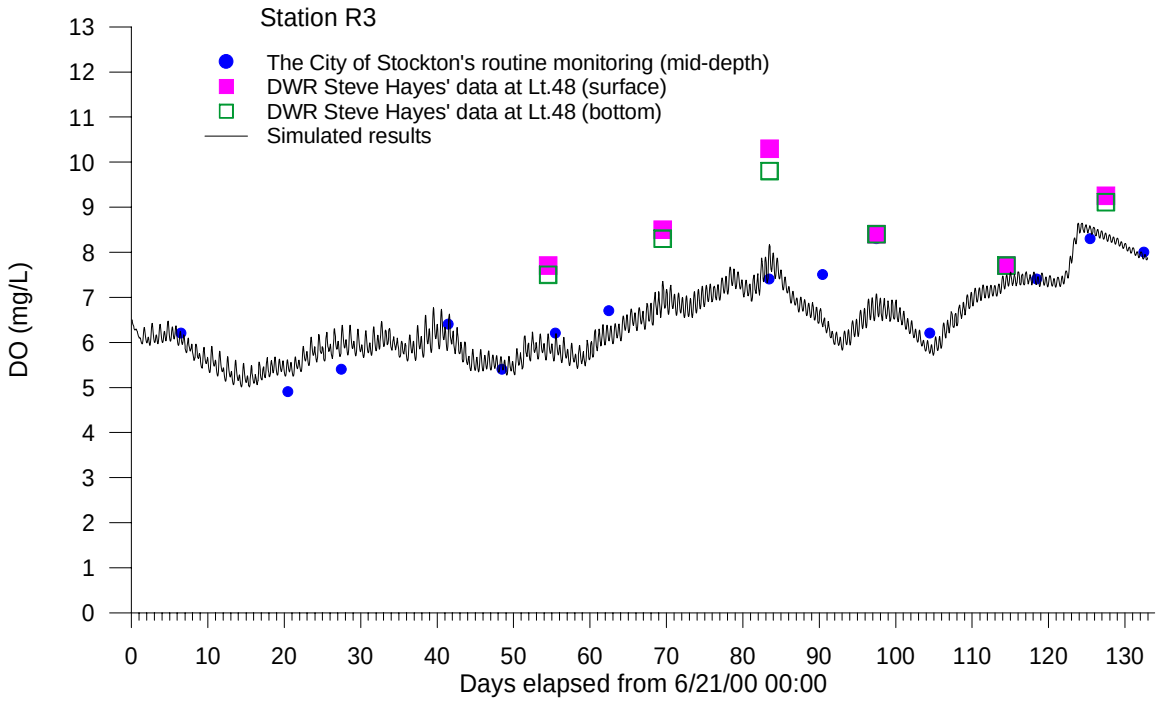

Figure III-51
Simulated and Observed DO for Station R3, 2000.

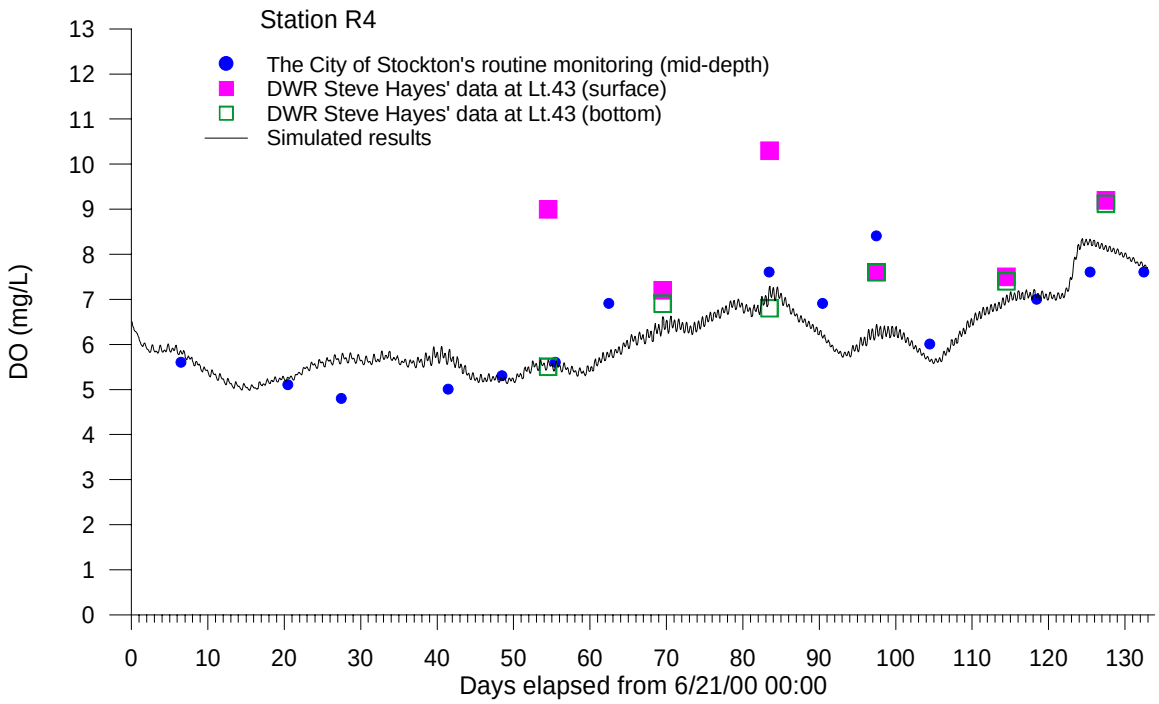

Figure III-52
Simulated and Observed DO for Station R4, 2000.

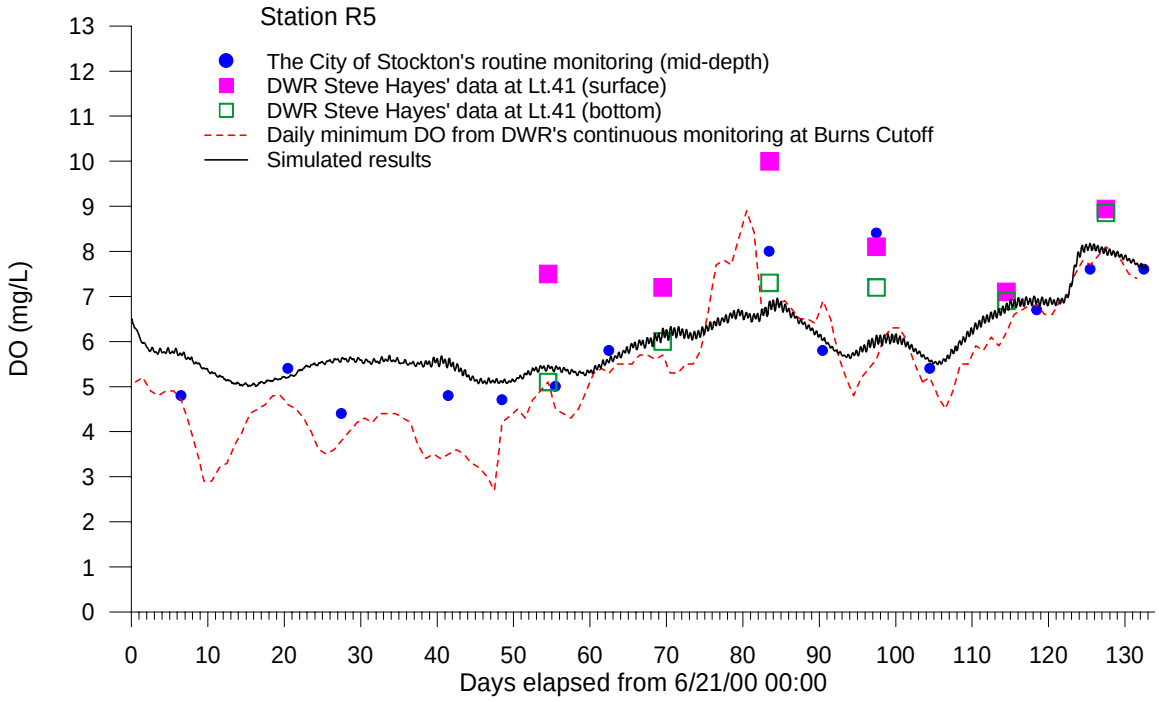

Figure III-53
Simulated and Observed DO for Station R5, 2000.

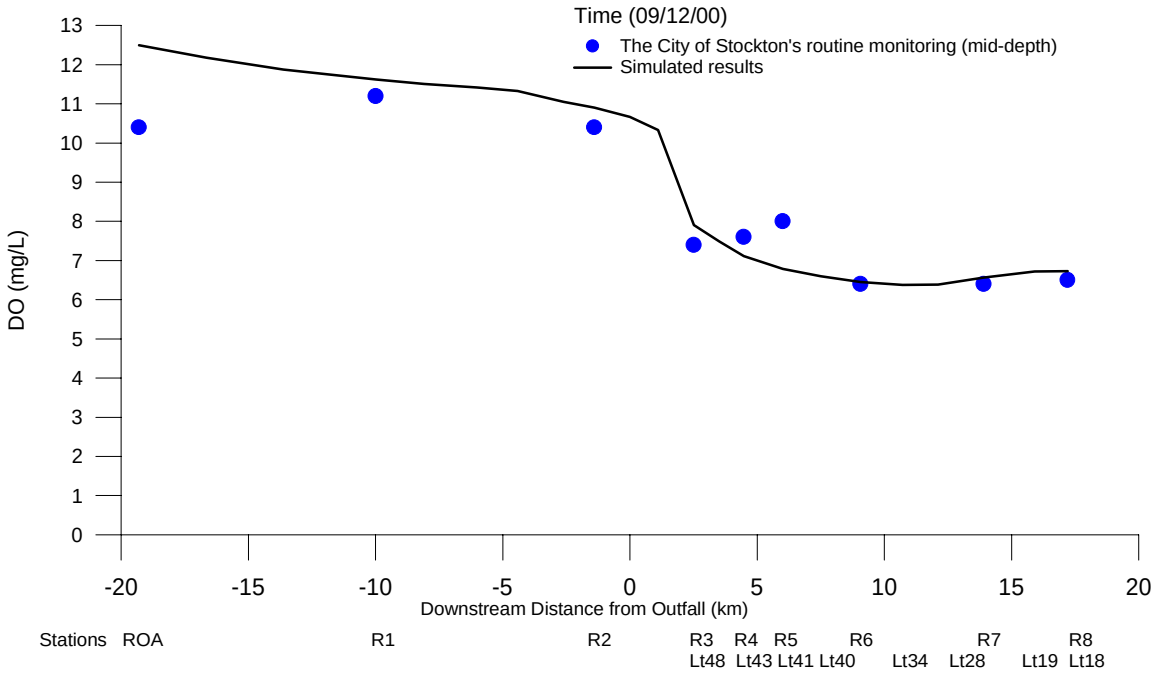

Figure III-54
Simulated and Observed Concentration Profile of DO for 09/12/00.

Algae Simulation

Figures III-55 and III-56 compare the simulated and observed chlorophyll-a for stations R3 and R5 respectively. The observed data was from the City of Stockton and Dr. Peggy Lehman of DWR. The model matched the seasonal variation of chlorophyll-a reasonably well.

Figure III-57 compares the simulated and observed concentration profile of chlorophyll-a for September 12, 2000. The model simulated the decreasing trend of chlorophyll-a from R3 to R8 due to light limitation.

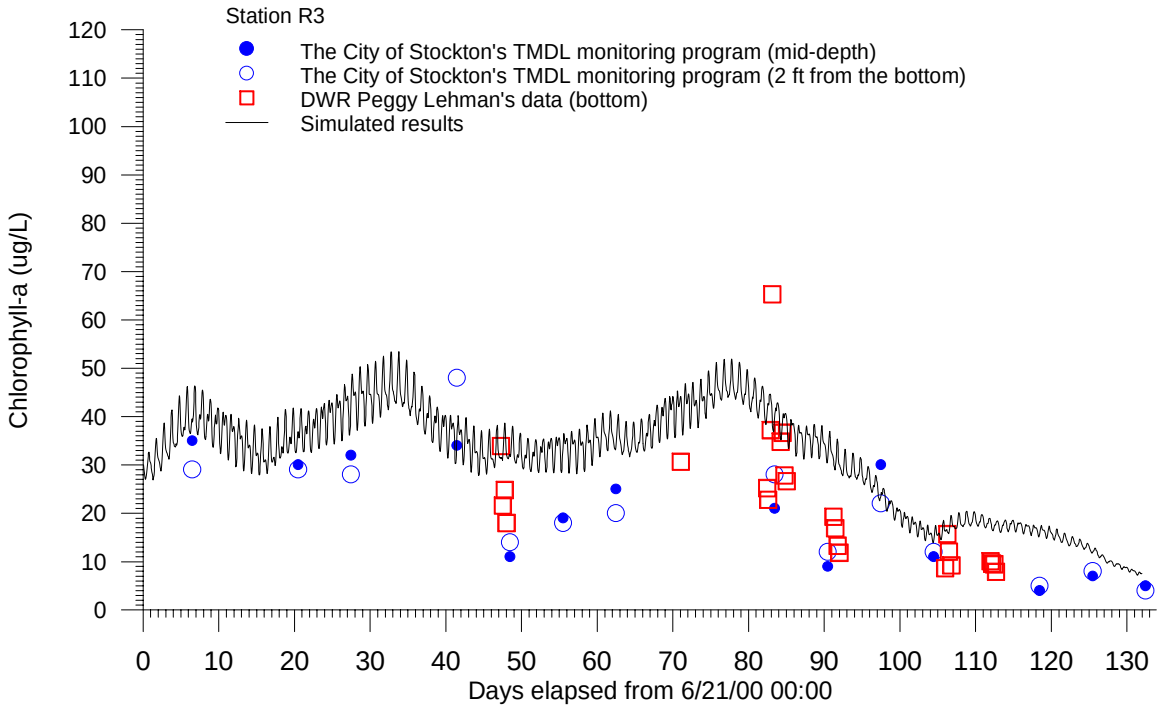

Figure III-55
Simulated and Observed Chlorophyll-a for Station R3, 2000.

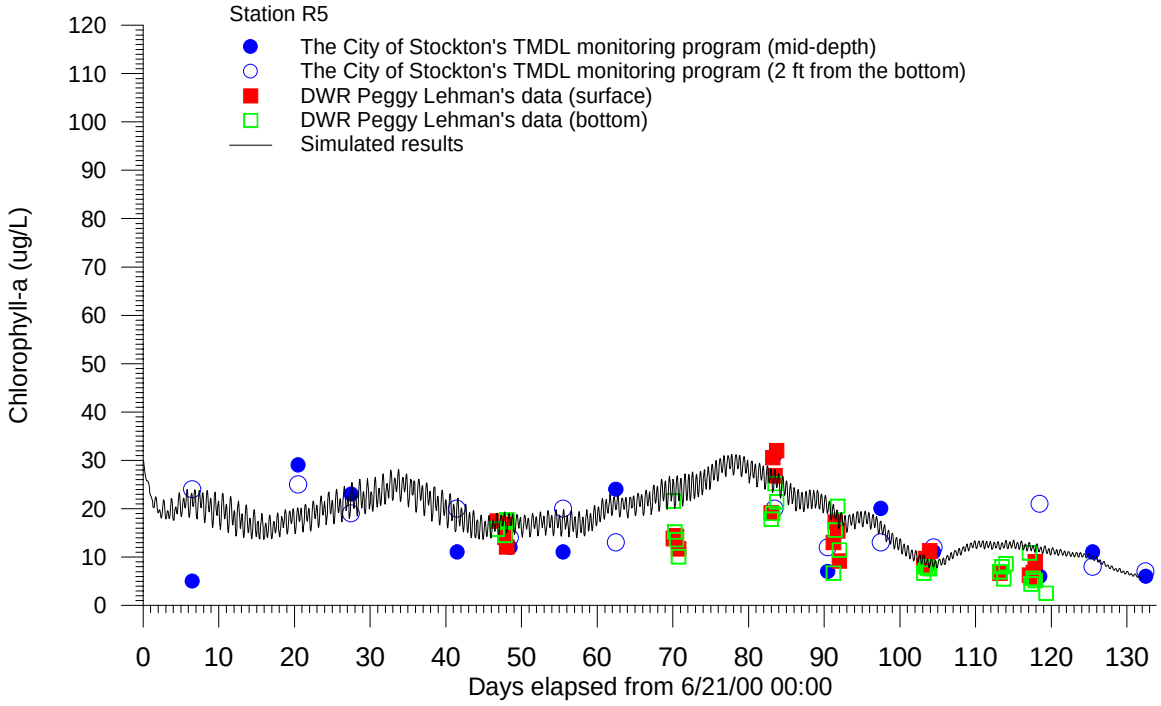

Figure III-56
Simulated and Observed Chlorophyll-a for Station R5, 2000.

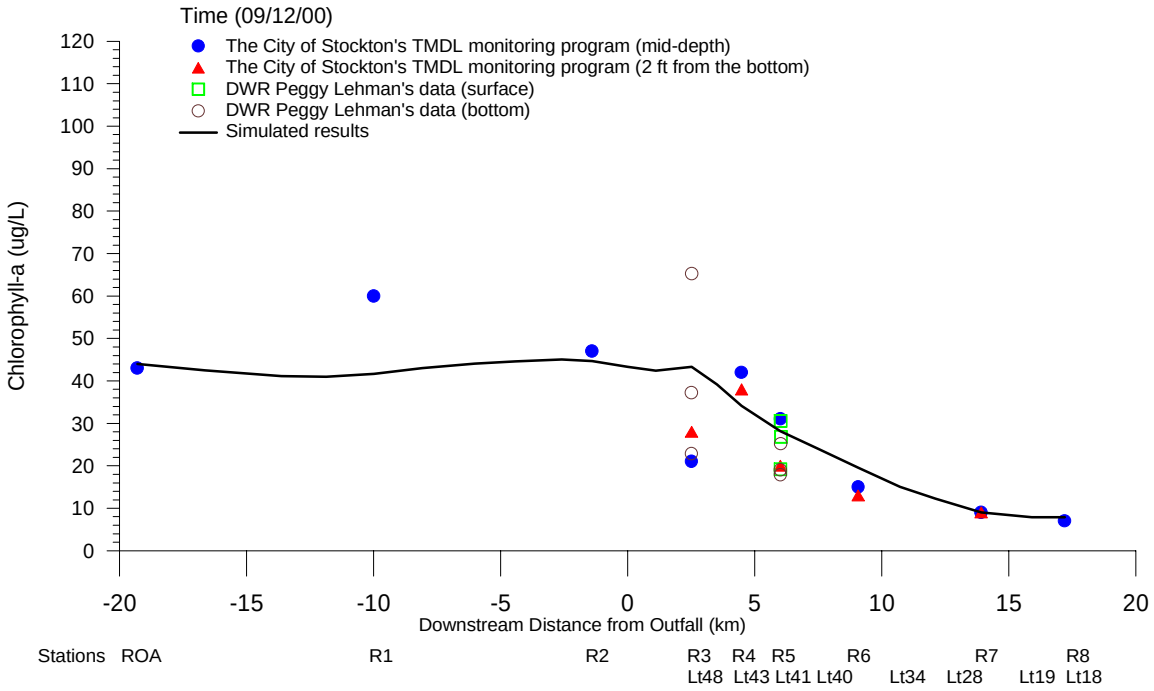

Figure III-57
Simulated and Observed Profile of Chlorophyll-a for 09/12/00.

Pheophytin Simulation

Figures III-58 and III-59 compare the simulated and observed pheophytin for stations R3 and R5 respectively. Figure III-60 compares the simulated and observed profile of pheophytin for September 12, 2000. The match was reasonable.

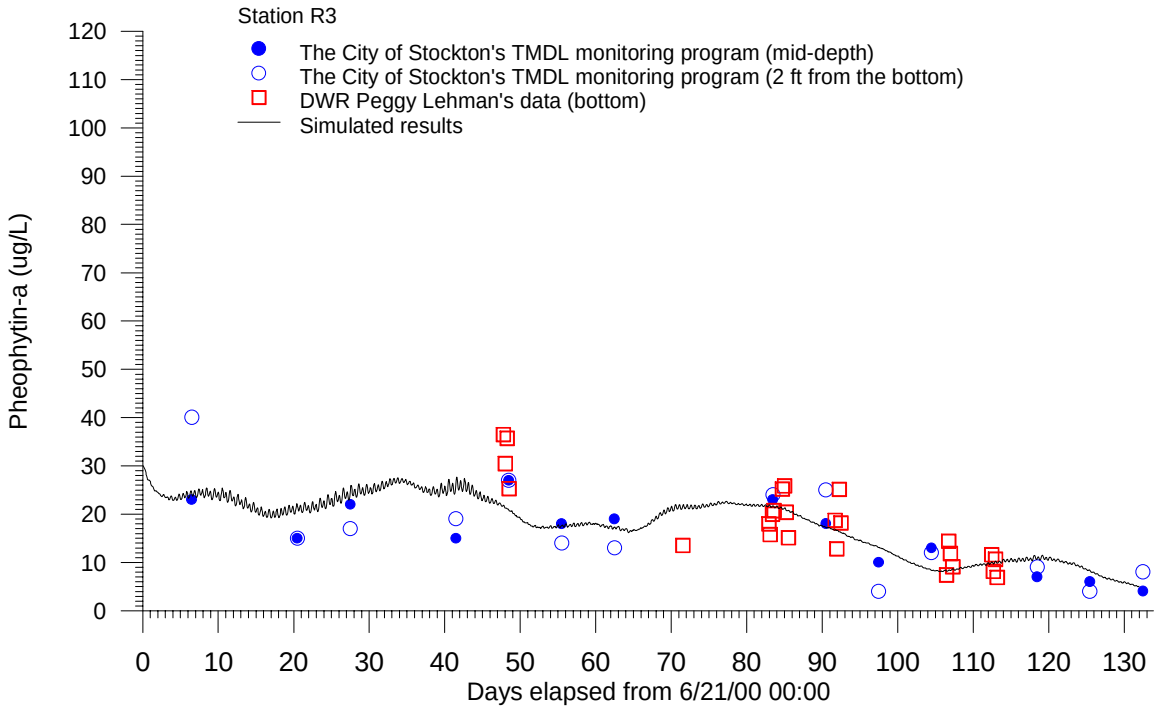

Figure III-58
Simulated and Observed Pheophytin for Station R3, 2000.

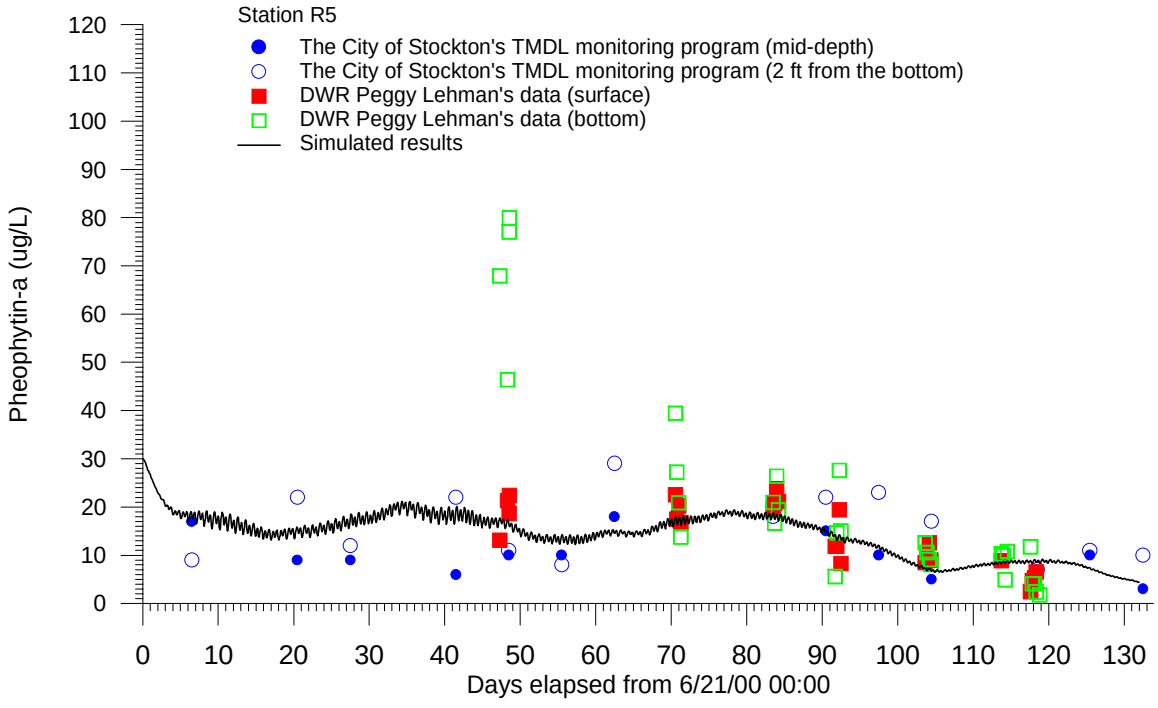

Figure III-59
Simulated and Observed Pheophytin for Station R5, 2000.

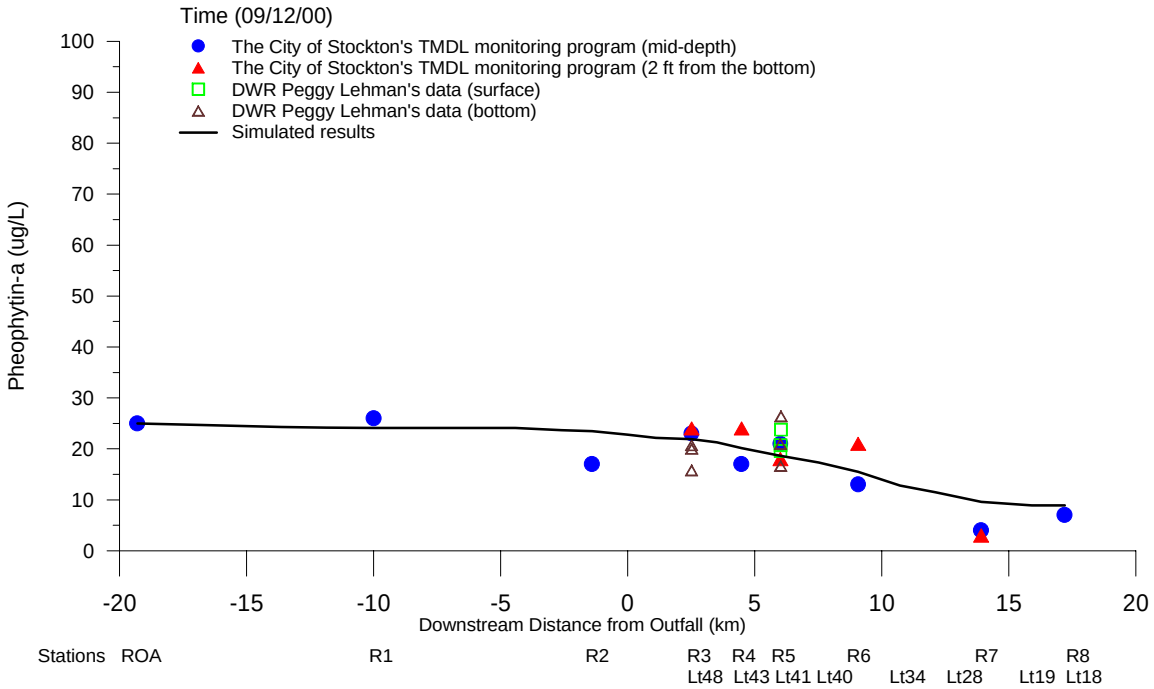

Figure III-60
Simulated and Observed Profile of Pheophytin for 09/12/00.

Ammonia Simulation

Figures III-61 and III-62 compare the simulated and observed ammonia for stations R3 and R5, respectively. Figure III-63 compares the simulated and observed ammonia profile in the San Joaquin River for September 12, 2000.

The model continued to show a rise in ammonia concentration due to higher ammonia discharge from Stockton RWCF from August to October of 2000. However, the river flow was higher in 2000 as compared to the flow in 1999. The river load of ammonia was also higher in year 2000 (Table III-2).

The model predicted a lower ammonia concentration for year 2000 than for year 1999 due to higher river flow and therefore higher dilution. The model also predicted a lower concentration gradient from R3 to R8. For some reason, the City of Stockton reported low ammonia concentration in a large number of samples for year 2000. Often, the concentrations were less than 0.2 mg/l, which was their detection limit. The low ammonia concentrations were reported when the RWCF effluent concentration was high. We suspect that there is a problem with the ammonia data for year 2000.

Dr. Peggy Lehman of DWR did report higher ammonia concentrations closer to the model predictions. Four of her values ranged from 0.15 to 0.8 mg/l at station R3 on September 12, 2000. On that day, the water might not have been well mixed.

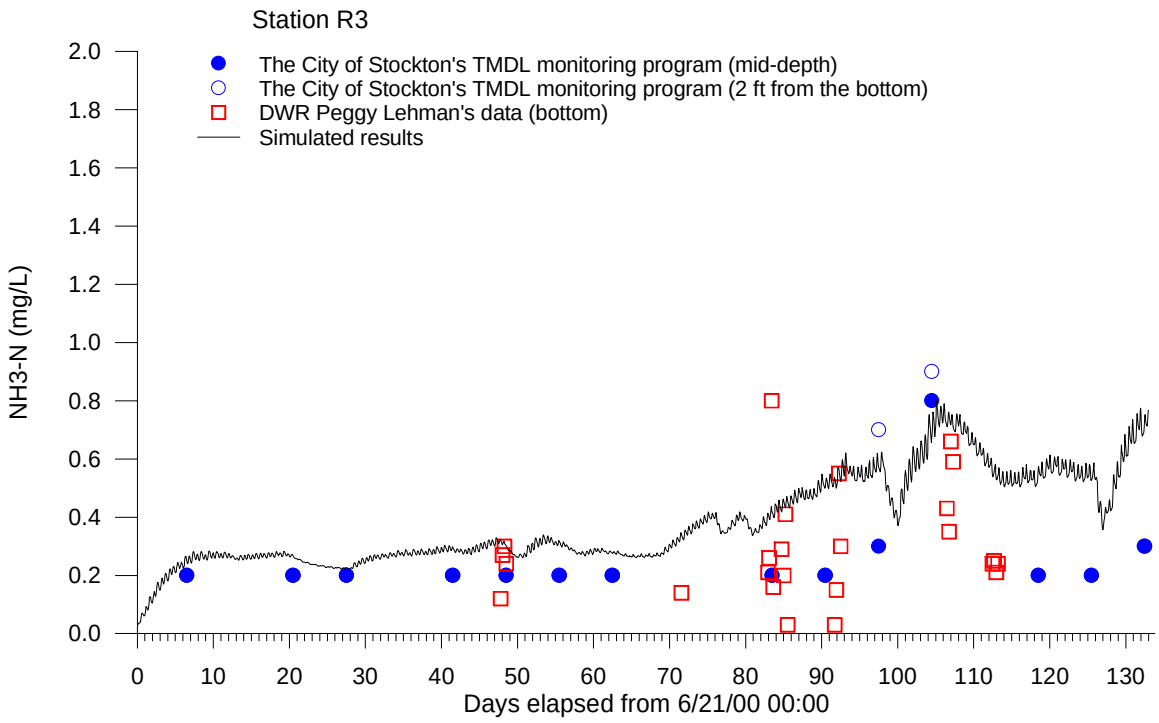

Figure III-61
Simulated and Observed Ammonia for Station R3, 2000

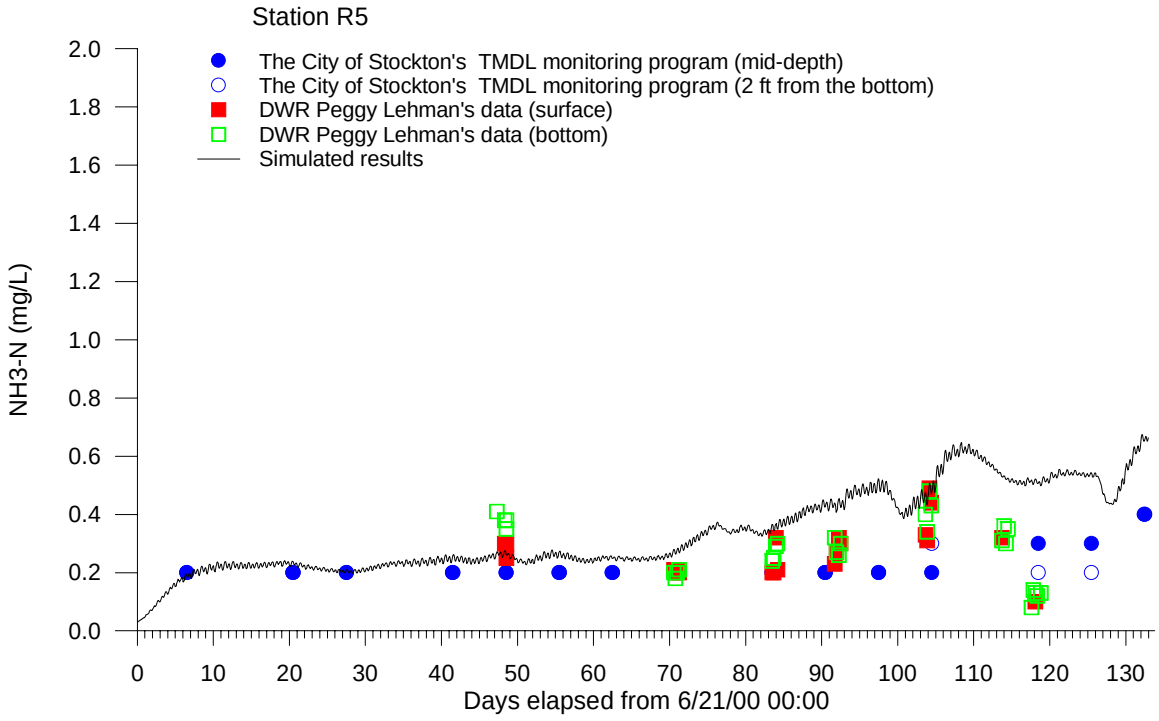

Figure III-62
Simulated and Observed Ammonia for Station R5, 2000.

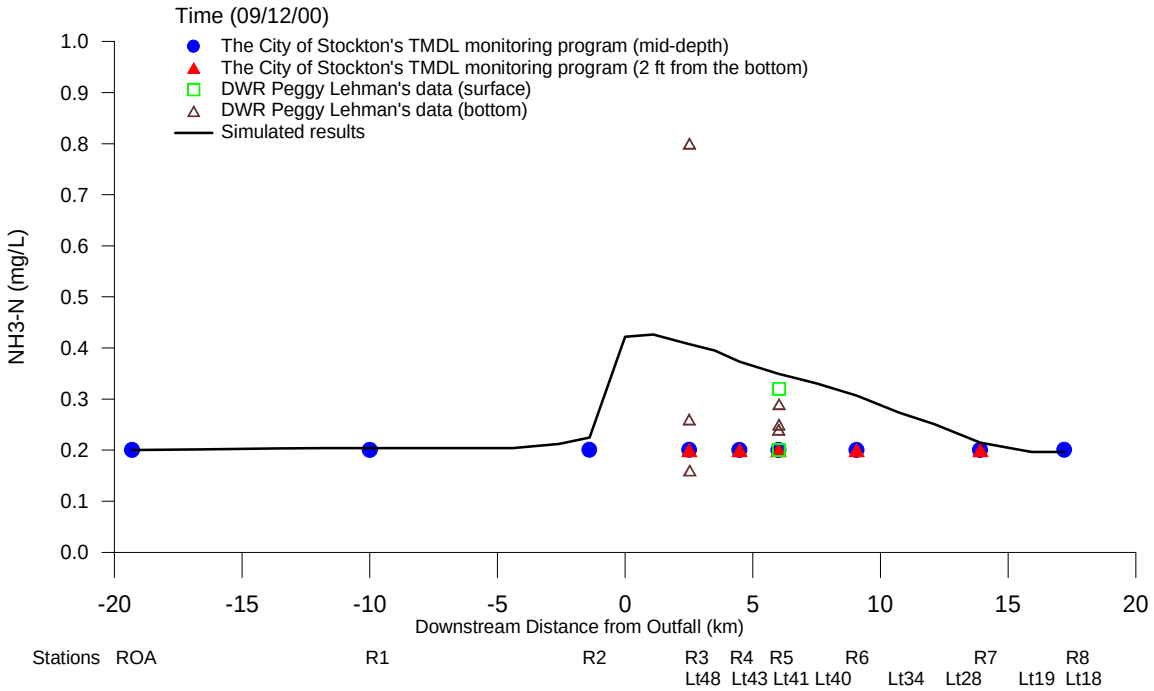

Figure III-63
Simulated and Observed Ammonia Profile for 09/12/00.

Nitrate Simulation

Figures III-64 and III-65 compare the simulated and observed nitrate for stations R3 and R5, respectively. Figure III-66 shows the simulated and observed concentration profile of nitrate for September 12, 2000.

The time series plots showed that the model tracked the seasonal variation of observed nitrate concentrations. The concentration profile showed that the model under predicted most nitrate concentrations for stations R3 through R8. Some data points did go as low as the model predictions.

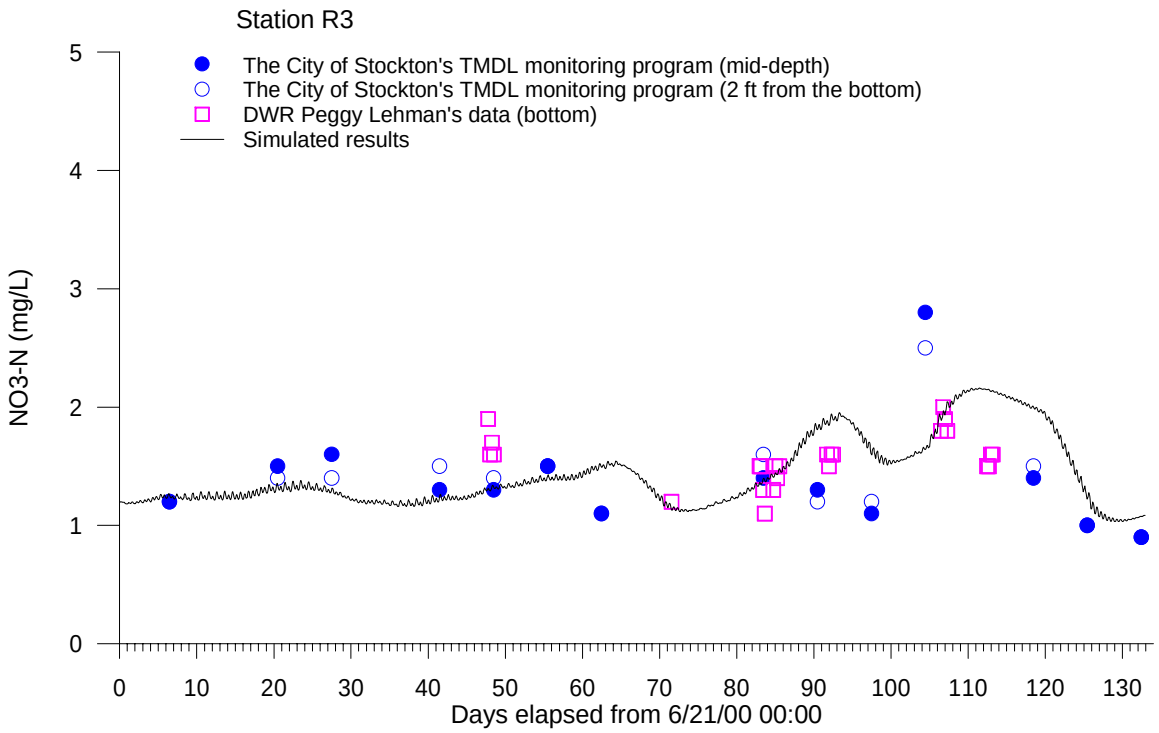

Figure III-64
Simulated and Observed Nitrate for Station R3, 2000.

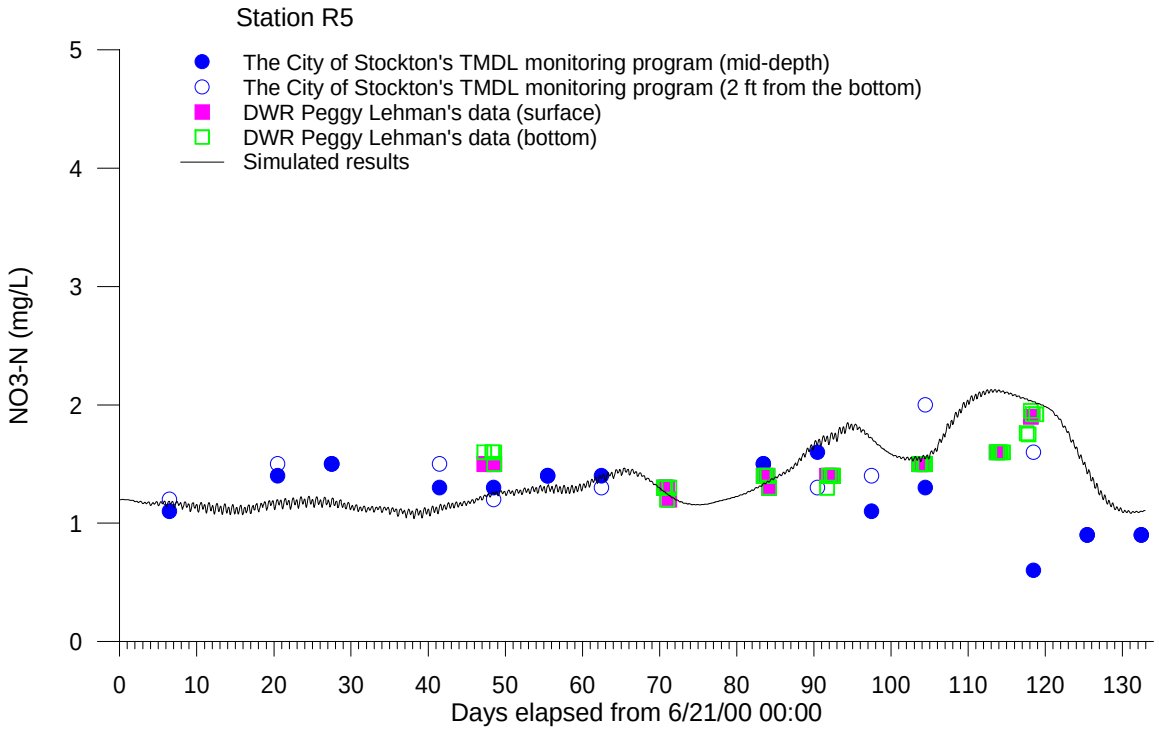

Figure III-65
Simulated and Observed Nitrate for Station R5, 2000.

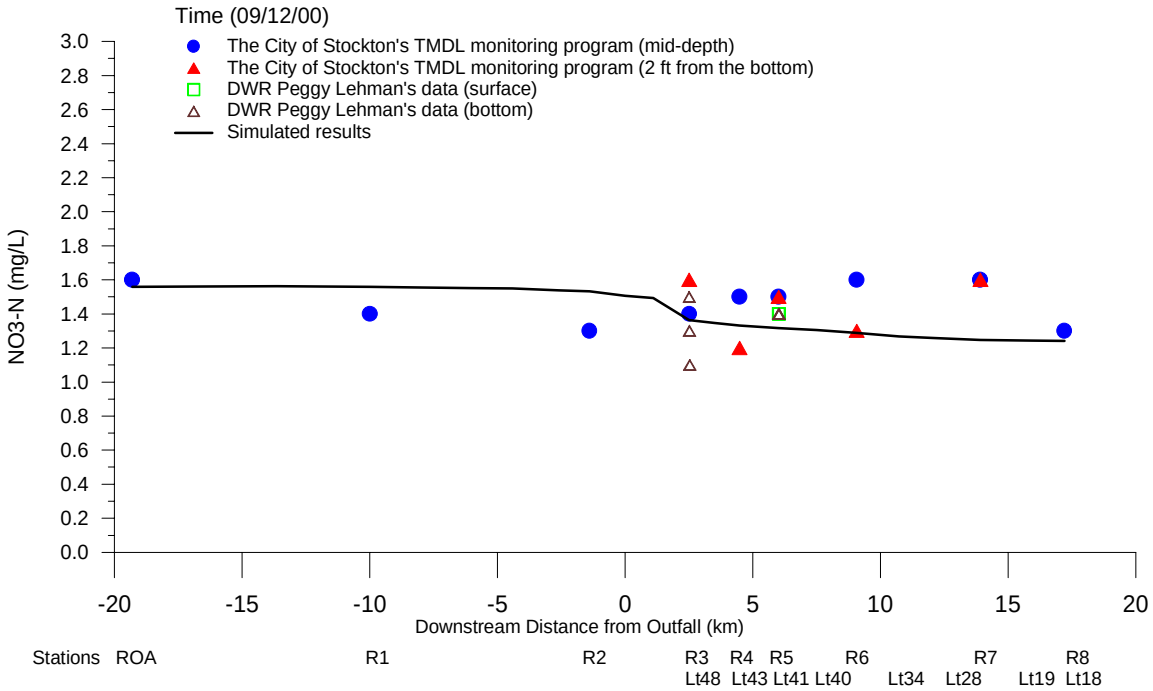

Figure III-66
Simulated and Observed Nitrate Profile for 09/12/00.

Phosphorus Simulation

Figures III-67 and III-68 compare the simulated and observed total phosphorus for stations R3 and R5 respectively. Figure III-69 compares the concentration profile of simulated and observed phosphorus for September 12, 2000. Overall, the model has tracked the observed values reasonably.

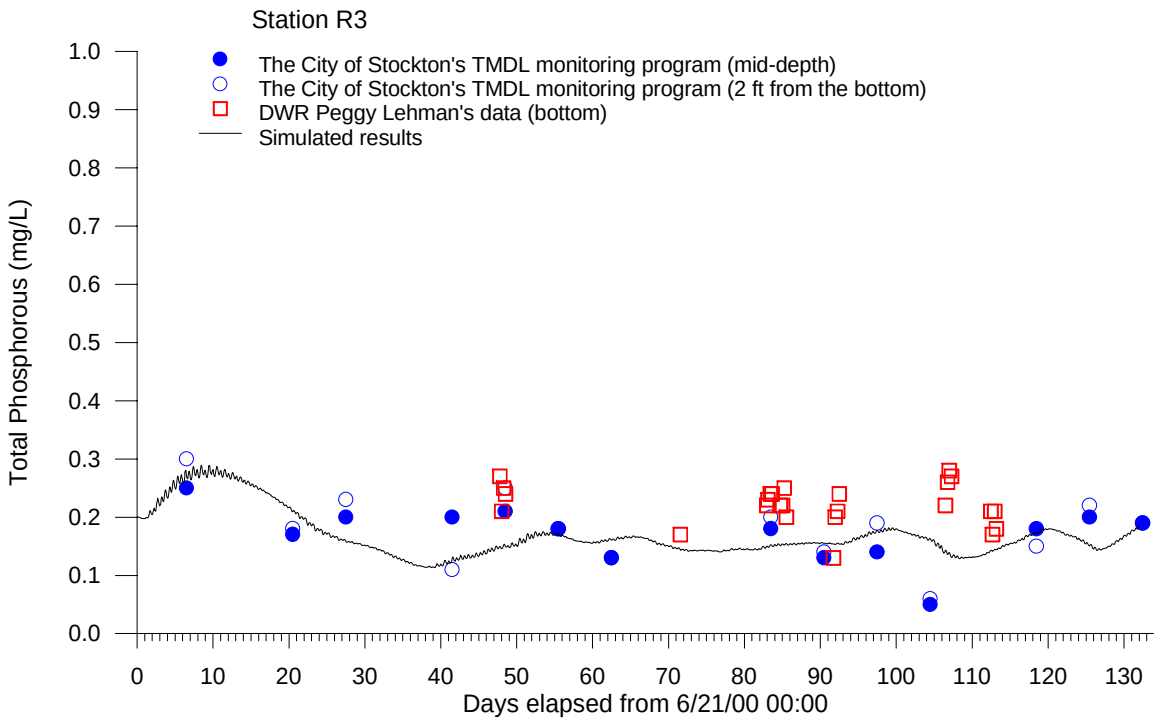

Figure III-67
Simulated and Observed Total Phosphorus for Station R3, 2000.

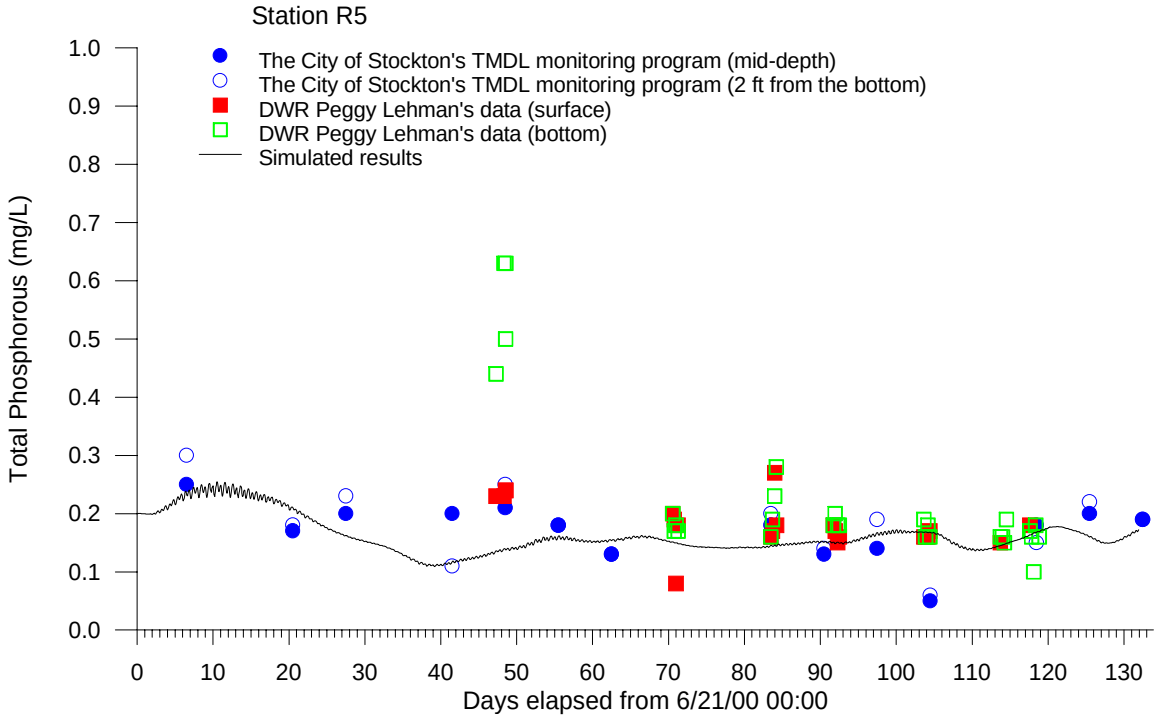

Figure III-68
Simulated and Observed Total Phosphorus for Station R5, 2000.

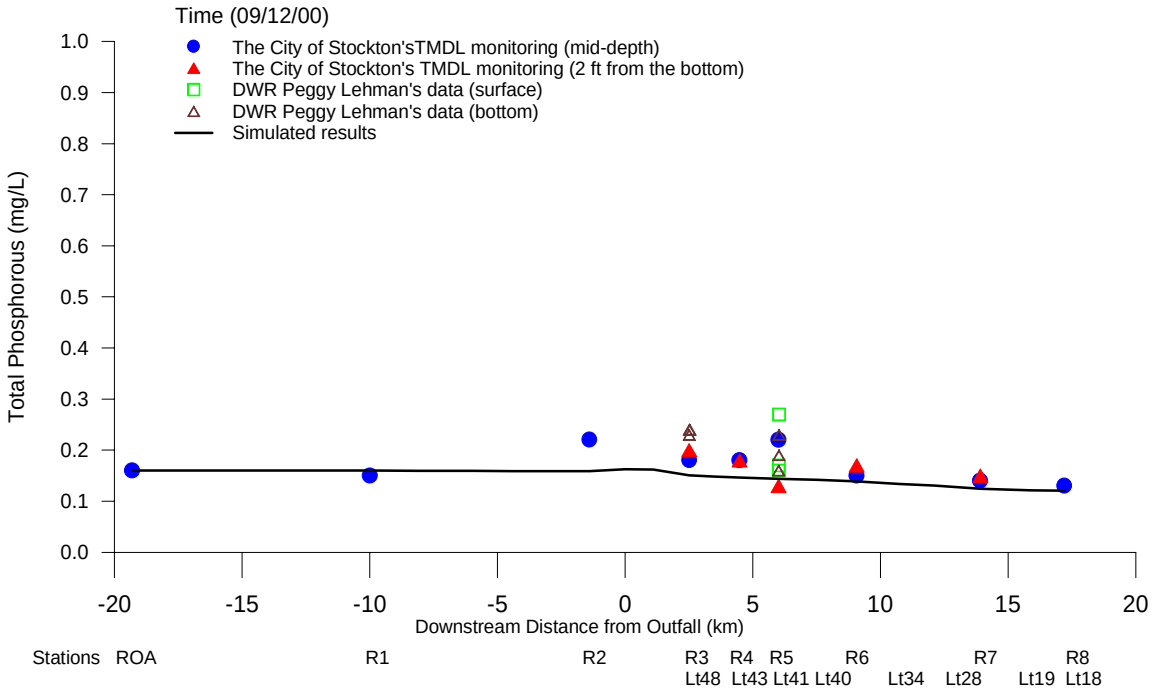

Figure III-69
Simulated and Observed Concentration Profile of PO4-P for 09/12/00.

TSS Simulation

Figures III-70 and III-71 compare the simulated and observed TSS for stations R3 and R5, respectively. Figure III-72 compares the simulated and observed concentration profile of TSS for September 12, 2000.

As it was in the case for 1999, the observed values of TSS varied widely. In general, the model matched the mid-depth values. The pattern of sedimentation indicated that highest sedimentation occurred at R4 in 1999 and at R3 in 2000.

Both the City of Stockton and Dr. Peggy Lehman of DWR reported very high TSS for stations R2 and R3 on September 12, 2000. The model could not account for those high values, because there was no exceptional high values in the river load data.

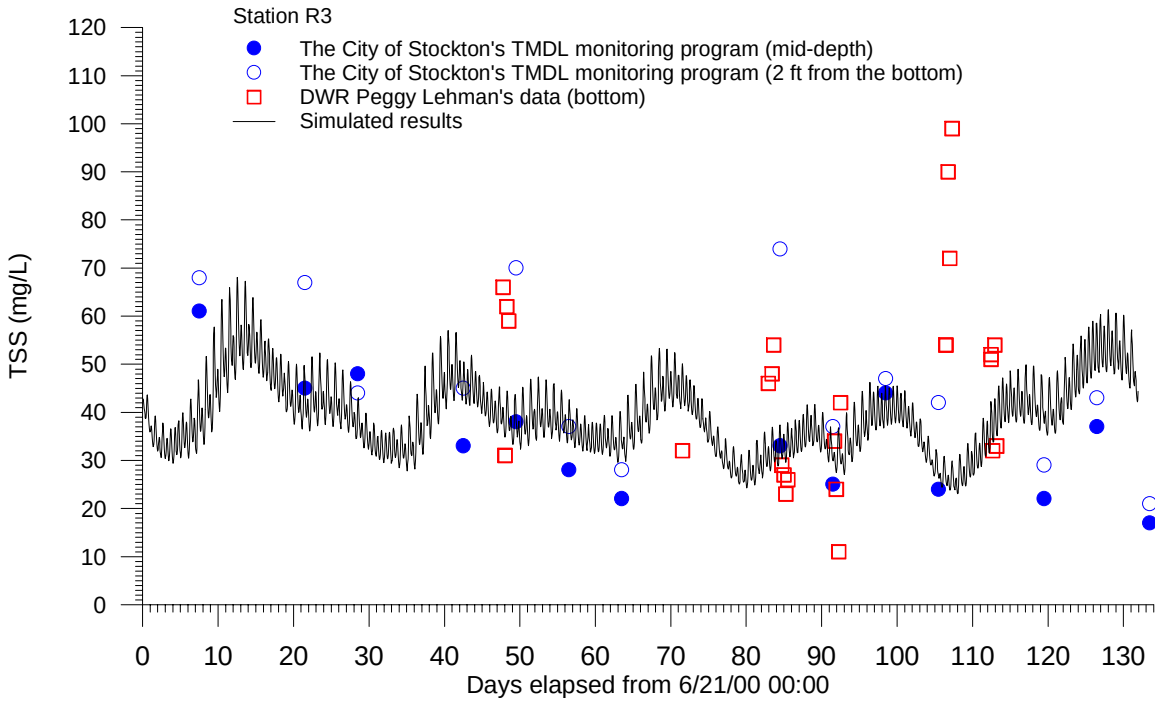

Figure III-70
Simulated and Observed Total Suspended Solids for Station R3, 2000.

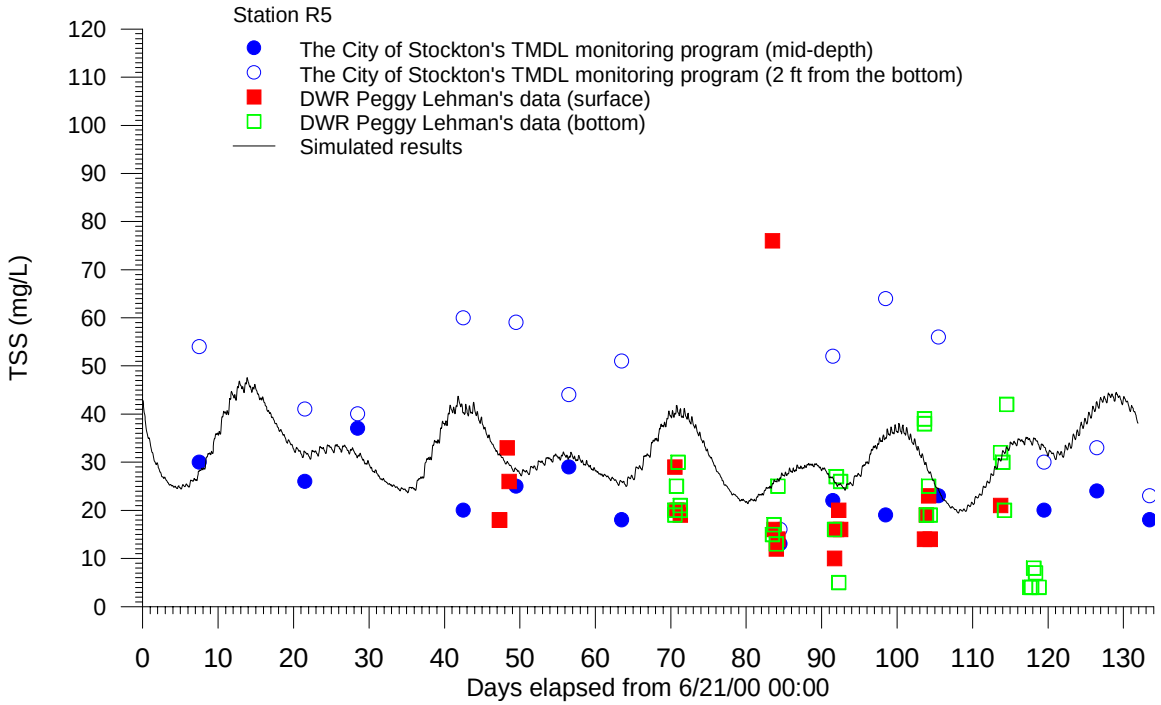

Figure III-71
Simulated and Observed Total Suspended Solids for Station R5, 2000.

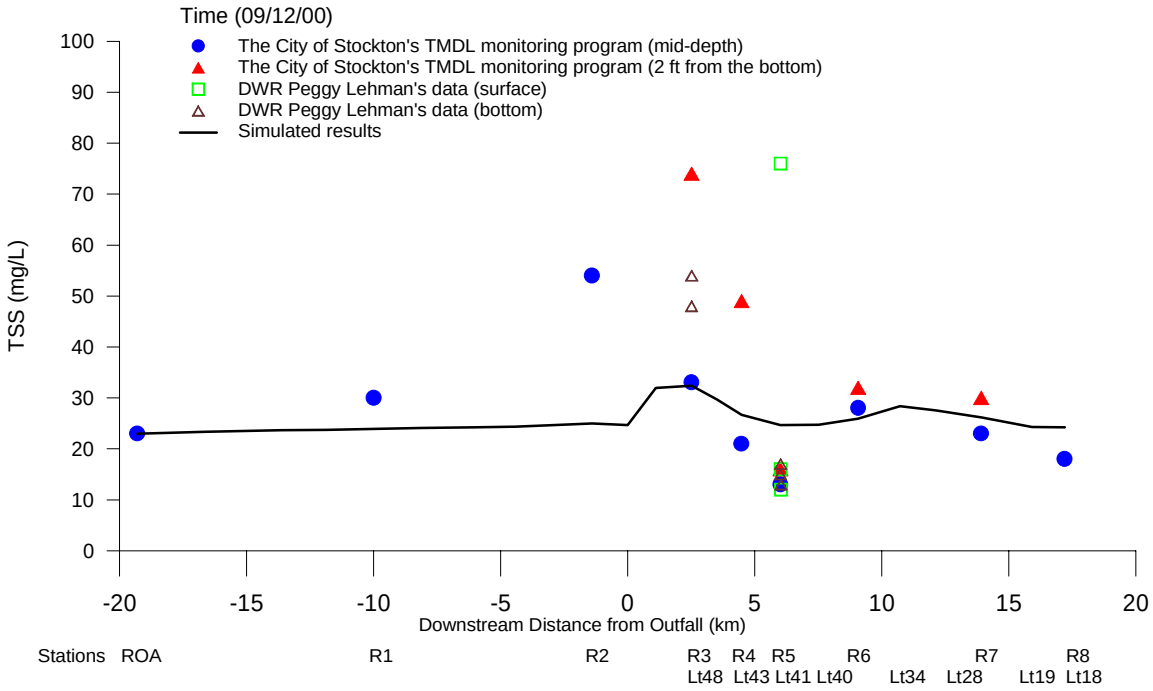

Figure III-72
Simulated and Observed Concentration Profile of TSS for 09/12/00.

VSS Simulation

Figures III-73 and III-74 compare the simulated and observed VSS for stations R3 and R5 respectively. Figure III-75 compares the simulated and observed concentration profile of VSS for September 12, 2000.

The model tracked the observed concentrations reasonably. As was in the case for 1999, most VSS brought in by the river load was retained in the Deep Water Ship Channel.

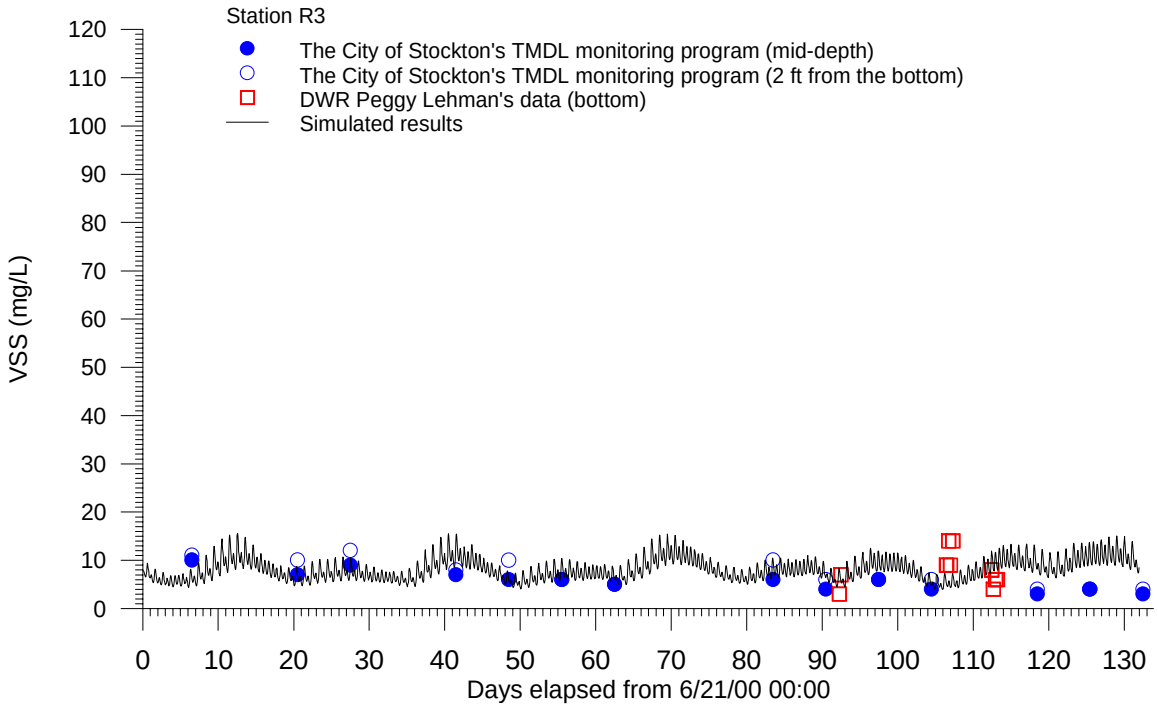

Figure III-73
Simulated and Observed VSS for Station R3, 2000.

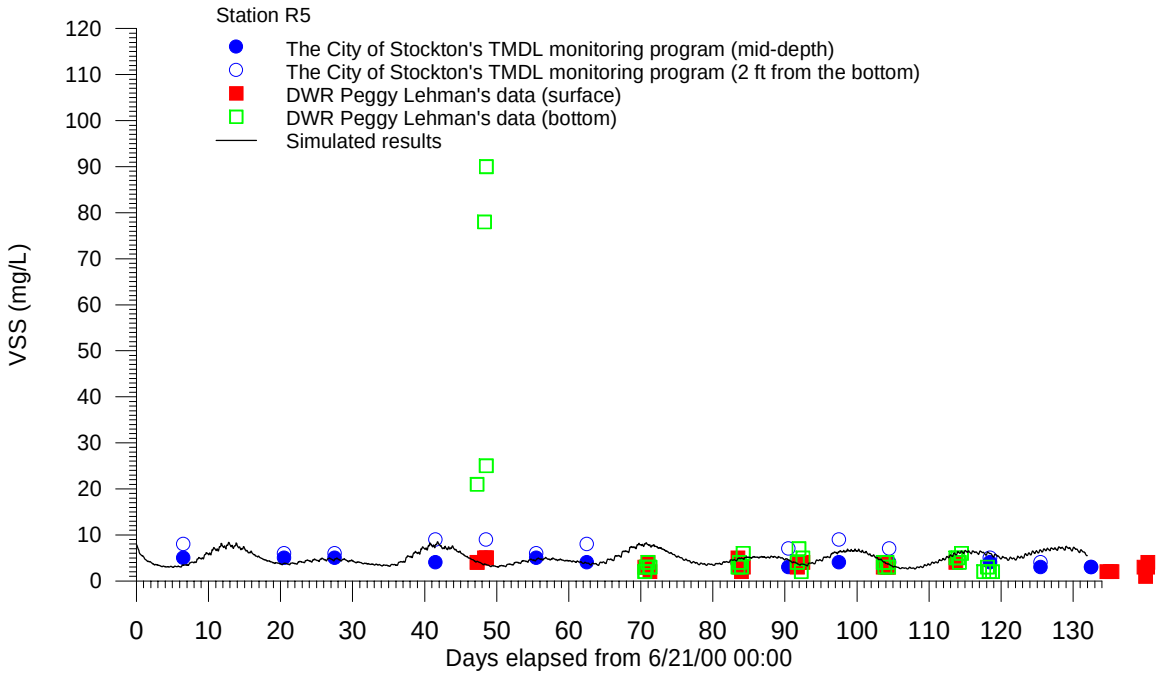

Figure III-74
Simulated and Observed VSS for Station R5, 2000.

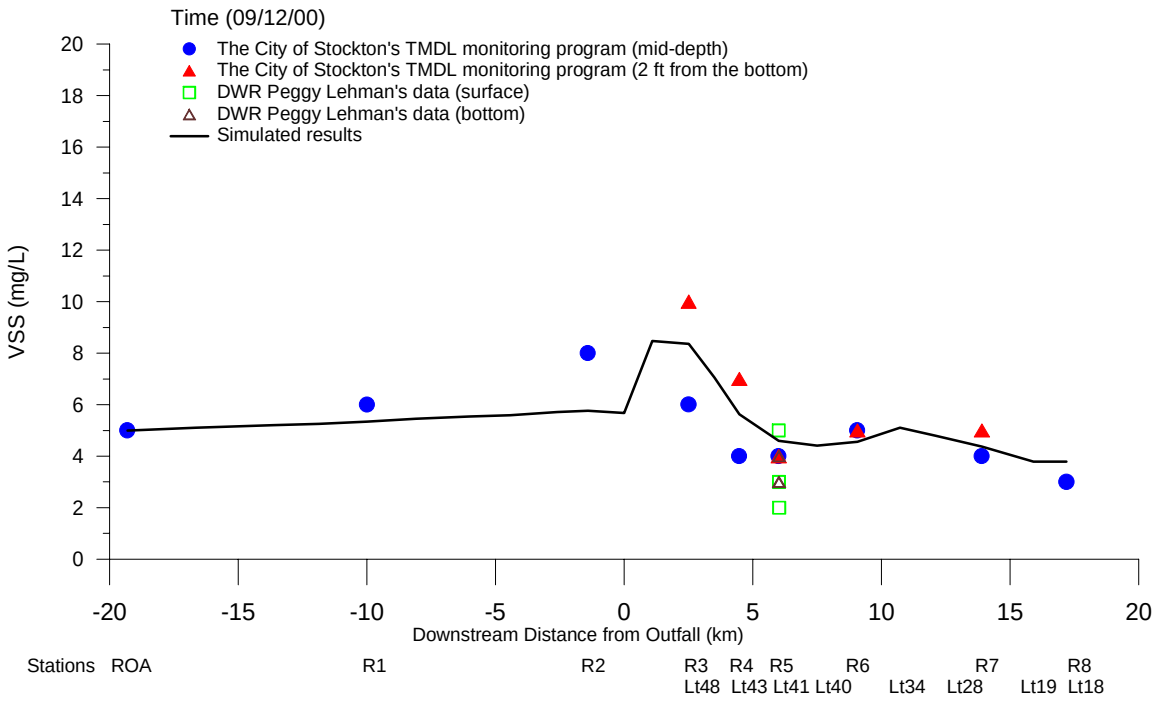

Figure III-75
Simulated and Observe Concentration Profile of VSS for 09/12/00.

2001 Simulation

Under a subcontract from Jones and Stokes, we ran the model for the year 2001 condition. Dr. Russ Brown of Jones and Stokes supplied the input data. We compiled other data needed for the model run.

For the 1999 and 2000 simulations, the meteorology data from Lodi station was used. This station no longer exists. We located a nearby Lodi West station as a substitute for the 2001 simulations.

The 2001 UVM flow data was incomplete. Dr. Russ Brown provided low and high estimates of UVM flow as shown in Figure III-76. Dr. Brown also furnished the concentrations of CBOD, ammonia, nitrate, phosphorus, chlorophyll, and pheophytin associated with the river flow.

Figure III-77 shows the Stockton discharge for 2001. The flow and effluent concentration data was obtained from the City of Stockton.

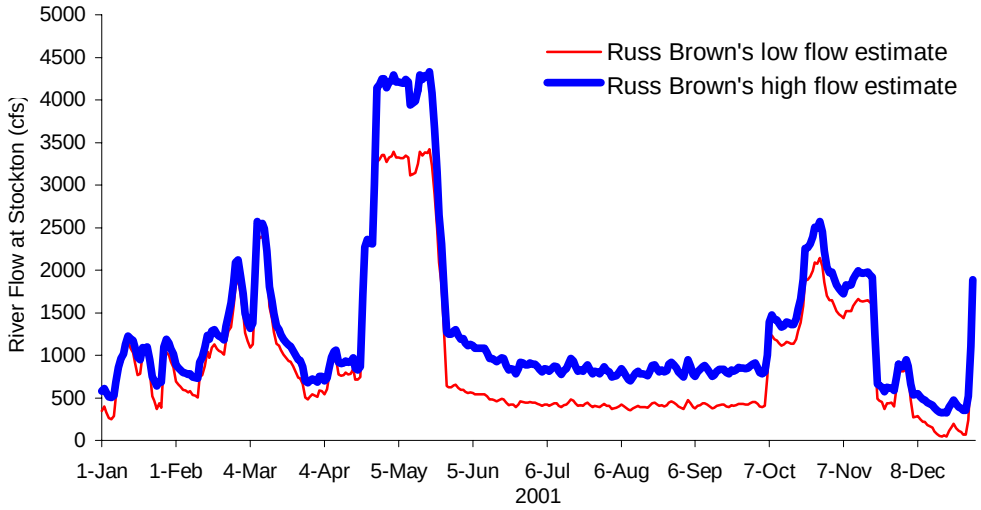

Figure III-76 UVM flow estimated by Dr. Russ Brown of Jones and Stokes.

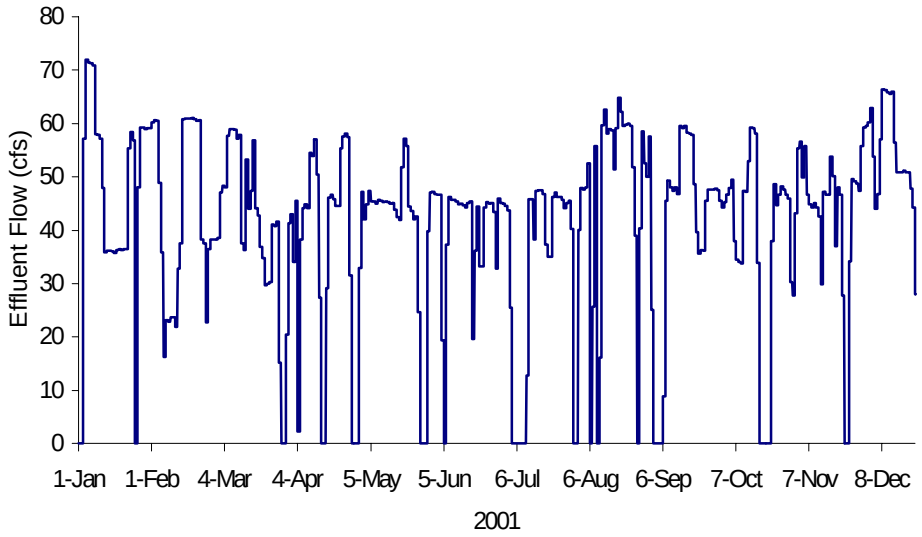

Figure III-77 Stockton Effluent Flow

Based on the data provided by Russ Brown of Dr. Jones and Stoke, the model was set up to run for the 2001 condition. The simulation was performed for both high and low estimates of UVM flows. The results for the high flow estimate were better.

The detailed model outputs were furnished to Dr. Russ Brown in spreadsheets. Dr. Brown will provide interpretations in his report. Figure III-78 compares the simulated and observed temperature at Rough & Ready Station. Figure III-79 compares simulated and observed DO at Rough & Ready Station. The model appears to work well for the 2001 condition, without any modification of calibrated coefficients.

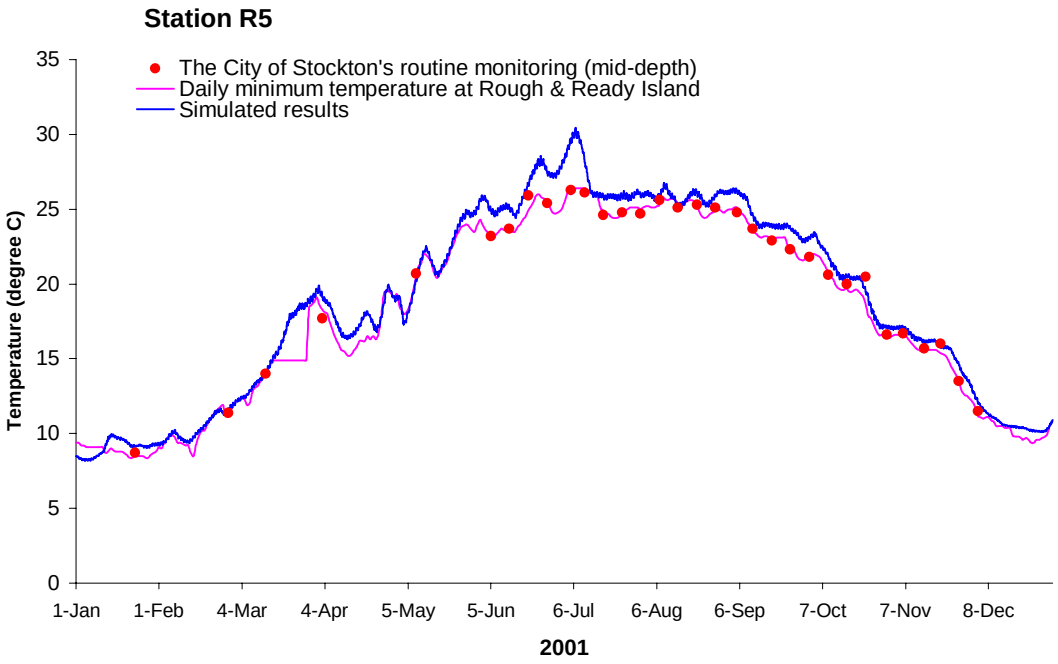

Figure III-78 Simulated and observed temperature for year 2001 at Rough & Ready Station

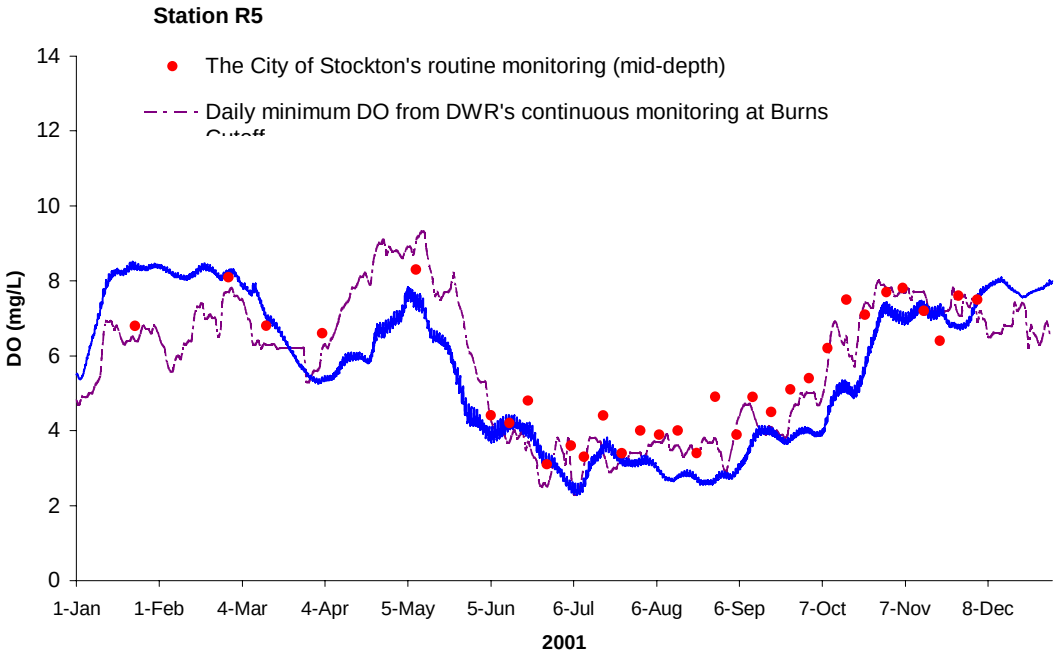

Figure III-79 Simulated and observed DO for year 2001 at Rough & Ready Station

As stated earlier, Dr. Russ Brown provided high and low estimates of UVM flows. The simulation with the higher estimate flow gave a better fit to observed DO. Figure III-80 shows the sensitivity of DO to the UVM flows.

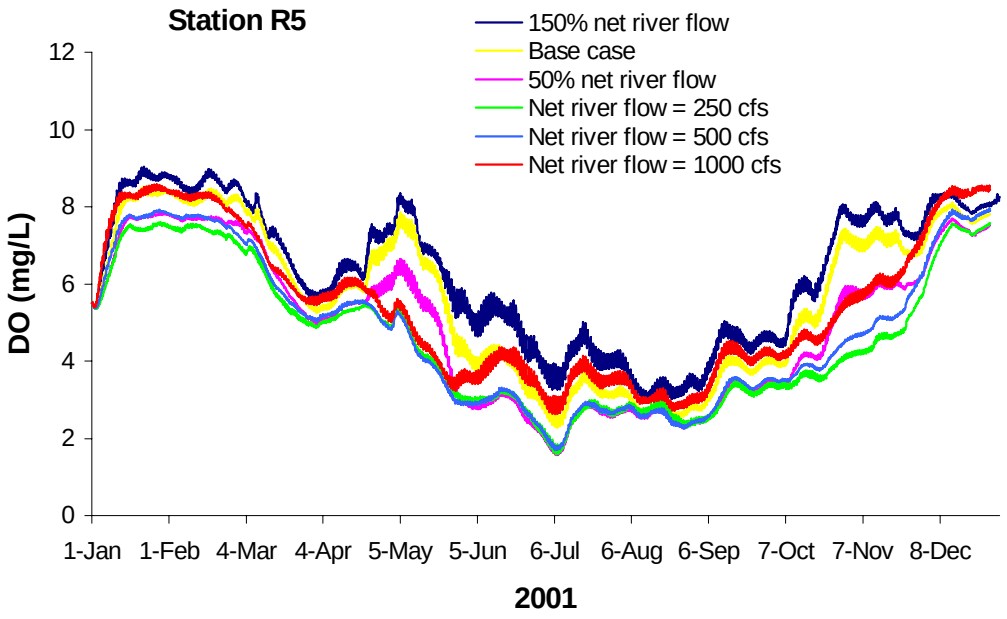

Figure III-80 Sensitivity of UVM flow on the DO at Rough & Ready Station for year 2001

Discussions

It was observed that there were more DO problems in 1999 than in 2000. This was caused by a number of factors. In the critical period of late fall, the river flow dropped drastically in 1999 (Figure III-2) and rose considerably in 2000 (Figure III-40). The water temperature in late fall was 18 degrees Celsius in 1999, about 2 degrees warmer than in 2000. During this critical period, the river load was also higher in 1999 (Figure VI-1) than in 2000 (Figure VI-2). The combined effect of those factors led to higher frequency of DO dropping below standard in 1999 than in 2000 sampling period.

The 2001 dataset is not very complete for UVM flow and river load. Without any adjustment made to the calibrated coefficients, however, the model appears to have simulated the 2001 condition well. This is remarkable considering the large number of estimates used to set up the model.

IV. Other Model Results

Introduction

The San Joaquin River DO model generates a large amount of outputs that can be dissected in many ways. In the previous chapter, we have compared the simulated and observed time series of data for various sampling stations and the concentration profile of water quality constituents for specific sampling dates.

In this chapter, we will make other comparisons that include frequency distribution and statistics. We will also compare the simulated and measured DO sinks and sources.

Frequency Distribution Analysis

The San Joaquin River DO model is driven by tides, meteorology, river flow (UVM), Stockton discharge etc. Each driving variable has its clock values (time series) collected by various agencies. The model integrates those time series to produce the time series of flow and water quality for various locations. The results are compared to clock values measured by still other investigators. Both timing and location can be off.

For that reason, the comparison of frequency distribution can sometimes be used to assess the reasonableness of model predictions. In this comparison, the time element is removed. The object is to determine whether the model predicted high, median and low values in the same frequency as the observed data.

The EPA model reviewers have requested the comparison of predicted and observed frequency distribution. In response to the request, we performed the analysis with 1996 data, which had a fairly complete data for the entire year. There were approximately 33 observations for each station, enough for the frequency distribution analysis. Figures IV-1 and IV-2 present the comparison of simulated and observed frequency distribution of DO for station R3 and R4, respectively. The match was excellent.

For 1999 and 2000, there are insufficient data points for individual stations. By pooling together the stations (R3 to R6) in the Deep Water Ship Channel, we can remove location element of the data, resulting with 68 data points for 1999 sampling period and 56 data points for 2000 sampling period. Figures IV-3 and IV-4 compare the simulated and observed frequency distributions of DO for 1999 and 2000, respectively.

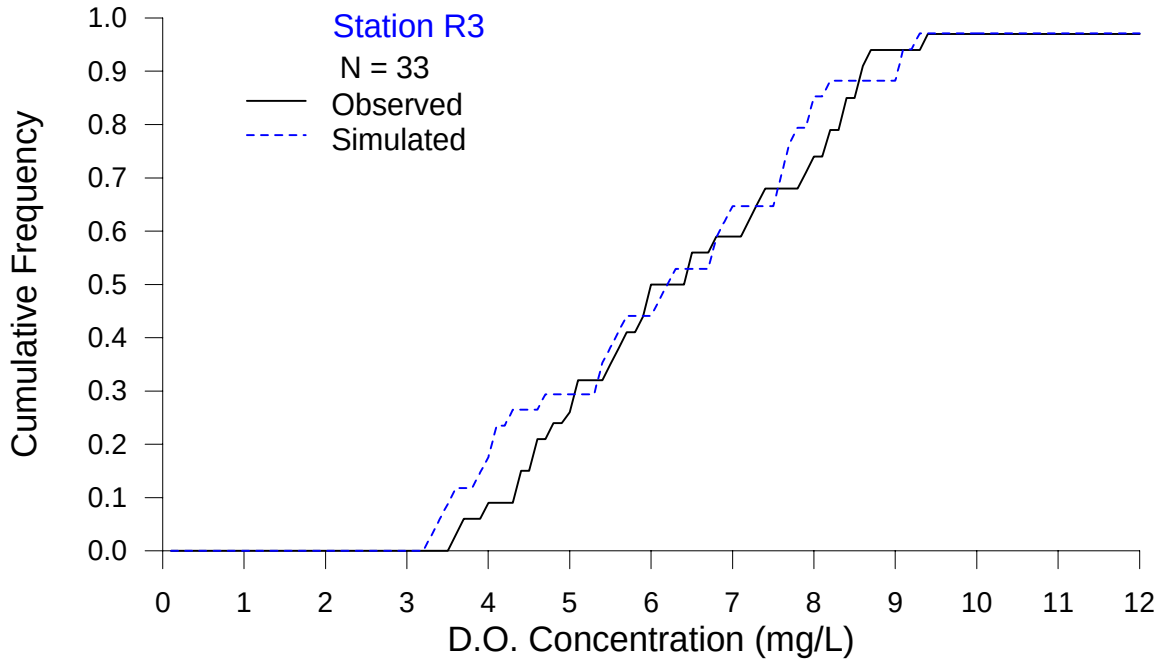

Figure IV-1
Simulated and Observed Frequency Distribution of DO for R3, 1996

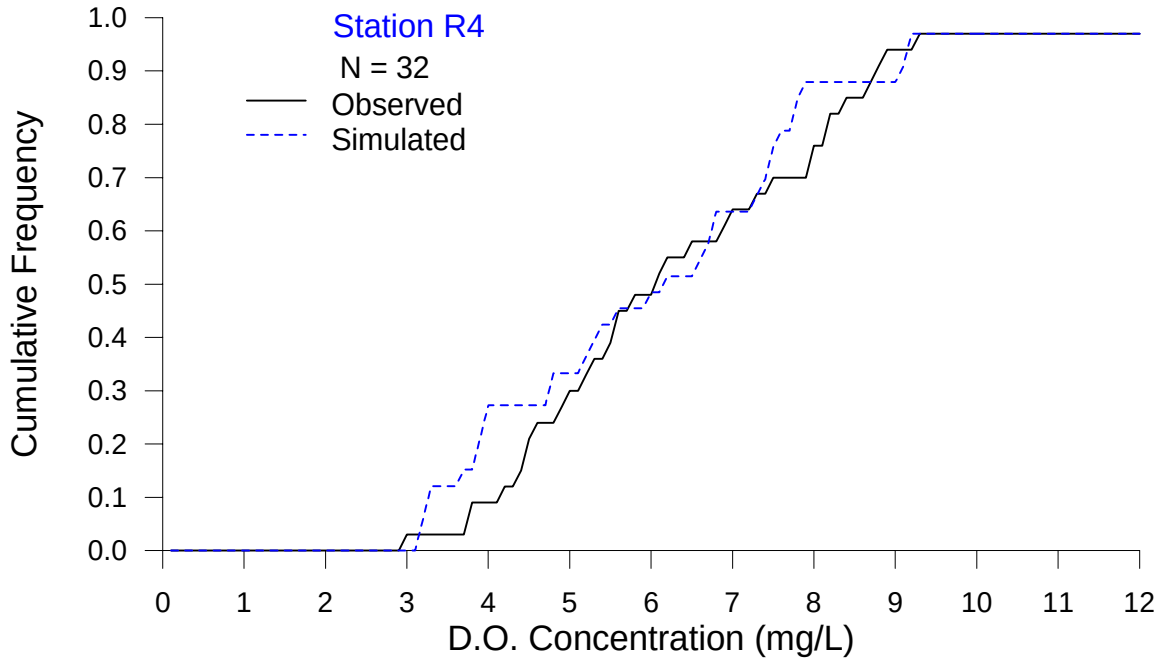

Figure IV-2
Simulated and Observed Frequency Distribution of DO for R4, 1996

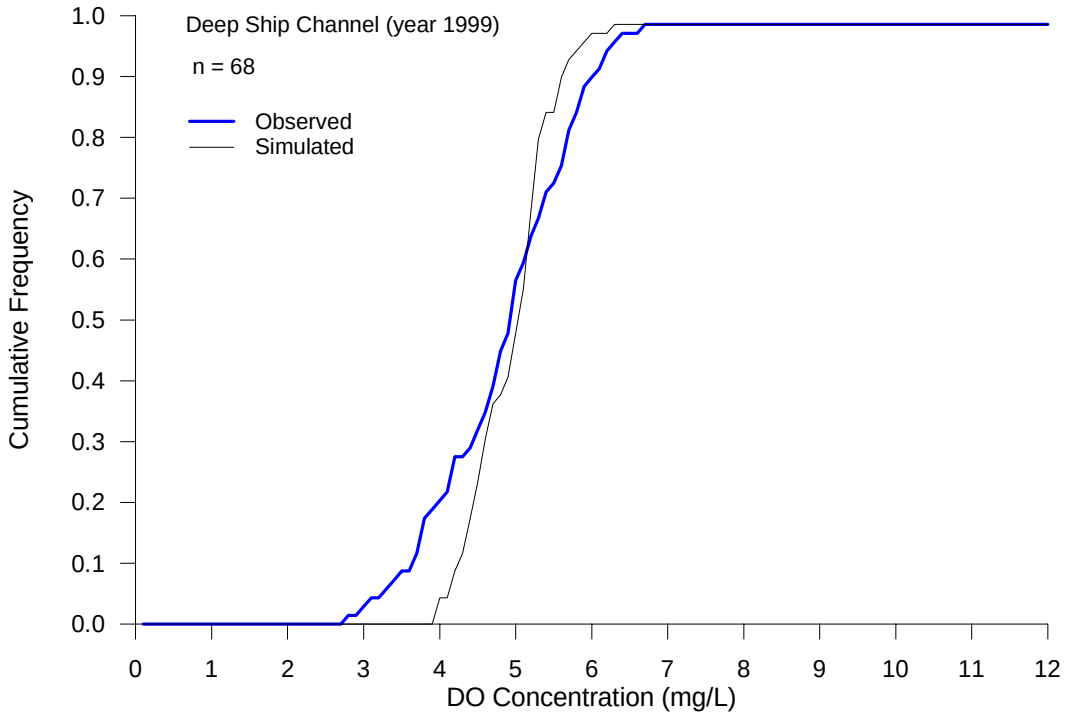

Figure IV-3
Simulated and Observed Frequency Distribution of DO in DWSC, 1999.

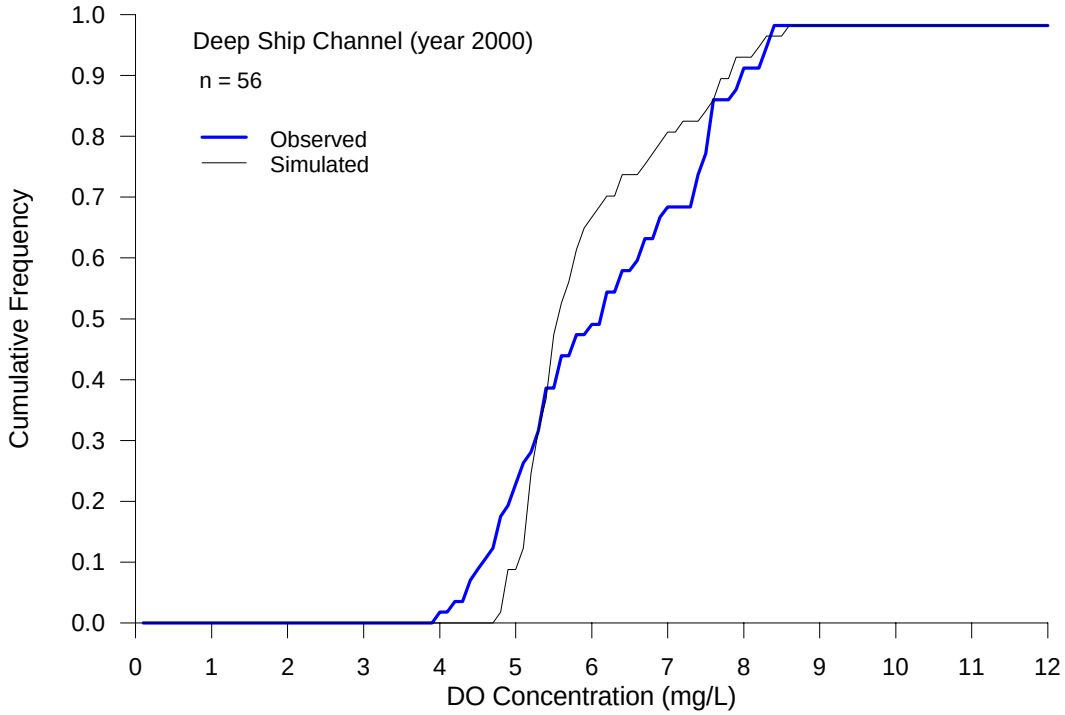

Figure IV-4
Simulated and Observed Frequency Distribution of DO in DWSC, 2000.

The number of data points is relatively small. There is also a question about whether the data points are representative of the Deep Water Ship Channel. However, the result shows that the model under predicted the low DO values for 1999 and 2000. This is not new information. Rather, it is the restatement of previous observation that the model did not track the episodic low DO.

Statistics

The range, average, mean relative error and mean absolute error of predicted DO were computed. The error was defined as the difference between the simulated and observed DO values for comparable time and location. The mean relative error was the average of the errors by allowing over prediction to cancel out the under prediction. The mean absolute error does not allow the over prediction to cancel out the under prediction.

Table IV-1 presents the results. Again, the model missed the low values of DO for both 1999 and Year 2000. During the year 1999 sampling period, the mean DO for the observed was 4.9 mg/l, compared to 4.9 mg/l for the simulated. The mean relative error was 0.1 mg/l and the mean absolute error was 0.59 mg/l. During the year 2000 sampling period, the mean DO for the observed was 6.2 mg/l, compared to 5.9 mg/l for the simulated. The mean relative error was –0.25 mg/l and the mean absolute error was 0.59 mg/l.

Table IV-1
Statistics of Simulated and Observed DO in DWSC

Parameters	Year 1999 Sampling Period	Year 2000 Sampling Period
Number of data points	68	56
Range of Observed DO, mg/l	2.8-6.7	4.0-8.4
Range of Simulated DO, mg/l	3.9-6.2	4.8-8.5
Mean of Observed DO, mg/l	4.9	6.2
Mean of Simulated DO, mg/l	4.9	5.9
Mean Relative Error, mg/l	0.1	-0.25
Mean Absolute Error, mg/l	0.59	0.59

Light Attenuation

The model calculates the light extinction coefficient as a function of suspended particles (i.e. the concentrations of TSS, VSS, and algae) in the water column. Thus, the light extinction coefficient can vary dynamically with the change of water turbidity.

Based on the simulated concentrations of TSS, VSS, and chlorophyll at station R3, the maximum light extinction coefficient was 1.46 per foot. The minimum light extinction coefficient was 0.55 per foot. Figure IV-5 compares the light attenuation curve measure

by Dr. Gary Litton of the University of Pacific on September 14, 2000 to the range of light attenuation curves predicted by the model.

In mid September, the model predicted low concentrations of TSS, VSS, and chlorophyll at R3. The measured light attenuation curve appears to match the predicted curve for the minimum light extinction coefficient.

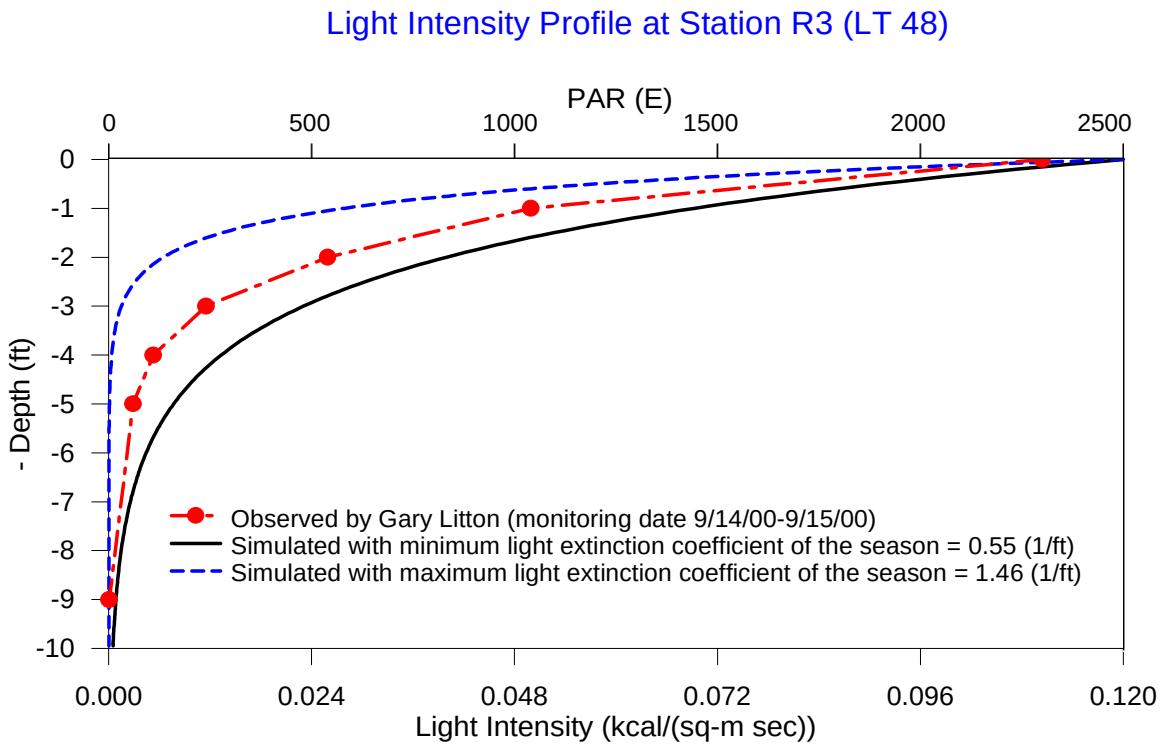

Figure IV-5
Observed and Simulated Range of Light Attenuation Through Water Column at R3

Algae in Turning Basin

As explained in Chapter II, the model could not simulate the high chlorophyll-a concentrations observed in the Turning Basin. This is because the model mixed the algae concentration to the entire water column. Biologists indicated that the algae, in the Turning Basin, resist vertical mixing. For that reason, the model was enhanced to accept the input data of mixing depth for algae.

A model simulation was performed with a mixing depth of 2 feet from the surface. Figure IV-6 and IV-7 present the simulated surface chlorophyll-a concentrations in the Turning Basin for 1999 and 2000, respectively.

The model results were compared to the data collected by Dr. Steve Hayes and Dr. Peggy Lehman, both of DWR. The model matched the observed data very well. The only exceptions were the 3 extreme low values measured by Dr. Peggy Lehman.

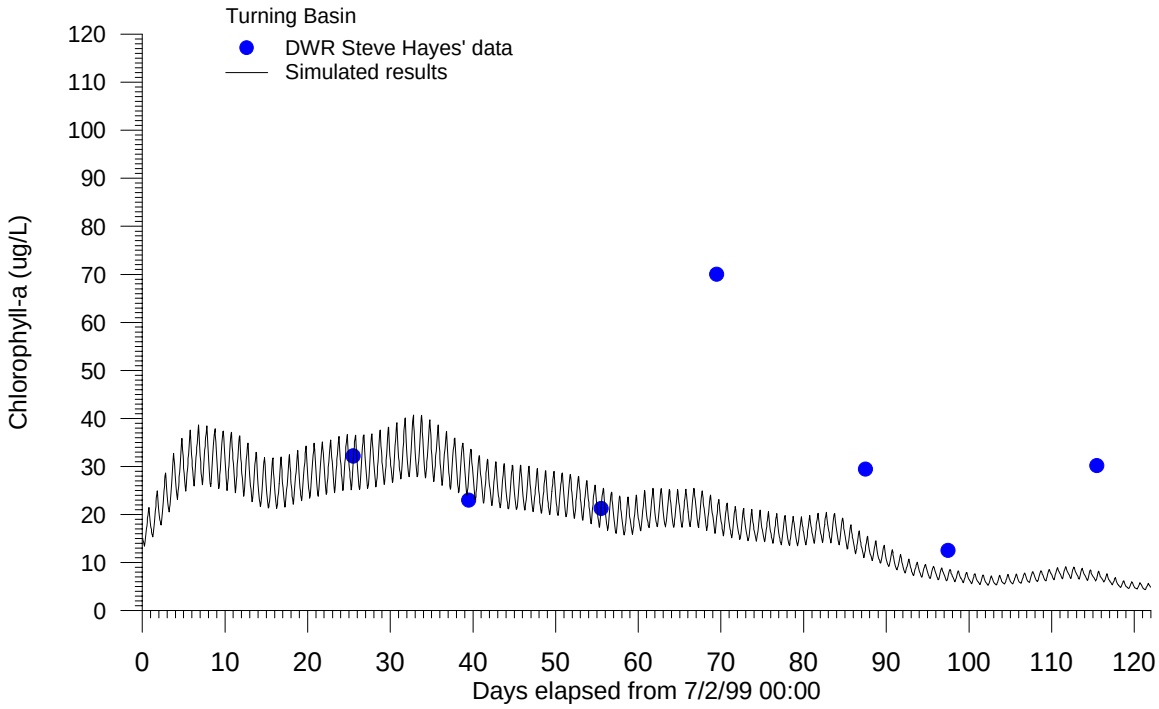

Figure IV-6
Simulated and Observed Surface Chlorophyll at Turning Basin, 1999.

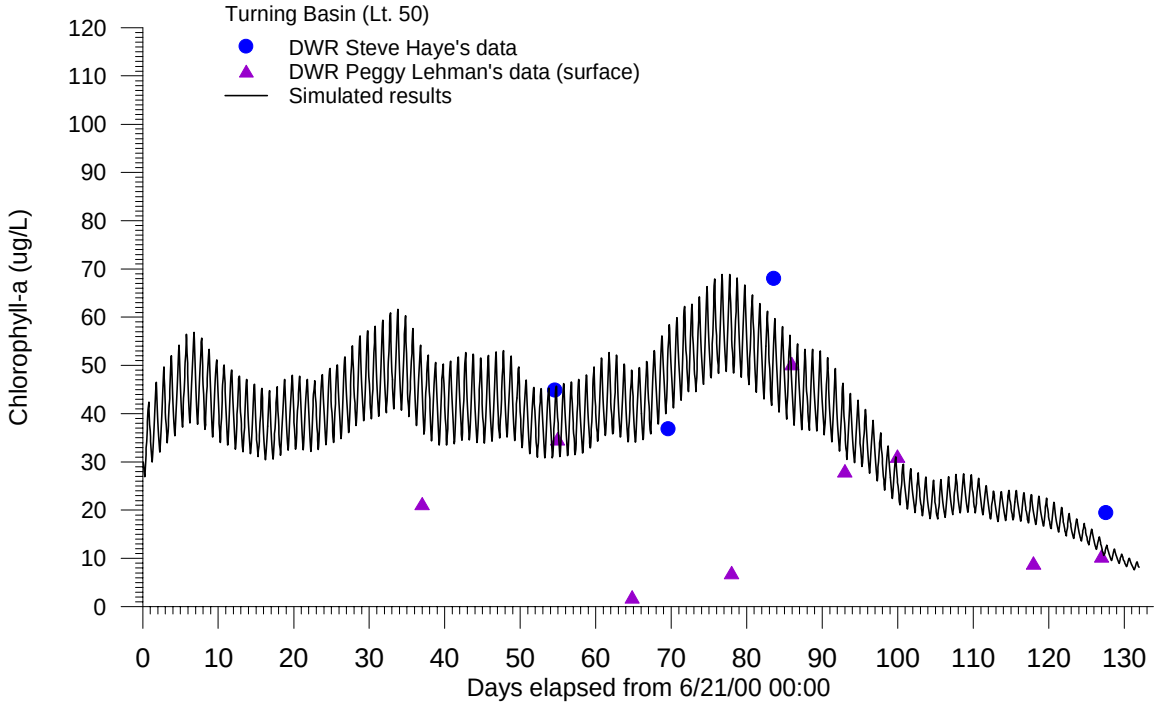

Figure IV-7
Simulated and Observed Surface Chlorophyll at Turning Basin, 2000.

Sinks and Sources of DO

The model calculates the hourly individual sink and source terms for each node. The sink terms include algae respiration, ammonia nitrification, sediment oxygen demand (SOD), and others (CBOD & VSS). The source terms include surface aeration and photosynthesis. Surface aeration can be a sink or a source depending on whether DO is super saturated. In DWSC, the surface aeration was a source.

The hourly sinks and sources of DO were averaged for each month over the 1999 and 2000 sampling periods. The sinks and sources for all nodes in DWSC were added to provide some idea about the important factors influencing the DO in the DWSC.

Tables IV-2 and IV-3 show the results for year 1999 and year 2000, respectively. Source terms have positive values and sink terms have negative values, all in Kg O_2/day.

Table IV-2
Monthly Simulated Fluxes of DO Sinks and Sources in DWSC, 1999.

Locations	Algae Photo Kg O_2/day	Algae Respiration Kg O_2/day	Ammonia Nitrification Kg O_2/day	SOD Kg O_2/day	BOD & VSS Kg O_2/day	Aeration Kg O_2/day
July	1080	-2700	-700	-1830	-4900	2900
August	960	-2500	-1200	-1800	-5100	2900
September	640	-1700	-2200	-1700	-6900	3600
October	210	-660	-2300	-1600	-5300	3400
Average	700	-1900	-1600	-1700	-5500	32000

Table IV-3
Monthly Simulated Fluxes of DO Sinks and Sources in DWSC, 2000.

Month	Algae Photo Kg O_2/day	Algae Respiration Kg O_2/day	Ammonia Nitrification Kg O_2/day	SOD Kg O_2/day	BOD & VSS Kg O_2/day	Aeration Kg O_2/day
June	2150	-4800	-960	-1900	-3200	2400
July	1770	-4500	-1400	-1870	-2900	2680
August	1600	-4200	-1600	-1900	-3050	2500
September	1600	-4390	-2080	-1720	-3040	1900
October	590	-1840	-2130	-1480	-3050	2200
Average	1500	-3900	-1600	-1800	-3000	2300

The differences between 1999 and 2000 results (Table IV-2 and Table IV-3) can be explained by the differences in the pollution loads (Table III-1 and Table III-2). The 1999 CBOD load was higher than the 2000 CBOD load, which led to a higher 1999 DO sink for CBOD and VSS (others). . The aeration flux for 1999 was higher, because the simulated DO was lower. The 1999 river load of algae (50 kg/d) was lower than the 2000 algae load (110 kg/day). Both algae respiration and algae photosynthesis were lower in 1999 than in 2000. Thus, the algae concentrations in DWSC were maintained through a continuous influx of algae in the river load

Because DWSC is a dynamic system, there was a monthly shift of fluxes for the DO sinks and sources. The DO sink due to ammonia nitrification increased from summer to fall, because of increasing ammonia load from Stockton RWCF. The decreasing trends of algae photosynthesis and algae respiration were caused by the decreasing trend of solar radiations from summer to fall. The decreasing trend of SOD from summer to fall was caused by decreasing water temperature.

Dr. Peggy Lehman of DWR used light and dark bottle experiments to measure the depth of photic zone, net photosynthesis in photic zone and respiration in aphotic zone in DWSC during the 2000 sampling period. The measurements were made in 7 sections on the main ship channel.

The data was used to calculate the photosynthesis, respiration, and net production of oxygen in DWSC. Table IV-4 shows the results. The calculation procedure is as follow:

1. The cross section of DWSC is assumed to be a reactangular, with a depth of 11.8 meters and a width of 131.3 meters. The total length is 1085 meters.

2. For each sampling date, the depth of photic zone was recorded. The depth of aphotic zone is the difference between the total depth (11.8 meters) and the depth of photic zone.

3. A single value of net photosynthesis was applied to the photic zone of all 7 sections. The day light hour was assumed to be 12 hours for all dates.

4. A single value of respiration was applied to the aphotic zone of all 7 sections.

5. The respiration in photic zone was assumed to be the same as in aphotic zone.

6. The photosynthesis production equals to the sum of net photosynthesis in photic zone (item 3) and respiration in photic zone (item 5).

7. The water column respiration equals to the sum of photic zone respiration and aphotic zone respiration.

Table IV-4
Photosynthesis and Respiration of Algae in DWSC (Dr. P. Lehman).

Dates	Photic zone depth, m	Photosynthesis Kg O_2/day	Respiration, Kg O_2/day	Net production Kg O_2/day
07-27/2000	2.31	16,500	-22,800	-6,300
08/14/2000	2.2	10,700	-12,700	-2,000
08-14d/2000	2.31	31,100	-31,500	-400
08-23/2000	2.26	8,400	14,000	-5,600
09-06/2000	2.26	8,390	-10,900	-2,510
09/12d/2000	2.0	6,770	-19,800	-13,030
09-14/2000	2.29	5,130	-14,100	-8,970
10-12/2000	2.20	3,950	-5,020	-1,070
10-16/2000	2.35	4,360	-5,020	-660
10-25/200	2.20	3,620	-3,220	+400
10-26d/2000	2.2	25,700	-16,000	+9,700
Average	2.23	11,300	-14,000	-2,600

To compare the model results (Table IV-3) to the measured (Table IV-4), we must first check the volume of DWSC used in the calculation. The model used the real time tidal volumes simulated by the model, which amounted to an average of 19.5 million cubic meters. Dr. Peggy Lehman used an assumed volume, which amounted to 15.5 million cubic meters. The volume difference was approximately 30% bigger for the model.

The average of the measured respirations was –14,000 kg/day. The number should be compared to the sum of algae respiration, ammonia nitrification, CBOD and VSS decay, simulated by the model. The sum was –8,500 kg/day. Thus, the model simulated a lower community respiration than that measured by the light and dark bottle technique.

The model predicted 1,500 kg/day for the average photosynthesis production of oxygen. The value was also one order of magnitude lower than the value of 11,300 kg/day, measured by the light and dark bottle experiment.

We must recognize that the flux simulation is not exactly the same as the light and dark bottle experiment. The model performs a real time simulation and calculates the fluxes based on the water quality concentrations that can vary spatially by nodes and temporary by hours. Photosynthesis is based on actual day light hours, which can vary from summer to fall. The model seeks to calculate the fluxed that may occur in the field.

The light and dark bottle experiment, on the other hand, used a grab sample taken at one time of the day to measure photosynthesis and respiration. The water in the bottle was not representative of the real water quality conditions that can vary with tides. Photosynthesis was measured with 12 hours of light. The total fluxes were calculated by applying a single measurement to all sections of the DWSC. Thus, the light and bottle experiment may not measure the true photosynthesis and respiration of the real system.

Surface and Bottom DO

The model assumes that the water is vertically mixed, which is mostly correct according to the available data. On occasions, the water may become stagnant, which leads to a transient stratification of some water quality parameters. These parameters may include DO, TSS, VSS, and algae. TSS, VSS and algae may settle quickly during the transient stratification period. DO can have stratification, because photosynthesis and aeration contribute oxygen to the surface water and the SOD, VSS, and algae consume oxygen from the bottom water. The stratification does not occur to TDS or chloride because they do not settle or interact with surface aeration or bottom sediment.

To estimate the maximum potential concentration difference between the surface and bottom DO, the following assumptions were made:

1. Photosynthesis and aeration add oxygen to the top two feet of water.

2. SOD consumes oxygen from the bottom foot of water.

3. VSS (pheophytin and detritus) and algae consume oxygen from the bottom foot of water.

4. Ammonia and CBOD are vertically mixed, so they do not contribute to the difference in surface and bottom DO.

Based on these assumptions, the model calculated the maximum potential difference in surface and bottom DO for each node. Figures IV-8 and IV-9 show the results for 1999 and 2000, respectively.

The model results indicate that the maximum potential DO difference can vary seasonably, due primary to the effect of algae. The difference is predicted to be higher in the summer, with a decreasing trend toward the fall, another indication of algal influence.

The DO difference was predicted to be high in the Turning Basin, but low at station R3, which is adjacent to the Turning Basin. In 1999, the DO difference was 4 mg/l at the Turning Basin and 1 mg/l at station R3 (Channel Point). In 2000, the model predicted a DO difference as high as 7 mg/l at the Turning Basin and less than 1.5 at station R3. Again, the model attributed most of the DO difference to the effect of algae.

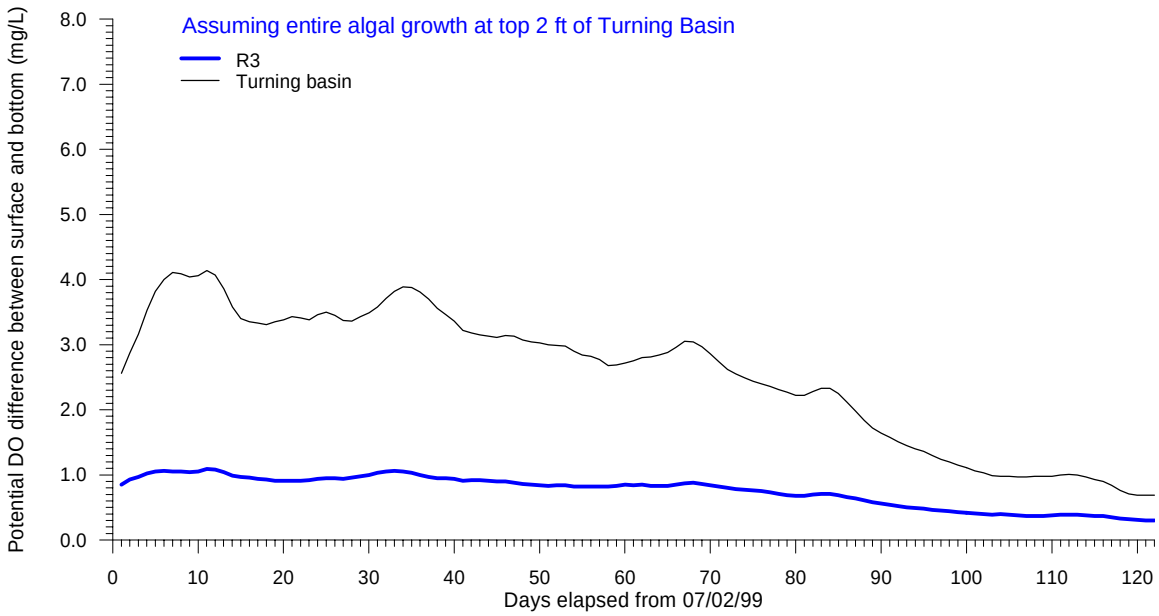

Figure IV-8
Simulated Surface and Bottom DO Difference for 1999.

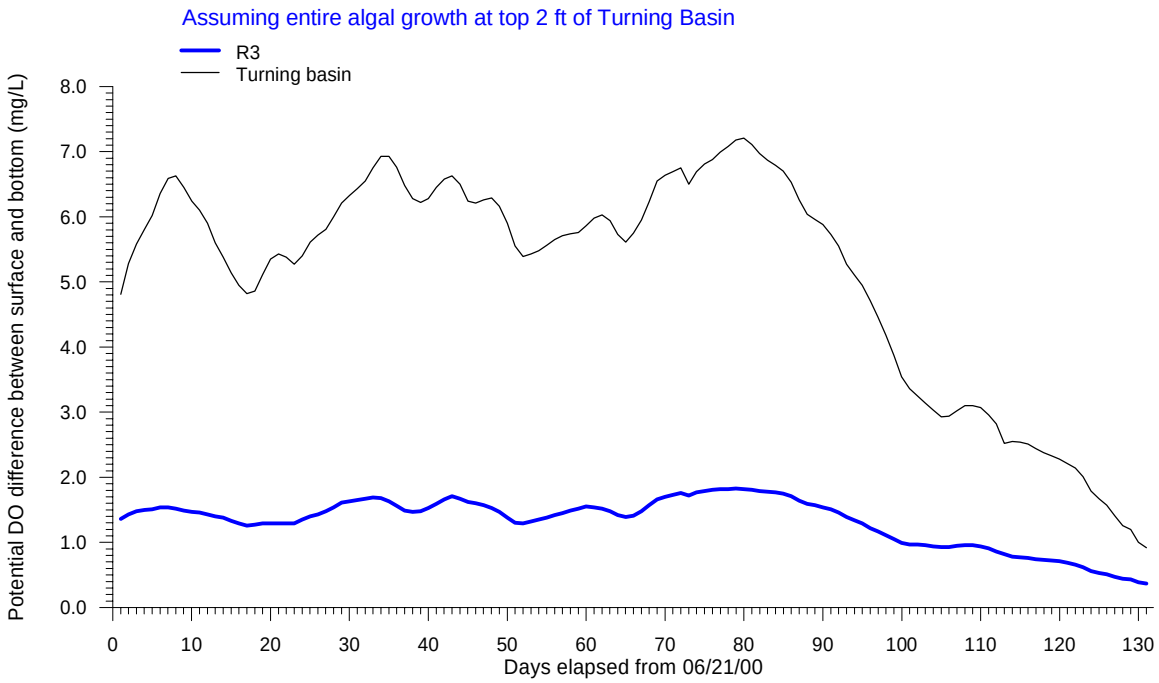

Figure IV-9
Simulated Surface and Bottom DO Difference for Year 2000.

Dr. Steve Hayes of DWR measured the DO difference at 14 stations. Table IV-5 presents the results for 3 locations (Turning Basin, Light 43, and Light 48).

Table IV-5
Measured Surface and Bottom DO Difference (Hayes of DWR)

Dates	Surface and Bottom DO Difference at Light 43, Mg/l	Surface and Bottom DO Difference at Light 48, mg/l	Surface and Bottom DO Difference at TB, mg/l
08-10-99	0.1	-0.4	5
08-26-99	2.2	0	7
09-09-99	2	0	12
09-27-99	0.5	0	6
10-07-99	0.1	0	0
10-25-99	0.1	-0.3	7
11-08-99	0.2	0.5	1
08-14-00	3.5	0.2	10
08-29-00	0.3	0.2	4
09-12-00	3.5	0.5	14
09-26-00	0	0	5
10-13-00	0	0	0

Some of the model predictions are confirmed by the observed data. The confirmed predictions are:

- The surface and bottom DO difference vary by locations. Large DO difference occurred at the Turning Basin. Negligible difference occurred at Light 48, which is immediately adjacent to the Turning Basin. A smaller difference occurred at Light 43, which is within the model node of station R3.

- The observed DO difference occurred in the summer and decreased toward the fall. By October, the DO difference mostly disappeared.

- The average DO difference for August and September was 7.5 for 1999, which was lower than the average of 8.3 for 2000 at the Turning Basin. This difference was caused by lower chlorophyll level in 1999.

However, the observed surface and bottom DO difference (10-14 mg/l) was substantially higher than the predicted difference (4-7 mg/l) at the Turning Basin. The predicted maximum difference was 4 mg/l for 1999 and 7 mg/l for 2000. The contrast was higher than the observed (7.5 for 1999 vs. 8.3 mg/l for 2000).

The discrepancy was probably caused by the difference in definition. In the model, the surface DO was the average concentration for the top 2 feet and the bottom DO was the average concentration for the bottom 1 foot. For the observed, grab samples were taken near the surface and bottom of the water column for the DO measurement. The surface sample can have a DO as high as 14 mg/l, which is super saturated.

In summary, the model predicted the top to bottom DO difference due to algae floating in the stratified Turning Basin to be 8 mg/l. When the river flow is high, this DO difference dropped to less than 1.5 mg/l at Channel Point, where the water from the Turning Basin mixed with San Joaquin river flow from the upstream. When the river flow is low, the mixing in the DWSC may not be complete. The top to bottom DO difference in the DWSC may stay as high as 3.5 mg/l by tidal excursion.

Sedimentation Flux

The model calculates the hourly sedimentation and scouring fluxes of TSS and VSS for each node. Figure IV-10 presents the simulated TSS sedimentation and scouring fluxes for station R3. The model predicts that the sedimentation and scouring fluxes varied with spring and neap tide and also with flood or ebb tide.

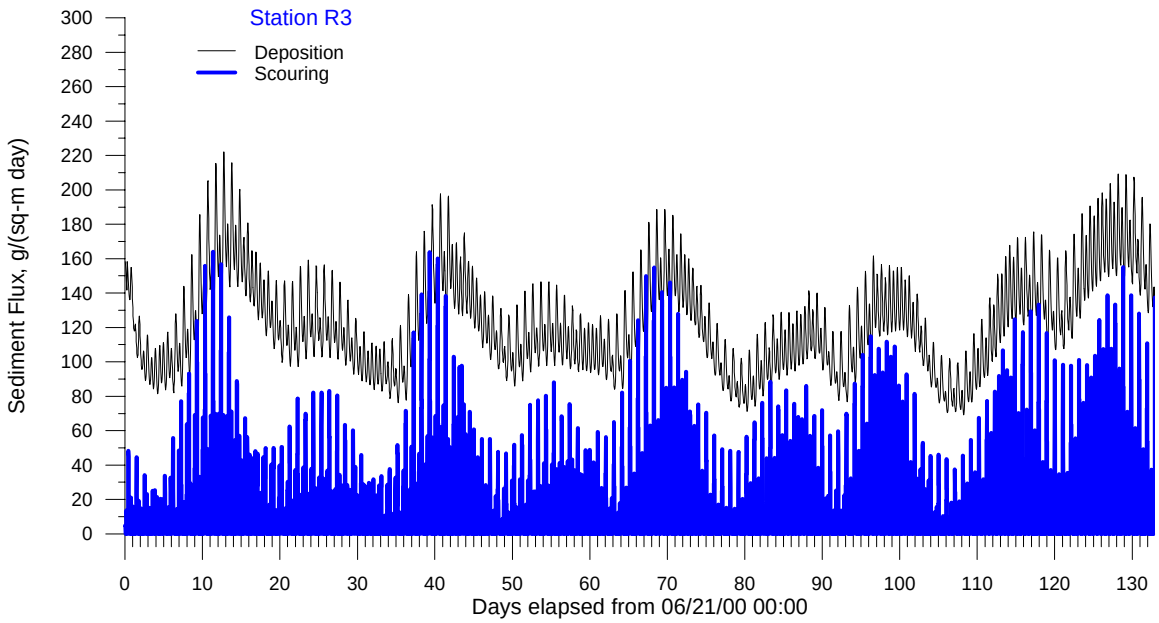

Figure IV-10
Simulated Sedimentation and Scouring Fluxed at Station R3.

Table IV-6 presents the simulated average sedimentation and scouring fluxes over the 4 months period for stations R3 through R6. For comparison, the TSS sedimentation fluxes measured by Dr. Gary Litton are presented in Table IV-7. The observed data showed that sedimentation fluxes did vary with spring, neap, flood, and ebb tides

Table IV-6
Simulated Average TSS Sedimentation and Scouring Fluxes at DWSC.

Station	Average TSS Sedimentation Flux $G/m^2/day$	Average TSS Scouring Flux $G/m^2/day$
R3	122	-15
R4	99	-22
R5	92	-30
R6	96	-132

Table IV-7
Measured TSS Sedimentation Fluxes (Dr. Gary Litton)

Dates	TSS sedimentation flux at Light 48, R3 $G/m^2/day$	TSS sedimentation flux at Light 43, R4 $G/m^2/day$	TSS sedimentation flux at Light 38, R6 $G/m^2/day$
07/26/2000	1,300	500	1,100
08/16/2000	2,000	1250	910
08/31/2000	2,230	-	1,200
09/14/2000	2,400	1,250	-
09/28/2000	700-3,200	900-2,000	840-1,300
10/19/2000	1,780-3,200	1,030-1,800	700-940
11/09/2000	3,100	380	400-840

As shown in Figure IV-10, the TSS sedimentation flux at station R3 can vary from 80 to 220 gram per square meter per day. The observed values varied from 700 to 3,200 gram per square meter per day.

However, the measured flux is at least one order of magnitude higher than the simulated. This is not surprising. Dr. Litton measured the TSS settling with mounted tubes. The particles inside the tube will normally settle faster due to the lack of turbulence. When the model used the settling velocity reported by Dr. Litton, all TSS settled out completely from the water column.

The reasonableness of simulated TSS sedimentation flux can be checked by another calculation. The bulk density of sediment may vary from 1.10 to 1.15 kilogram per cubic meter on a wet weight basis (Ariathurai and Arulanandan 1984). Mackenthun and Stefan (1998) in their study of sediment oxygen demand measured the characteristics of sediment. For sediment with a bulk density of 1.129 to 1.137 g/cm^3, the density of dry solid ranged from 0.27 to 0.23 g/cm^3. Hayter (1984) compiled bed density data to support his modeling effort. The bed density ranged from 190 to 260 kg/m^3. Assuming a dry density of 0.25 g/cm^3 (250 kg/m^3), the net sedimentation flux of 122 $g/m^2/day$ translates to 0.6 feet per year of sediment.

This sedimentation rate is based on the average of 4.5 months from June to October of 2000. The annual simulation would include high flow period when TSS concentration and TSS sedimentation are higher. The sediment accumulation could be more than one foot per year.

Dr. Gary Litton measured an average TSS sedimentation flux of 2,200 gram per square meter per day at Light 48 (R3). Using the same conversion factor, the sediment accumulation rate is 10.5 feet per year, which would be too large. The measured TSS sedimentation decreased from Light 48 (R3) toward Light 38 (R6). The model simulated a decrease from R3 to R5. The simulated sedimentation at R6 was slightly higher than at R5.

The model also simulates scouring flux, which was not measured. The simulated scouring flux increased from station R3 to R6. At R6, the model predicted a small net scour.

Corps of Engineers performed bathymetric survey of DWSC annually. We checked the bathymetric maps of 1999 and 2000. We determined that the sediment accumulation rate was 0 to 3 feet per year depending on locations. Sediment accumulation was more pronounced at station R3. Some scouring was indicated downstream of station R6. Thus, the model prediction was reasonable.

Figure IV-11 presents the fluxes of VSS deposition and scouring at station R3. Table IV-8 presents the average deposition and scouring fluxes of VSS for stations R3 to R6. Table IV-9 presents the VSS sedimentation fluxes measured by Dr. Litton.

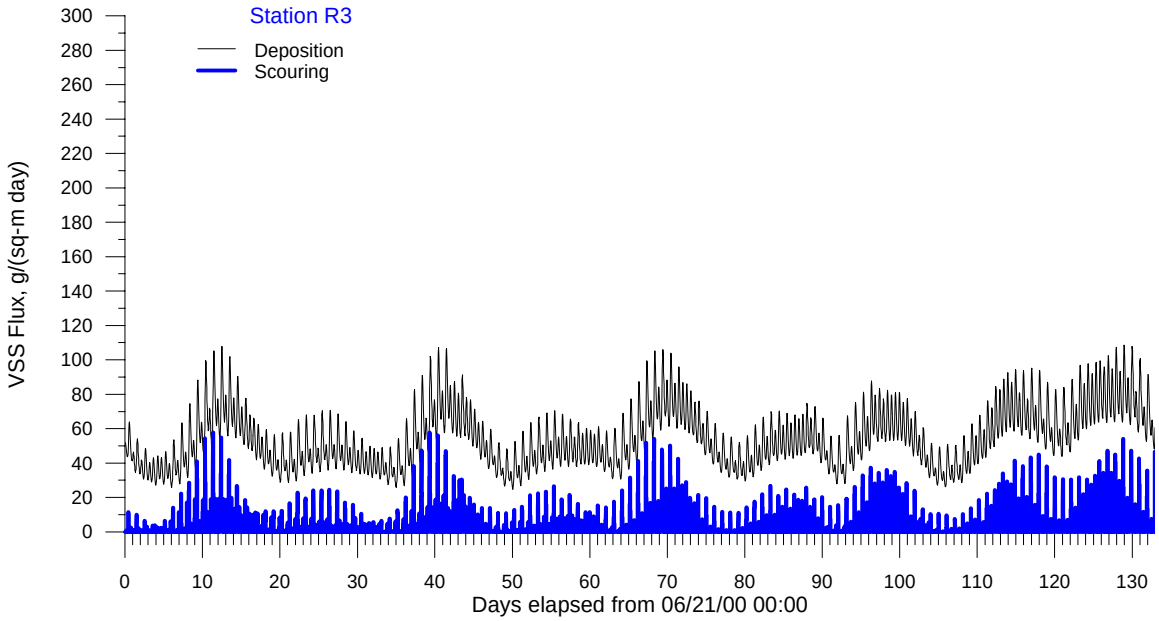

Figure IV-11
Simulated VSS Sedimentation and Scouring Fluxes at Station R3.

Table IV-8
Simulated Average VSS Sedimentation and Scouring Fluxes at DWSC.

Station	Average VSS Sedimentation Flux $G/m^2/day$	Average VSS Scouring Flux $G/m^2/day$
R3	54	-3
R4	38	-5
R5	34	-8
R6	37	-50

Table IV-9
Measured VSS Sedimentation Fluxes (Dr. Gary Litton)

Dates	VSS sedimentation flux at Light 48, R3 $G/m^2/day$	VSS sedimentation flux at Light 43, R4 $G/m^2/day$	VSS sedimentation flux at Light 38, R6 $G/m^2/day$
07/26/2000	108	41	86
08/16/2000	175	106	79
08/31/2000	160	74	118
09/14/2000	210	120	
09/28/2000	74-250	89-200	86-137
10/19/2000	139-250	85-200	72-86
10/09/2000	65-230	26-38	7-46

As in the case of TSS sedimentation, the VSS sedimentation fluxes measured by mounted tube is higher that the simulated values. For station R3, the simulated VSS sedimentation flux varied from 35 to 100 gram per square meter per day. The measured VSS sedimentation fluxes varied from 75 to 250 gram per square meter per day. The model also predicted a higher VSS sedimentation flux for R3 than for R5 or R6. The river load of VSS settles first at R3 and then move on to settle at R4, R5, and R6.

V. Sensitivity Analyses

Introduction

The dynamic estuary model requires a large number of coefficients and boundary conditions. The numerical values of the model input can be obtained from measurements performed in the laboratory or in-the field. Not all parameters can be measured accurately. The measurement performed at one time may not hold true all the times. Often, many of the parameters are not measured directly. One has to rely on estimate based on literature values reported elsewhere.

There are uncertainties in the input data, which can lead to uncertainty in model predictions. In this chapter, the model is used to determine how the model prediction can vary with a given percentage of change in the input value. The decision makers can then take the model uncertainty into account, when they make environmental decisions based on model predictions.

Methodology

The dynamic model estuary model makes predictions for a large number of variables for every hour at every node. It would be confusing to look at the sensitivity of each prediction with respect to the input data.

Chris Foe of the Central Valley Regional Water Quality Control Board proposed an integrative parameter called Maximum Daily DO Deficit (MDDOD). Based on the concept, we derive an index for DO deficit as follows:

The DO deficit (DOD) is a measure of DO below 5 mg/l.

$$DOD = 5.0 - DO \text{ , for DO} < 5 \text{ mg/l} \qquad \text{(V-1)}$$

The DO deficit is zero when the DO concentration is above 5 mg/l.

The model calculates 24 hourly DO values for each day. The lowest DO value of a day is used to calculate the maximum DO deficit of the day.

$$MDOD(day) = 5.0 - \min\{DO(hr)\} \qquad \text{(V-2)}$$

Equation V-2 can be expressed in mass unit as follow,

$$MDOD(day) = [5.0 - \min\{DO(hr)\}]V \qquad \text{(V-3)}$$

where V is the average volume of the node in cubic meter. After unit conversion, MDOD(day) is in the unit of kilograms O_2.

The index of DO deficit over a period can be calculated by,

$$IDOD(period) = \sum_{n=1}^{ndays} [MDOD(day)/ndays] \qquad \text{(V-4)}$$

IDOD is an index of DO deficit, because it represents only the mass of DO deficit for the worse hour of the day. The average volume may not be the actual volume of the node when the worse DO occurs. However, IDOD is a good indicator for the DO deficit for any point in the tidal estuary.

The overall DO deficit for the main stem of the DWSC can be calculated by summing the IDOD for all nodes within the Deep Water Ship Channel.

The objective of a water quality management plan is to eliminate the DO deficit in the DWSC. The IDOD is therefore a useful parameter to evaluate the model sensitivity.

For the sensitivity analysis of this study, a base case is first established by running the model using the calibrated coefficients for the period from June 1 to October 31 of 2000. Allowing the model to stabilize from the initial condition, the IDOD is calculated by averaging the maximum daily DO deficits of DWSC for 133 days from June 21 to October 31, 2000.

The model simulation is then performed with an increase or a decrease of model coefficient. The change of IDOD with respect to the change of model coefficient is evaluated with the model.

The sensitivity analyses were performed for two classes of parameters, i.e. rate coefficients and boundary conditions. The results are discussed in two separate sections below.

Sensitivity of Model Coefficients

Individual Sensitivity

The rate coefficients selected for sensitivity analyses include the decay rates of ammonia, CBOD, and detritus. Their theta (θ) values for temperature correction are also evaluated. Their numerical values for the base case have been reported in Chapter 3 and summarized again in Table V-1.

Table V-1
Parameter Values of Base Case

Coefficients	Parameter Value
Ammonia nitrification rate	0.05 per day
Theta (θ) value for nitrification	1.08
CBOD decay rate	0.1 per day
Theta (θ) value for CBOD decay	1.04
Detritus decay rate	0.01 per day
Theta (θ) value for detritus decay	1.02

The IDOD for the base case is 456 kilogram of DO. The sensitivity of change in IDOD is evaluated by the percent change from the base case value (456 kg of O_2). Table V-2 summarizes the results of sensitivity analyses.

Table V-2
Sensitivity of IDOD with Respect to Model Coefficients

Model Coefficient	Percent changes Of model coefficient	Percent change Of IDOD
Ammonia nitrification	+5%	+10%
	-5%	-10%
	+10%	+21%
	-10%	-19%
θ value of nitrification	+5%	+71%
	-5%	-46%
	+10%	+166%
	-10%	-76%
CBOD decay	+5%	-5%
	-5%	+5%
	+10%	-9%
	-10%	+10%
θ value of CBOD decay	+5%	+38%
	-5%	-34%
	+10%	+77%
	-10%	-60%
Detritus decay	+5%	+21%
	-5%	-19%
	+10%	+44%
	-10%	-35%
θ value of Detritus decay	+5%	+178%
	-5%	-75%
	+10%	+490%
	-10%	-96%

The results shown in Table V-2 reveal the followings:

1. An increase in decay rate for reactions that consume DO leads to an increase of IDOD. The only exception is CBOD decay rate, which decreases with increasing decay rate. The reason is that the model converts CBOD to ultimate BOD internally for the calculation of BOD decay. A smaller CBOD decay rate leads to a higher ultimate BOD.

2. Higher IDOD with lower BOD decay rate is caused by the high hydraulic residence time that allows the ultimate BOD to be oxidized completely within DWSC even at a lower decay rate.

3. The response of IDOD to the change of model coefficient is nonlinear. A change of model coefficient from 5% to 10% leads to more than a doubling of IDOD.

4. IDOD is more sensitive to a change of theta value than the rate coefficient itself. This is because the temperature speeds up the decay rate exponentially.

5. The IDOD is most sensitive to detritus, because of its high river load (18,000 kg/day VSS). The IDOD is least sensitive to CBOD decay because of its low river load (1,500 kg/day CBOD).

6. High sensitivity of a model coefficient actually makes it easier for model calibration. In the highly integrated model, all parameters are related to each other. A wrong coefficient for the ammonia decay coefficient will not only lead to a poor match in ammonia concentrations but also an error in dissolved oxygen and nitrate concentrations.

Combined Sensitivity

To determine the combined sensitivity of model coefficients, two approaches have been used. One approach is the Monte Carlos simulations, in which the mean and standard deviation of individual model coefficients are provided as input to the model. In each time step, the model program will randomly select a value for each coefficient and use it in the simulation. The Monte Carlos simulation will require an extensive change of the model program and also detailed information about the statistical characteristics of model coefficients. For that reason, it was not possible to perform the Monte Carlo simulation with the DO model at this time.

The other approach is the Jackknife technique, in which the range of parameter values for model coefficients is specified. For example, the rate coefficients for the three decay coefficients are assumed to vary as follows:

Mode Coefficients	Range of Parameter Values				
CBOD decay rate	-10%	-5%	+0%	+5%	+10%
Ammonia decay rate	-10%	-5%	+0%	+5%	+10%
Detritus decay rate	-10%	-5%	+0%	+5%	+10%

The percent of variation is from the base case shown in Table V-1. A list of simulation cases can be prepared for different combinations of parameter values. There are 125 possible combinations with five possible values for each of the three model coefficients. The model was set up to run all those cases to evaluate the statistical spread of model predictions.

Figure V-1 shows the results of Jackknife simulations. The probability distribution appears to skew toward lower deficit values. The mode of predicted DO deficit is 300 to 350 kg. The mean is 470 kg and the standard deviation is 150 kg. The broad distribution of predictions indicates that the model is equally sensitive to all three key decay coefficients for BOD, ammonia, and detritus.

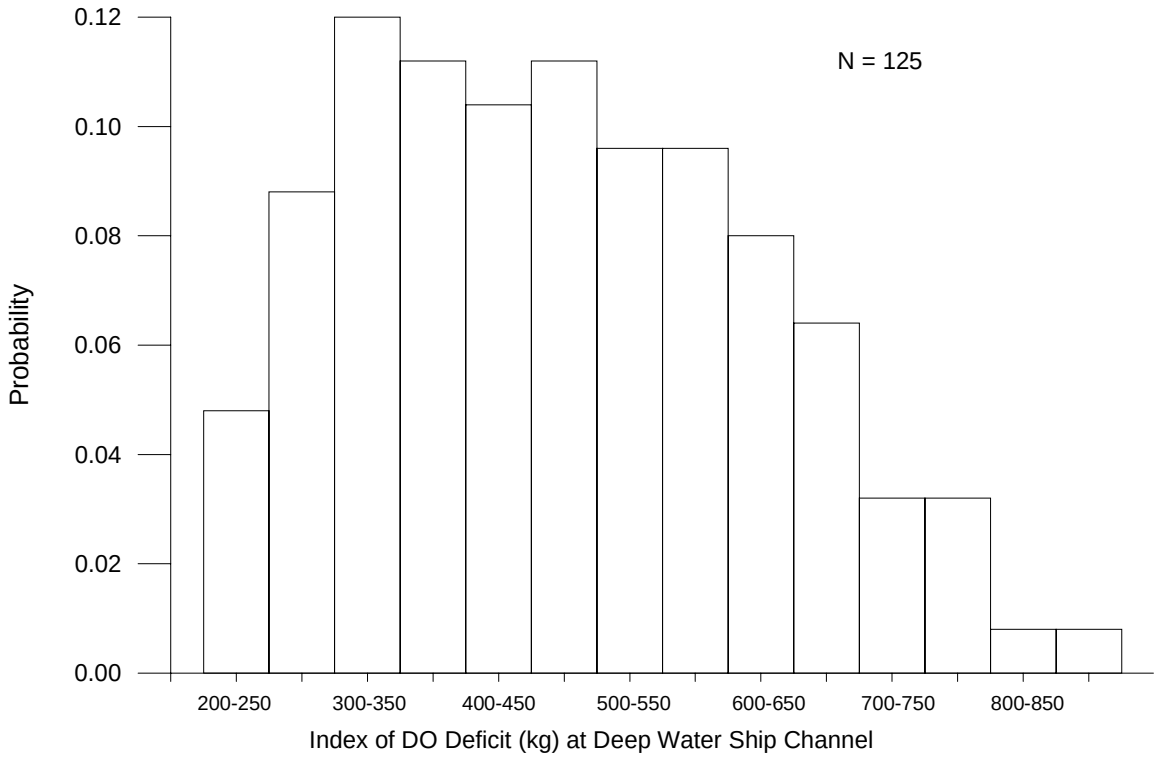

Figure V-1
Probability Distribution of DO Deficit

Sensitivity of Boundary Conditions

The boundary conditions selected for sensitivity analyses include river flow, river load, and Stockton load. The base condition is the same as the one used in the sensitivity analysis of model coefficients. The base case IDOD is still 456 kg of DO.

The boundary condition of river flows are increased or decreased by 5% and 10% every day. The change in IDOD with respect to the change in river flow is evaluated with the model.

For the change of river load, it is assumed that the river flows stay the same. But, the concentrations of all pollutants (ammonia, nitrate, CBOD, chlorophyll, etc.) are increased or decreased by 5% and 10%. The change of Stockton load is handled in the same way, i.e. the change is made on concentrations not on the flow.

Table V-3
Sensitivity of IDOD with Respect to Boundary Conditions

Boundary Conditions	Percent changes Of boundary conditions	Percent change Of IDOD
River flow	+5%	-15%
	-5%	+16%
	+10%	-28%
	-10%	+34%
River load of all pollutants	+5%	+50%
	-5%	-34%
	+10%	+185%
	-10%	-76%
Stockton load	+5%	+5%
	-5%	-5%
	+10%	+11%
	-10%	-10%

Based on the information presented in Table V-3, following observations are made:

1. The DO deficit in DWSC is very sensitive to rive flow. A 5% increase of river flow will reduce DO deficit by 15%. A 5% decrease of river flow will increase DO deficit by 16%.

2. The DO deficit in DWSC is more sensitive to flow decrease than flow increase. Doubling the flow increase from 5% to 10% will decrease the DO deficit from

15% to 28%. However, doubling the flow decrease from 5% to 10% will increase the DO deficit from 16% to 34%.

3. The DO deficit in DWSC is most sensitive to the river load of all pollutants from upstream. A 5% increase in river load increases the DO deficit by 50%. A 10% increase in river load increases the DO deficit by 185%. A 5% decrease in river load decreases the DO deficit by 34%. A 10% decrease in river load decreases the DO deficit by 76%.

4. The DO deficit in DWSC is sensitive Stockton load, but less sensitive than the river load. A 5% increase of Stockton load will raise the DO deficit by 5%. A 5% decrease of Stockton load will reduce the DO deficit by 5%.

5. By far, the DO deficit is more sensitive to change in boundary conditions than the change in the parameter values of model coefficients.

VI. Management Scenarios

Introduction

In the previous chapters, we have described the model calibration, in which the model was used in hind casting mode. The input data that reflects the actual 1999 and 2000 conditions was inputted to the model. Based on the input data, the model predicted the flow and water quality conditions at various locations in the San Joaquin River and at various times. The model predictions were compared to the data observed at various locations and times to ensure the model accuracy.

Analyses so far have shown that the dissolved oxygen concentration dropped below standard sometimes and somewhere in the Deep Water Ship Channel. In this chapter, the model is used in predictive mode to evaluate the management scenarios that can be implemented to raise the dissolved oxygen. In predictive mode, the input data is prepared to reflect proposed management scenarios.

Most management scenarios involve the reduction of waste loads that contribute oxygen consuming materials to the receiving water. For the San Joaquin River, the load reduction requirement is a function of river flow.

Methodology

The methodology has been used to perform the strawman's loading analyses, using the 1999 data. The preliminary results based on the earlier model have been submitted to Dr. Chris Foe of the Central Valley Regional Water Quality Control Board, who is preparing a report for the results.

With the current version of the calibrated model, the strawman's loading analyses were repeated for both 1999 and 2000 conditions. This section describes the results of strawman's loading analyses.

Index of DO Deficit

The main objective of water quality management for the San Joaquin River is to eliminate dissolved oxygen deficit in the Deep Water Ship Channel. For that reason, the model is used to predict the index of DO deficit (IDOD) described in the previous chapter. A proposed management scenario becomes an acceptable alternative, when it leads to a zero value of IDOD.

The IDOD described herein is defined a little different than the term maximum daily dissolved oxygen deficit used in the 1999 strawman' loading analyses. The maximum daily dissolved oxygen deficit was defined as the sum of maximum daily dissolved oxygen deficits for the entire simulation period. Since it is cumulative, the numerical

value can increase with the number of days in the simulation period. In this report, IDOD is calculated by dividing the cumulative value by the number of days in the simulation period, as described in the previous chapter.

Management Options

The management options to control dissolved oxygen in the San Joaquin River includes river flow, Stockton load, and river load. Tides, temperature, and sediment oxygen demand (SOD) are important, but they are not considered controllable for this analysis.

The river flow, river load, and Stockton load can be controlled separately. For example, the river flow can be manipulated by reservoir releases, Delta export pumping, operation of the barrier at the head of Old River, and/or re-circulation of Delta water. The river load can be controlled by the upgrade of treatment plants and the application of best management practices (BMP) to reduce the pollutant concentrations in the nonpoint loads from farms, dairy, and wetlands upstream of Vernalis. The Stockton load can also be reduced by upgrading its RWCF.

Under the hind cast mode of model simulation, the input data for river flow was assigned to the actual daily flow measured at the UVM station near Stockton. The purpose is for the model to simulate the flow and water quality under the actual condition, so that the model predictions can be compared to the data observed in the real system. For the predictive mode of model simulation, the input data for river flow is maintained constant. However, the model can be run under the hypothetical flows of 250, 500, 750, 1000, 1500, and 2000 cfs. By this way, it is possible to find out the combination of river flow and load reduction needed to eliminate DO deficit.

Stockton Load

Stockton effluent contains CBOD, NH3, algae, Pheophytin, and VSS. The daily flows and pollutant concentrations for the simulation period of year 2000 were inputted to the model. The model calculates the daily mass loadings of pollutants by multiplying the flow and pollutant concentrations. The concentrations of individual pollutants are tracked. Each pollutant decays at its own rate and consumes its equivalent dissolved oxygen in the receiving water.

River Load

The river flow also contains CBOD, NH3, algae, Pheophytin, and VSS. The daily flows for the management scenarios are assumed to be constant, as explained earlier. However, the real pollutant concentrations for the simulation period of year 2000 were inputted to the model. The model calculates the daily mass loadings of pollutants by multiplying the assumed river flow and actual pollutant concentrations. The model decays each pollutant at its own rate and consumes dissolved oxygen in the receiving water.

Equivalent Ultimate BOD

Both Stockton load and river load contain oxygen consuming materials. For comparative analysis, it is desirable to use a common currency for all oxygen consuming materials. The appropriate common currency is the equivalent ultimate BOD (EUBOD) defined as follow:

$$
\begin{aligned}
EUBOD = Q[&CBODu \\
&+4.57*KNH3/KBOB*CNH3 \\
&+R/KBOD*a*CALGAE \\
&+4.57*KNH3*KPHEO/KBOD*CPHEO \\
&+4.57*KNH3*b*KDETR/KBOD*CDETR \\
&+(1-b)*KDETR/KBOD*c*CDETR] \qquad \text{(VI-1)}
\end{aligned}
$$

where Q is the volumetric discharge rate. CBODu is the ultimate BOD converted from BOD5. KBOD is BOD decay rate (0.1 per day). KNH3 is ammonia decay rate (0.05 per day). R is algae respiration rate (0.25 per day). KPHEO is pheophytin decay rate (0.1 per day) and KDETR is detritus decay rate (0.01 per day). All rate constants are for the standard temperature of 20 degrees Celsius.

The constant “a” is milligram of oxygen consumed per milligram of algae respired (2.0). The constant “b” is the nitrogen content of detritus (0.08), which is released as ammonia. Constant “c” is milligram of oxygen consumed per milligram of detritus decayed (1.6).

CBOD is concentration of BOD. CNH3 is the concentration of ammonia. CALGAE is concentration of algae. CPHEO is the concentration of pheophytin and CDETR is the detritus concentration.

Management Scenarios

A management scenario can include a combination of individual control options, i.e. river flow, river load, and Stockton load. The options for river flow are 250, 500, 1000, 1500, and 2000 cfs.

Under each of the flow condition, the model is first run for 100% of Stockton load together with 100% of river load. Subsequently, the model is run for various combinations of Stockton load and River load. For example, a scenario is run for 2000 cfs of river flow, 100% of Stockton load, and 75% of river load.

It must be noted that the reduction of river load and Stockton load are derived from the lowering of pollutant concentrations, not from the change of river flow and/or Stockton discharge. Since the DO deficit in DWSC is sensitive to river flow, a load reduction by decreasing flow can sometimes lead to counter intuitive results.

Loading Comparison

The daily equivalent CBOD of Stockton and river loads were calculated according to Equation VI-1. The results for the 1999 loads are presented in Figure VI-1. The results for the 2000 loads are presented in Figure VI-2.

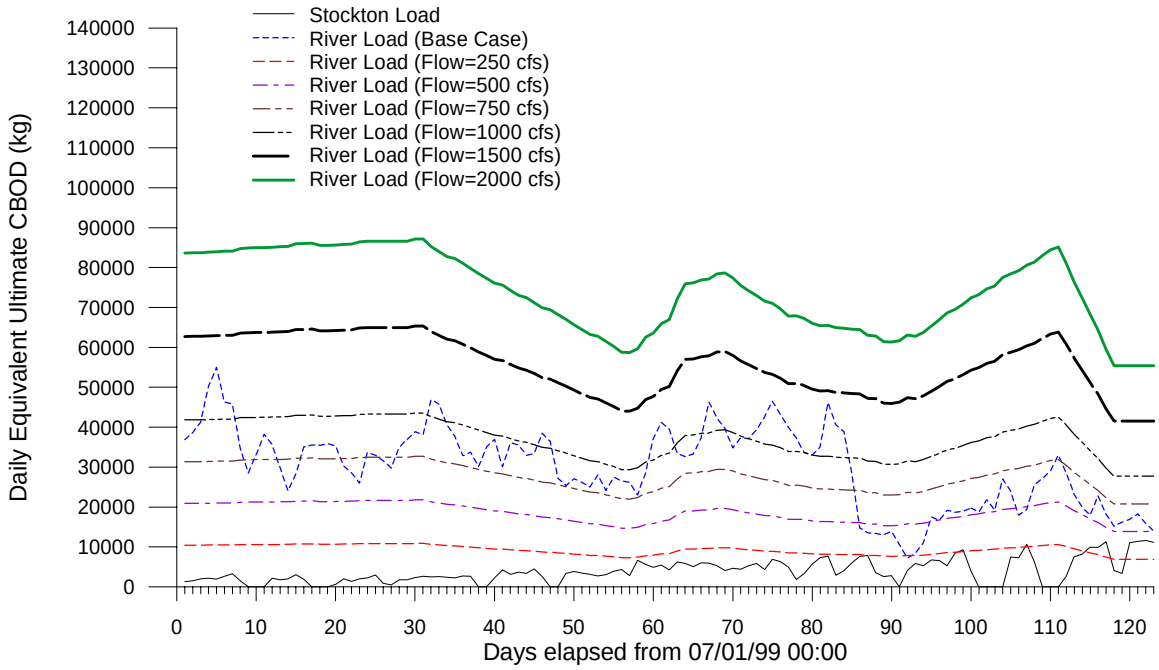

Figure VI-1
River Load and Stockton Load for the 1999 Simulation Period

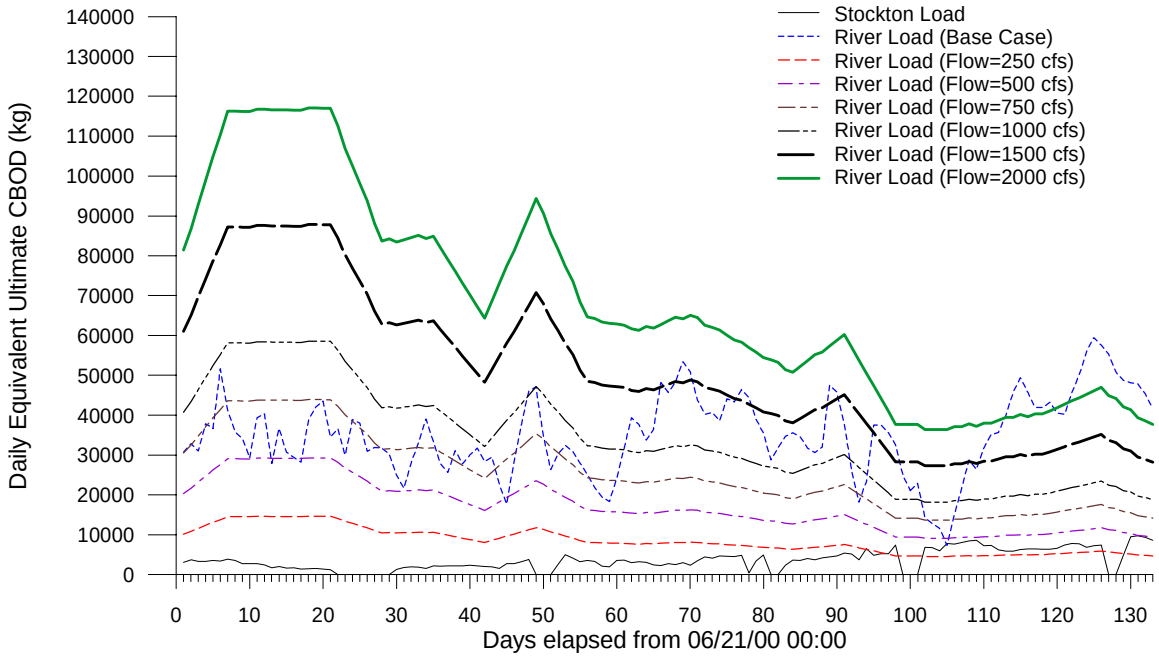

Figure VI-2
River Load and Stockton Load for the 2000 Simulation Period

The bottom line is for Stockton load (Figures VI-1 and VI-2). Based on the results shown in Figures VI-1 and VI-2, the average daily equivalent ultimate BOD was calculated. The results are presented in Table VI-1.

The Stockton load is approximately 13% of the river load in 1999 and 10% of the river load in 2000. The actual Stockton load was 3,900 kg per day of equivalent BOD for 1999 as compared to 3,600 kg per day for 2000. The actual river load for 2000 was 35,000 kg of equivalent BOD, higher than 30,000 kg of the 1999 equivalent BOD. This was caused by a substantially higher river flow in year 2000 than in year 1999. The actual pollutant concentrations were lower in year 2000 than in year 1999. As a result, the river load for the constant flow condition becomes higher for 1999 than for 2000.

Table VI-1
Average Daily Equivalent BOD of River Load and Stockton Load

Items	Average Daily Equivalent BOD for Year 1999 Kilogram per day	Average Daily Equivalent BOD for Year 2000 Kilogram per day
Stockton load	3,900	3,600
River load	30,100	35,000
River load at 250 cfs	9,200	8,500
River load at 500 cfs	18,400	17,000
River load at 750 cfs	27,700	25,500
River load at 1000 cfs	36,900	34,000
River load at 1500 cfs	55,300	51,000
River load at 2000 cfs	73,800	68,000

Effect of River Flow

The model was exercised to calculate the index of DO deficit in the DWSC for 100% Stockton load and 100% river load. The results are shown in Table VI-2.

Table VI-2
DO Deficit Under Various Flow Conditions

San Joaquin River Flow At Stockton, cfs	Index of DO Deficit With 100% Stockton Load and 100% River Load for Year 1999, kg O_2	Index of DO Deficit With 100% Stockton Load and 100% River Load for Year 2000, kg O_2
250	8170	1360
500	7600	1180
750	5860	380
1000	4070	32
1500	1670	0
2000	650	0

The results show the importance of river flow on dissolved oxygen deficit in the Deep Water Ship Channel of San Joaquin River. Under the year 2000 condition, the index of DO deficit disappears as the river flow exceeded 1,500 cfs, due to a shorter residence time and a higher assimilative capacity.

The DO deficit under the year 1999 condition was substantially higher. The index of DO deficit remained at 650 kg O2 even at the high flow of 2000 cfs. This is caused by higher Stockton load and river load for the 1999 simulation.

The analysis clearly demonstrated the importance of river flow on DO deficit. It also showed the need to reduce Stockton load and river load even at high river flow in order to eliminate the DO deficit.

Deficit at Low Flow

The model was exercised to determine the DO deficit under the low flow condition of 250 cfs. The results are summarized in Table VI-3. The results show that the DO deficit cannot be eliminated by any reasonable load reduction schemes for Stockton and upstream dischargers. The river flow of 250 cfs is too low to be considered as a part of solution for low DO problem in the DWSC.

Table VI-3
DO Deficit Under Low Flow Condition of 250 cfs

Loading Condition	1999 Index of DO Deficit in DWSC, kg O_2	2000 Index of DO Deficit in DWSC, kg O_2
100% Stockton load and 100% river load	8170	1360
100% Stockton load and 75% river load	6400	600
100% Stockton load and 50% river load	4690	200
100% Stockton load and 25% river load	3200	60
100% river load and 75% Stockton load	6440	640
100% river load and 50% Stockton load	4850	430
100% river load and 25% Stockton load	3460	300

Deficit at High Flow

The model was exercised to determine the DO deficit under the high flow condition of 1000 cfs. The results are presented in Table VI-4.

Under the year 2000 condition, the DO deficit can be eliminated with 100% Stockton load and 75% river load. However, some minor DO deficit will remain with 100% river load and 25% Stockton load.

Under the year 1999 condition, the DO deficit can be eliminated only if the river load is reduced by 75%. If nothing is done to the upstream pollutants, the DO deficit remains at 2120 kg of O_2 with a 75% reduction of Stockton load.

The model suggested that a river flow higher than 1000 cfs is a part of the solution to the DO problem. With a sufficient high river flow, a reasonable combination of load reductions from Stockton and upstream dischargers can be devised to solve the DO problem in DWSC.

Table VI-4
DO Deficit Under High Flow Condition of 1000 cfs

Loading Condition	1999 Index of DO Deficit in DWSC, kg O_2	2000 Index of DO Deficit in DWSC, kg O_2
100% Stockton load and 100% river load	4000	30
100% Stockton load and 75% river load	1240	0
100% Stockton load and 50% river load	61	0
100% Stockton load and 25% river load	0	0
100% river load and 75% Stockton load	3320	16
100% river load and 50% Stockton load	2670	7
100% river load and 25% Stockton load	2120	1

Deficit Without DWSC

According to the historic record, the San Joaquin River was only 7 feet deep. The river was dredged to 35 feet to accommodate the ocean going cargo ships that visit the Stockton Harbor for agriculture products. The model was exercised to calculate DO deficit under the historic condition of San Joaquin River without DWSC. The results are presented in Table VI-5.

Table VI-5
DO Deficit Under Historic Channel Depth of 7 Feet

San Joaquin River Flow At Stockton, cfs	1999 Index of DO Deficit With 100% Stockton Load and 100% River Load, kg O_2	2000 Index of DO Deficit With 100% Stockton Load and 100% River Load, kg O_2
250	96	120
500	58	49
750	7	0
1000	0	0
1500	0	0
2000	0	0

Under the 1999 condition, the DO deficit would not have occurred with a river flow of 1000 cfs and 100% of both Stockton load and river load. Under the 2000 condifition, the river flow for a zero DO deficit is 750 cfs. When the river is shallow, the river has a short residence time for the same river flow. The pollutants are flushed out of the river section. The re-aeration is high and sufficient to replenish DO.

While it is of interest to show the effect of DWSC on DO, it is not a realistic alternative to solve the DO problem by eliminating the deep water ship channel, which is vital to the agricultural industry of the San Joaquin Valley. However, the calculation shows that DWSC is a responsible party to the DO problem in San Joaquin River.

VII. Summary and Conclusions

Summary

The Lower San Joaquin River DO model contains hydrodynamic and water quality modules. The hydrodynamic module simulates the tidal movement of water. The water quality module performs heat budget and mass balance calculations to predict water temperature and concentrations of BOD, nutrients (ammonia, nitrate, phosphate), algae (chlorophyll-a), and dissolved oxygen. With the CALFED 2000 grant, the model was expanded to include volatile suspended solid (VSS), total suspended solid (TSS), and pheophytin. Algorithms were added to simulate the settling of suspended particles, the scouring of sediment from bottom, and their effects on sediment oxygen demand (SOD). The model was also enhanced to simulate the growth of flagellate algae that stays in the top two feet of the Turning Basin.

The river flow, meteorology, tide, Stockton discharge and upstream water quality concentrations for 1999 and 2000 were inputted to the model. The model simulated the dynamic variations of flow and water quality at various points of the San Joaquin River. The model predictions were compared to the observed values in time series and concentration profiles, collected by various investigators under the CALFED grant..

Comparisons were also made for the frequency distribution of water quality, statistics of model accuracy, fluxes of DO sinks and sources, the surface and bottom difference of DO, and sedimentation fluxes of TSS and VSS. Sensitivity analyses were performed for the model coefficients of BOD, ammonia, and VSS decay rates, as well as the boundary conditions of river flow, river load and Stockton load.

After calibration, the model was used to evaluate effectiveness of various management scenarios that may be devised to raise the DO above the 5 mg/l standard. The management scenarios include various combinations of river flow, Stockton load, and river load from the upstream boundary.

Conclusions

Based on the results presented in this report, following conclusions can be made:

1. The model predictions have reasonably matched the observed tidal current, water temperature, dissolved oxygen, chlorophyll-a, phoephytin, ammonia, nitrate, phosphate, total suspended solid, and volatile suspended solid.

2. Due to a lack of detailed time varying boundary conditions, the model did not capture some of the episodic low DO, observed in the field. During the 1999 sampling period, the range of observed DO was 2.8 to 6.7 mg/l, compared to the range of 3.9 to 6.2 mg/l for the simulated. The mean DO for the observed

was 4.9 mg/l, compared to 4.9 mg/l for the simulated. The mean relative error was 0.1 mg/l and the mean absolute error was 0.59 mg/l. During the 2000 sampling period, the range of observed DO was from 4.0 to 8.4 mg/l, compared to the range of 4.8 to 8.5 mg/l for the simulated. The mean DO for the observed was 6.2 mg/l, compared to 5.9 mg/l for the simulated. The mean relative error was –0.25 mg/l and the mean absolute error was 0.59 mg/l.

3. For the 2000 sampling period, the model calculated an average of 1,500 kilogram per day of oxygen produced by algae in the DWSC. The values measured by the light and dark bottle experiments have an average of 11,300 kg/day. The simulated community respiration was –8,500 kg/day of oxygen. The light and dark bottle result was –14,000 kg/day.

4. Numerous assumptions were made in using the light and dark bottle results to calculate the fluxes of photosynthesis and respiration in the DWSC. These assumptions may make the model results not directly comparable to the values calculated from the light and bottle experiment.

5. For the main stem of deepwater ship channel (DWSC) and the 2000 sampling period, the DO sources were 1500 kg/day for photosynthesis and 2300 kg/day for aeration. The DO sinks were –3900 kg/day for algae respiration, 1600 kg/day for ammonia nitrification, 1800 kg/day for sediment oxygen demand, 3000 kg/day for CBOD and VSS decay. So, the major DO sinks were algae respiration and the decay of CBOD and volatile suspended solids. The sink due to ammonia nitrification was surprisingly moderate, probably due to the fact that high ammonia discharge occurred only in the latter half of the sampling period.

6. The potential DO difference between the surface and bottom water was due primary to the effect of algae. The difference is predicted to be as high as 7 mg/l in the Turning Basin in the summer, decreasing toward the fall. The predicted DO difference is only 1.5 mg/l at R3 (Lights 43 and 48), immediately adjacent to the Turning Basin. The observed data confirmed the general pattern of model predictions, however, the observed maximum surface to bottom DO difference was 8.3 mg/l for the year 2000, as compared to 7 mg/l for the simulated.

7. The simulated sedimentation flux of TSS was 122 grams per square meter per day at station R3 (Light 48), decreasing to 92 grams per square meter per day at station R5 (light 41). The simulated scouring flux of TDS was –15 grams per square meter per day at R3 increasing to –30 grams per square meter per day at R5 (Light 41). The measured sedimentation flux was one order of magnitude higher because TSS settled faster inside the mounted tubes due to the lack of turbulence.

8. The DO deficit was most sensitive to river load, river flow, and Stockton load, in that order. A 5% increase in river load increases the DO deficit by 50%. A 10% increase in river load increases the DO deficit by 185%. A 5% decrease in river load decreases the DO deficit by 34%. A 10% decrease in river load decreases the DO deficit by 76%. The theta values were also very sensitive due to the exponential function used to adjust temperature effect. However, their values have a small range of variation. The decay coefficients were sensitive, but not as sensitive as the boundary conditions and theta values.

9. River flow, river load, and Stockton load are key control measures to solve the DO problems of the DWSC. At the low flow of 250 cfs, no reasonable reduction of Stockton load and/or upstream loads can help raise the DO above 5 mg/l. At the high flow of 1500 cfs, reasonable reductions of Stockton load and river load can meet the DO standard.

10. The DO deficit would disappear if the DWSC were eliminated and the San Joaquin River were returned to its historic water depth of 7 feet. The model simulation showed that deepening the channel was, in part, responsible for the deterioration of DO due to increase of residence time. However, the DWSC is economically too important to be eliminated.

11. The Lower San Joaquin River DO model is reasonably calibrated and is ready to evaluate the efficacy of management alternatives that can eliminate the DO deficit in the DWSC of San Joaquin River.

VIII. Questions and Answers

This chapter provides a simple answer to each of the frequently asked questions about the DO model:

1. Did the model simulate the hydrodynamics of the DWSC?

   Answer: Yes
   Evidence: The predicted tidal velocities matched the ADCP measurements.

2. Did the model simulate the water quality of the DWSC?

   Answer: Yes. The model predictions matched the mid-depth temperature, ammonia, nitrate, detritus (VSS), suspended sediment, algae, pheopyhtin, dissolved oxygen, and others, measured at various stations in the DWSC.
   Evidence: Comparison plots shown in the final report.

3. Did the model simulate the DO in the DWSC accurately?

   Answer: Accurate enough for decision making
   Evidence: Observed mean was 6.2 mg/l compared to 5.9 mg/l simulated. Relative error was –0.25 mg/l. Absolute error was 0.59 mg/l

4. Did the model simulate the lowest DO found in the DWSC?

   Answer: No
   Evidence: Observed range of DO was 4 to 8.4 mg/l compared to 4.8-8.5 mg/l simulated. The minimum DO might occurred at deep samples not simulated by the model, or was controlled by the boundary condition, which was not specified in the input data.

5. What are the major sources of oxygen to the DWSC?

   Answer: Surface aeration and photosynthesis oxygenation
   Evidence: Aeration supplied 2,300 kg/d of oxygen and photosynthesis supplied 1,500 kg/d of oxygen.

6. What are the major sinks of oxygen in the DWSC?

   Answer: Algae respiration and decay of VSS and then nitrification
   Evidence: DO sinks were 3,900 kg/d algae respiration, 3,000 kg/d VSS and BOD decay, and 1,600 kg/d nitrification.

7. Does the model include organic nitrogen as DO sink?

   Answer: Yes.
   Evidence: The model does not simulate organic nitrogen separately. But, organic nitrogen is contained in detritus, algae, and pheophytin. These constituents release ammonia during their decay. Ammonia is then subjected to nitrification, which consumes DO.

8. What was the relative importance of algal respiration on DO in the DWSC?

   Answer: Important particularly during the algal blooms in the upstream.
   Evidence: It contributed 37% of DO sinks in the DWSC. (note: this statement contradicted Dr. Peggy Lehman, whose analysis might not have included periods with algal blooms).

9. What were the most sensitive factors for DO in the DWSC?

   Answer: Temperature, river load, river flow, Stockton load in that order.
   Evidence: Sensitivity analysis results, presented in the final report.

10. What was the simulated algal growth in the DWSC relative to the amount brought in by the river load from upstream?

    Answer: About the same (note: this is consistent with Dr. Peggy Lehman).
    Evidence: Simulated in-situ growth was 107 kg/d of chlorophyll-a. The river load was 114 kg/d of chlorophyll-a.

11. What is the most limiting factor for algae growth in the DWSC?

    Answer: Light (note: this is consistent with Dr. Peggy Lehman)
    Evidence: Sharp light attenuation with depth and high nutrient concentrations relative to their half saturation values.

12. What was the magnitude of Stockton load relative to river load from upstream?

    Answer: River load was 10 times of the Stockton load.
    Evidence: River load of oxygen consuming organic matter was 35,000 kg/d as compared to 3,600 kg/d for the Stockton load.

13. How important is the river flow on DO deficit in the DWSC?

    Answer: Very important
    Evidence: The DO deficit in the DWSC was 1,360 kg when river flow was 250 cfs. The DO deficit became zero at the river flow of 1,500 cfs.

14. How important was the channel depth to DO in the DWSC?

Answer: Very important
Evidence: DO deficit in the DWSC became zero when channel depth was reversed from current 35-40 feet back to historical 8 to 10 feet.

15. What is the reasonable option for raising DO above 5 mg/l in the DWSC?

Answer: Maintaining a river flow of 1,000 cfs and reducing Stockton and river loads by 20% (or preferably 25% for a margin of safety).
Evidence: Model simulations and professional judgment.

IX. References

Ariathurai, R. and K. Arulanandan. 1984. “An Electrical Method to Measure In-situ Sediment Densities”, in Estuarine Cohesive Sediment Dynamics, A. J. Mehta, Editor, Springer-Verlag, New York, pp. 206-218.

Beaseley, D.B., and L.F. Higgins, 1991. “ANSWERS User’s Manual”, Publication No. 5, Agriculture Engineering Department, University of Georgia, Coastal Plain Experiment Station, Tifton, GA.

Brown, L.C. and T.O. Barnwell, Jr. 198.5. Computer Program Documentation for the Enhanced Stream Water Quality Model QUAL2E, EPA/600/3-85/065, US EPA Environmental Research Laboratory, Athens, GA August 1985.

Chen, C. W. 1970. "Concepts and Utilities of Ecologic Model", Jour of Sanitary Engineering Division, ASCE, Vol. 96, No SA5, October 1970, pp. 1085-1907.

Chen, C. W. and G.T. Orlob. 1975. "Ecologic Simulation for Aquatic Environments", in Systems Analysis and Simulation in Ecology, Vol. III, B. Patten, Editor, Academic Press, pp.475-588.

Chen, C. W., D. Leva, and A. Olivieri 1996. "Modeling Fate of Copper Discharge to San Francisco Bay", Jour of Environmental Engineering, ASCE, Vol. 122, No. 10, pp. 924-934.

Chen, C.W. and W. Tsai. 1997.“Evaluation of Alternatives to Meet the Dissolved Oxygen Objectives of the Lower San Joaquin River”, Report to California State Water Resources Control Board, Sacramento, CA., Systech Engineering, Inc. San Ramon, CA.

DWR. 2000. “Methodology for Flow and Salinity Estimates in the Sacramento-San Joaquin Delta and Suisun Marsh”, 21st Annual Progress Report to the State Water Resources Control Board, June 2000.

Feigner, K.D. and H.S. Harris. 1970. Documentation Report FWQA Dynamic Estuary Model, Federal Water Quality Administration.

Graf, W.H. 1971. Hydraulics of Sediment Transport. McGraw-Hill Book Company, New York, NY, p96.

Hayter, E.J. 1984. “Estuarial Sediment Bed Model”, in Estuarine Cohesive Sediment Dynamics, A. J. Mehta, Editor, Springer-Verlag, New York, pp. 326-359.

Mackenthun, A.A. and H.G Stefan. 1998. “Effect of Flow Velocity on Sediment Oxygen Demand: Experiments”, Jour of Environmental Engineering, Vol. 124, No. 3, pp. 222-230.

Roache, P.J. 1972. “Computational Fluid Dynamics”, Hermosa Publishers, Albuquerque, New Mexico.

Schanz, R. and C.W. Chen. 1993. “City of Stockton Water Quality Model, Volume 1. Model Development and Calibration”, Report to City of Stockton, PWA and Systech Engineering, Inc.

Tang, L. and E.E. Adams. 1995. “Effect of Divergent Flow on Mass Conservation in Eulian-Lagrangian Transport Schemes”, in Eastuarine and Coastal Modeling, Proceedings of the 4th International Conference, October, 1995, pp. 107-115.